FINAL REPORT
(March 1, 1985 to February 29, 1989)

AERODYNAMIC AND KINETIC PROCESSES IN FLAMES

(AFOSR 85-0147)

For Review by

Dr. Julian Tishkoff
Air Force Office of Scientific Research
Bolling Air Force Base

Submitted by
Professor Chung K. Law
Department of Mechanical and Aerospace Engineering
Princeton University
Princeton, NJ 08544

September, 1989

Unclassified
SECURITY CLASSIFICATION OF THIS PAGE

REPORT DOCUMENTATION PAGE

Form Approved
OMB No. 0704-0188

1a. REPORT SECURITY CLASSIFICATION: Unclassified	1b. RESTRICTIVE MARKINGS
2a. SECURITY CLASSIFICATION AUTHORITY	3. DISTRIBUTION/AVAILABILITY OF REPORT: Approved for public release; distribution is unlimited.
2b. DECLASSIFICATION/DOWNGRADING SCHEDULE	
4. PERFORMING ORGANIZATION REPORT NUMBER(S)	5. MONITORING ORGANIZATION REPORT NUMBER(S): AFOSR-TR-90-0087
6a. NAME OF PERFORMING ORGANIZATION: University of California at Davis; 6b. OFFICE SYMBOL (If applicable)	7a. NAME OF MONITORING ORGANIZATION: AFOSR/NA
6c. ADDRESS (City, State, and ZIP Code): Davis, California 95616	7b. ADDRESS (City, State, and ZIP Code): Building 410, Bolling AFB DC 20332-6448
8a. NAME OF FUNDING/SPONSORING ORGANIZATION: AFOSR/NA; 8b. OFFICE SYMBOL (If applicable): NA	9. PROCUREMENT INSTRUMENT IDENTIFICATION NUMBER: AFOSR-85-0147
8c. ADDRESS (City, State, and ZIP Code): Building 410, Bolling AFB DC 20332-6448	10. SOURCE OF FUNDING NUMBERS: PROGRAM ELEMENT NO. 61102F; PROJECT NO. 2308; TASK NO A2; WORK UNIT ACCESSION NO.

11. TITLE (Include Security Classification)
(U) Aerodynamic and Kinetic Processes in Flames

12. PERSONAL AUTHOR(S)
C. K. Law

13a. TYPE OF REPORT	13b. TIME COVERED	14. DATE OF REPORT (Year, Month, Day)	15. PAGE COUNT
Final Report	FROM 1985 TO 1989	1989 - 9 - 15	73

16. SUPPLEMENTARY NOTATION

17. COSATI CODES			18. SUBJECT TERMS (Continue on reverse if necessary and identify by block number)
FIELD	GROUP	SUB-GROUP	Flame Dynamics, Flame Kinetics, Turbulent Flames, Soot Formation, Methane-Air Combustion.

19. ABSTRACT (Continue on reverse if necessary and identify by block number)

In this program an extensive experimental, numerical and analytical study of the dynamics and chemical kinetics of flames was conducted. Specific phenomena investigated included an asymptotic simulation of hydrocarbon oxidation kinetics, an analysis of nonadiabatic flame propagation in dissociation equilibrium, a 3-step modeling of diffusion flames, detailed experimental and numerical determination of the laminar flame speeds of methane/air mixtures, experimental and analytical quantification of the propagation, extinction and interaction of laminar flames, experimental quantification of the structure and propagation of turbulent premixed flames in stagnation flow, and the influence of dilution, inert addition, preferential diffusion, and aerodynamic straining on soot formation in diffusion flames. A total of fourteen journal publications resulted from the present program.

20. DISTRIBUTION/AVAILABILITY OF ABSTRACT	21. ABSTRACT SECURITY CLASSIFICATION
☒ UNCLASSIFIED/UNLIMITED ☒ SAME AS RPT. ☒ DTIC USERS	Unclassified
22a. NAME OF RESPONSIBLE INDIVIDUAL: Julian M Tishkoff	22b. TELEPHONE (Include Area Code): (202) 767-0465; 22c. OFFICE SYMBOL: AFOSR/NA

DD Form 1473, JUN 86 Previous editions are obsolete. SECURITY CLASSIFICATION OF THIS PAGE

Unclassified

Table of Contents

RESEARCH ACCOMPLISHMENTS

During the grant period worthwhile contributions have been made on the qualitative and quantitative understanding of flames. These contributions can be approximately grouped into four categories: (1) Kinetic structure of laminar flames; (2) Aerodynamic structure of laminar flames; (3) Structure of turbulent premixed flames; (4) Soot formation in laminar diffusion flames. The accomplishments are summarized in the following, while the details can be found in the published journal papers.

1. Kinetic Structure of Laminar Flames

The emphasis in this area is in understanding and quantifying the detailed and semi-global kinetics of fuel/oxidizer systems undergoing combustion.

1.1 Asymptotic Simulation of Hydrocarbon Oxidation Kinetics

In this study we have used large activation energy matched asymptotic analysis to resolve the detailed reaction process of paraffin/air oxidation as represented by the four-step semi-global reaction mechanism determined from Princeton's flow reactor. Four major regimes respectively representing fuel pyrolysis, hydrogen and carbon monoxide production, hydrogen oxidation, and carbon monoxide oxidation were identified. Embedded within these four major regimes are fifteen sub-regimes. Unlike previous asymptotic studies of reaction systems with complex chemistry, transitions between these sub-regimes are not governed by the different orders of activation energies but rather by the creation/destruction and thereby availability of the various intermediates. Explicit expressions were derived for the characteristic time scales associated with each sub-regime. Analytical results agree well with

the experimental flow reactor data.

This work is reported in Publication No. 1.

1.2 Nonadiabatic Flame Propagation in Dissociation Equilibrium

An intriguing question in the fundamental study of the structure and extinction of flames is the influence of product dissociation on the extinguishability of flames. Recently Williams and Peters have analyzed the diffusion flame structure and found that product dissociation facilitates flame extinction. In the present study we have analyzed the premixed flame structure allowing for product dissociation. Analytical solutions have been obtained with an explicit expression for the burning rate eigenvalue as a function of the dissociation and heat loss parameters. These reveal the interesting results that dissociation alone cannot cause extinction of an adiabatic flame. In retrospect this is reasonable because the effect of dissociation is equivalent to reducing the heat of combustion, which lowers the flame temperature but does not alter the basic structure of the laminar flame propagation which does not exhibit any extinction behavior.

Analysis has also been performed allowing for volumetric heat loss. In this case it was found that extinction is facilitated in the simultaneous presence of dissociation and heat loss.

This work is reported in Publication No. 2.

1.3 Kinetic and Thermal Structure of Diffusion Flames

We have analyzed the structure of a diffusion flame supported by a representative branching-termination reaction scheme

$$F + R_1 \rightarrow 2R_2$$

$$O + R_2 \rightarrow 2R_1$$

$$R_1 + R_2 + M \rightarrow 2P + M$$

where F is the fuel, O the oxidizer, M a third body, and R_1 and R_2 are regenerated radicals. The analysis yields three types of flame behavior, depending on the efficiency of the recombination reaction. Of particular interest is the fast recombination regime in which branching and recombination take place in the same, thin reaction zone. An explicit extinction criterion has been derived which respectively specialize to a kinetic extinction limit and a thermal extinction limit; in the latter case we recover Linan's extinction criterion. This work is reported in Publication No. 3.

1.4 Experimental and Numerical Determination of Laminar Flame Speeds of Methane/Air Mixtures under Reduced and Elevated Pressures

The laminar flame speed S_L^o is an important physico-chemical parameter of a combustible mixture because it contains the basic information regarding its diffusivity, exothermicity and reactivity. However, in spite of the extensive efforts expended to accurately determine their values, wide systematic spreads in the reported experimental data still exist even though in many instances the experiments appear to have been carefully executed. Recently, it has been suggested that these systematic discrepancies are likely caused by the coupled effects of flame stretch and preferential diffusion. Specifically, it has been demonstrated both theoretically and experimentally that the flame response can be qualitatively reversed when the flame stretch changes from positive to negative (e.g. expanding spherical flame versus the Bunsen flame), and when the mixture's effective Lewis number crosses a critical value typically around unity (e.g. lean methane/air and rich propane/air mixtures versus rich methane/air and lean propane/air mixtures).

A particularly serious implication of the stretch-induced flame response

is the potential falsification of the kinetic information determined or validated through comparison between the numerically-calculated and experimentally-determined results. In view of this concern, we have recently proposed a stagnation-flow based methodology through which stretch effects can be systematically subtracted out such the S_L^o can be unambiguously determined.

In the present investigation we have accurately determined the S_L^o of methane/air mixtures under reduced and elevated pressures. While these data are of practical interest in its own right in terms of high-pressure combustion, we note in addition that these data also carry significant kinetic information because pressure not only influences the frequency of molecular collision but also differentiates the relative efficiencies of the two-body branching reaction versus the three-body termination reaction. Thus they provide additional constraints for the validation of the kinetic schemes.

The experimental data have been compared with the numerically-calculated values obtained by assuming different kinetic mechanisms. Consequently, the C_1 mechanism of Miller and C_2 mechanism of Warnatz both accurately reproduce our experimental data over the extensive concentration and pressure ranges tested. The relative superiority of these two schemes cannot be further resolved.

This work is reported in Publication No. 4.

1.5 Laminar Flame Speeds of Methane/"Air" Mixtures as a Function of Stoichiometry, Pressure and Flame Temperature

The work of 1.4 has been extended to the determination of laminar flame speeds of methane/"air" mixtures over the stoichiometric range from very lean to very rich, the pressure range from 0.25 to 2 atm, and flame temperature range from 1,550 and 2,250 K; independent variation in the flame temperature

is achieved by substituting nitrogen in the air by an equal amount of argon or carbon dioxide. These data are expected to be useful for the partial validation of proposed kinetic mechanisms. In the present study numerical simulation of the experimental flame speeds has been conducted by using a C_1 mechanism and a full C_2 mechanism. The calculated results agree well with the experimental data, for both the C_1 and C_2 mechanisms, except for the very rich mixtures for which there is substantial over-prediction by the C_2 mechanism. Sensitivity analyses have also been performed where appropriate for enhanced insight into the controlling elementary reactions.

This work is reported in Publication No. 5.

1.6 Experiments on Extinction of Diffusion Flames

In this study we experimentally investigate the theoretical results of 1.3. The theory predicts that, because of the simultaneous presence of branching and termination reactions, the density-weighted extinction strain rate of a diffusion flame increases only linearly with pressure, while the conventional formulation assuming only a one-step second-order overall reaction predicts a quadratic dependence. The experiment was conducted by using the counterflow diffusion flame configuration. Experimental results indeed reveal a linear dependence.

This work is reported in Publication No. 6.

2. Aerodynamic Structure of Laminar Flames

The emphases here are on the influence of stretch and preferential diffusion on flames.

2.1 Propagation and Extinction of Stretched Premixed Flames

Practically all realistic flames are subjected to aerodynamic stretching,

manifest through flow nonuniformity, flame curvature, or flame/flow unsteadiness. These processes can profoundly affect the flame from those prescribed by the classical one-dimensional planar flame propagation theory, which is frequently the one used in modeling practical combustion phenomena.

The two most important parameters characterizing stretched flames are the stretched flame speeds and the states of extinction when certain critical stretch rates are exceeded. Unfortunately, these data have not been obtained. Therefore, the first contribution of the present study is an accurate determination of these values as functions of stoichiometry and stretch for both methane/air and propane/air mixtures. These results further show that the flame speed is finite at the state of extinction and that the extinction limits for nearly adiabatic, stretchless, and planar flames appear to correspond to the flammability limits of the respective mixtures. It is suggested that kinetic termination could be the dominant extinction mechanism at the flammability limits.

This work is reported in Publication No. 7.

2.2 Interaction Between Laminar Flames

Modeling of turbulent combustion can be frequently facilitated by approximating the turbulent flame as an ensemble of laminar flamelets. It is clear that, contrary to previous modeling efforts in which such flamelets are assumed to be isolated ones, they are actually in close proximity and therefore should interact strongly with each other.

In a previous study we have experimentally mapped the extinction limits of two interacting laminar premixed flames. Subsequently a theory has been formulated for the extinction of this interacting system. The results show good agreement with the experimental data for lean methane/air mixtures but

not lean butane/air mixtures.

In the present study we first argued that such a discrepancy is a consequence of the unity Lewis number assumption in the theory. The theory was subsequently extended to allow deviation of the Lewis numbers from unity. Satisfactory agreement with all experimental data was then obtained.

This work is reported in Publication No. 8.

2.3 Dynamics of Stretched Flames

This is an invited review paper presented at the 22nd Combustion Symposium. Here recent advances in the understanding of the structure, propagation and extinction of laminar flames under the influence of stretch, as manifested by the existence of flame curvature, flow nonuniformity, and flame motion, are reviewed. The emphasis is on premixed flames because of the richness and subtlety of the phenomena involved. The review distinguishes the influences of the tangential and normal velocity gradients on the flame response, both at the hydrodynamic scale and within the flame structure, and emphasizes the importance of the preferential diffusion nature of heat and mass transport, as well as the extent to which the flame can freely adjust its location in response to stretch in order to achieve complete reaction. It is then demonstrated that stretch has only minimal effect on an adiabatic, unrestrained, diffusionally-neutral flame with complete reaction in that the temperature, propagation rate, and thickness of the flame are invariant to stretch, and that stretch alone cannot extinguish such a flame. In the presence of preferential diffusion and/or when the flame movement is restrained, the response of the flame to stretch becomes more sensitive and extinction is also possible. The concept of flame stretch is applied to interpret such practical flame phenomena as flame stabilization and flame-

front instability, determination of laminar flame speeds and flammability limits, concentration and temperature modifications in flame chemistry, and modeling of turbulent flames. The properties of stretched diffusion flames are then briefly discussed. The review closes with suggestions for further research.

This paper is designated as Publication No. 9.

3. Structure of Turbulent Premixed Flames

3.1 Structure and Propagation of Turbulent Premixed Flames

Previous experimental studies on turbulent premixed flames have used either the Bunsen flame configuration or the V-flame stabilized by a rod. Data obtained from these two flame configurations, however, are complicated by the uncertainty in the flame orientation and the eddies generated in the flame stabilization region. In the present investigation we have adopted the stagnation flame as our model configuration. The advantages here are the planar nature of the flame which is also normal to the bulk flow, and the absence of fluctuations generated by the holding region.

Using this flame configuration, experiments have been conducted covering equivalence ratios of 0.67 to 1.16, incident turbulence intensities of 0.1 to 0.7 m/s, and global stretch rates of 100 to 230/sec. Results on turbulence statistics show that in crossing the flame the increase in fluctuation is more pronounced in the normal component, while the Reynolds stress remains almost zero, and that the velocity joint probability density function is bimodal for rich flames and mono-modal for lean flames. Turbulent flame speeds determined as functions of the equivalence ratio and turbulence intensity agree well with those in the literature.

This work is reported in Publication No. 10.

3.2 Velocity and Scalar Fields of Turbulent Premixed Flames in Stagnation Flow

Detailed experimental measurements of the scalar and velocity statistics of premixed methane/air flames stabilized by a stagnation plate are reported. Conditioned and unconditioned velocity of two components and the reaction progress variable are measured by using a two-component laser Doppler velocimetry technique and Mie scattering technique, respectively. Experimental conditions cover equivalence ratios of 0.9 and 1.0, incident turbulence intensities of 0.3 to 0.45 m/s, and global stretch rates of 100 to 150 sec^{-1}. The experimental results are analyzed in the context of the Bray-Moss-Libby flamelet model of these flames. The results indicate that there is no turbulence production within the turbulent flame brush and the second and third order turbulent transport terms are reduced to functions of the difference between the conditioned mean velocities of the axial and transverse components. The result of normalization of these relative velocities by the respective velocity increase across laminar flames suggest that the mean unconditioned velocity profiles are self-similar.

This work is reported in Publication No. 11.

4. Soot Formation in Laminar Diffusion Flames

In this series of studies the effects of dilution, preferential diffusion, inert addition, and aerodynamic straining on soot formation in laminar diffusion flames were quantified.

4.1 Dilution and Temperature Effects on Inert Addition on Soot Formation in a Counterflow Diffusion Flame

The isolated effects of fuel dilution and flame temperature variation on

soot formation have been investigated experimentally for counterflow diffusion flames. The methodology of isolation through temperature adjustment involves changing the concentration of the fuel by diluting it with nitrogen and then increasing the maximum temperature of the diluted flame back to that of the undiluted flame by replacing a portion of the nitrogen in the oxidizer flow with an equal portion of argon. Soot quantities are determined by using light-scattering and extinction techniques, flame temperatures by thermocouple measurements, and velocities by LDV mapping. Results on ethylene show that both temperature and dilution contribute to a reduction in the soot volume fraction and dilution accounts for a substantial amount of this reduction. It is further found that the soot formation rate and specific surface area are linearly dependent on the initial fuel concentration, while the specific surface growth rate is insensitive to its variation. Finally, the soot formation process is insensitive to a wide range of fuel ejection rates for the present counterflow diffusion flame established in the forward stagnation region of a porous cylinder.

The work is reported in Publication No. 12.

4.2 Preferential Diffusion and Concentration Modification in Sooting Counterflow Diffusion Flames

An experimental investigation has been conducted on the influence of the mobility of inert additives on soot formation in propane and ethylene counterflow diffusion flames. Inerts used were helium, neon, argon, or krypton, and the results show that while the mobility of the inert has practically no effect when a small amount of inert is added to the oxidizer side, the influence is significant when added to the fuel side in that krypton, being the least mobile inert, yields the greatest soot loading while

helium, being the most mobile, yields the least. By relating the spatially-resolved soot volume fractions to the corresponding profiles of temperature, velocity and species concentrations, it is demonstrated that this influence on soot loading is likely caused by concentration modifications of the fuel and the soot precursors due to the different mobilities of the inert additives.

This work is reported in Publication No. 13.

4.3 Experiments on the Sooting Limits of Aerodynamically-Strained Diffusion Flames

An experimental study has been performed with axisymmetric counterflow diffusion flames to investigate the influence of aerodynamic straining on the relevant sooting limits of the lower alkanes. The limits are defined by the critical strain rate at which either soot luminosity, soot particle scattering, or fluorescence is negligible compared to the appropriate background signal. These critical strain rates are found to be greatest for the sooting limit based on the fluorescence signal, and least for that based on luminosity. The fluorescence signal, if attributed to polycyclic aromatic precursors, yields a limit that can be interpreted as the extinction of soot precursors and is suggested to be a possible limit for identifying a completely nonsooting flame condition. The separate effects of flame temperature and fuel concentration on the critical strain rates for soot extinction have also been studied. The results are indicative of how temperature and concentration influence the soot particle inception process and they show that both are potentially important parameters. The critical strain rates display an Arrhenius temperature dependence and this dependence is similar for all alkanes considered.

This work is reported in Publication No. 14.

PUBLICATIONS

1. "Asymptotic Simulation of the Four-Step Global Kinetics of Hydrocarbon/Air Mixtures under Flow Reactor Conditions," by M. Birkan and C.K. Law, Combustion Science and Technology, Vol. 51, pp. 145-207 (1987).

2. "Theory of Nonadiabatic Flame Propagation in Dissociation Equilibrium," by B.H. Chao and C.K. Law, Twenty-First Combustion Symposium, The Combustion Institute, Pittsburgh, PA, pp. 1793-1802 (1988).

3. "Asymptotic Structure and Extinction of Diffusion Flames with Chain Mechanism," by M. Birkan and C.K. Law, Combustion and Flame, Vol. 73, pp. 127-146 (1988).

4. "Laminar Flame Speeds of Methane/Air Mixtures Under Reduced and Elevated Pressures," by F. Egolfopoulos, P. Cho, and C.K. Law, Combustion and Flame, Vol. 76, pp. 375-391 (1989).

*5. "Experimental and Numerical Determination of Laminar Flame Speeds of Methane/(Ar, N_2, CO_2)-Air Mixtures as Function of Stoichiometry, Pressure, and Flame Temperature," by D.L. Zhu, F.N. Egolfopoulos and C.K. Law, Twenty-Second Combustion Symposium, The Combustion Institute, Pittsburgh, PA, pp. 1539-1545 (1989).

6. "Extinction of Counterflow Diffusion Flames with Branching-Termination Chain Mechanisms: Theory and Experiment," by C.K. Law, Lecture Notes in Physics Series, Vol. 299: Mathematical Modelling in Combustion Science (J. Buckmaster and T. Takeno, eds.), Springer-Verlag, pp. 147-156 (1988).

7. "Propagation and Extinction of Stretched Premixed Flames," by C.K. Law, D.L. Zhu, and G. Yu, Twenty-First Combustion Symposium, The Combustion Institute, Pittsburgh, PA, pp. 1419-1426 (1988).

8. "Extinction of Interacting Premixed Flames: Theory and Experimental Comparisons," by S.H. Chung, J.S. Kim and C.K. Law, Twenty-First Combustion Symposium, The Combustion Institute, Pittsburgh, PA, pp. 1845-1851 (1988).

*9. "Dynamics of Stretched Flames," by C.K. Law, Twenty-Second Combustion Symposium, The Combustion Institute, Pittsburgh, PA, pp. 1381-1402 (1989). **Invited Paper**

10. "Structure and Propagation of Turbulent Premixed Flames Stabilized in a Stagnation Flow," by P. Cho, C.K. Law, J. Hertzberg, and R.K. Cheng, Twenty-First Combustion Symposium, The Combustion Institute, Pittsburgh, PA, pp. 1493-1499 (1988).

*11. "Velocity and Scalar Fields of Turbulent Premixed Flames in Stagnation Flow," by P. Cho, C.K. Law, R.K. Cheng, and I. Shepherd, Twenty-Second Combustion Symposium, The Combustion Institute, Pittsburgh, PA, pp. 379-386 (1989).

12. "Dilution and Temperature Effects of Inert Addition on Soot Formation in a Counterflow Diffusion Flame," by R.L. Axelbaum, W.L. Flower, and C.K. Law, Combustion Science and Technology, Vol. 61, pp. 51-73 (1988).

*13. "Preferential Diffusion and Concentration Modification in Sooting Counterflow Diffusion Flames," by R.L. Axelbaum, C.K. Law, and W.L. Flower, Twenty-Second Combustion Symposium, The Combustion Institute, Pittsburgh, PA, pp. 2019-2026 (1989).

*14. "Experiments on the Sooting Limits of Aerodynamically-Strained Diffusion Flames," by D.X. Du, R.L. Axelbaum, and C.K. Law, Twenty-Second Combustion Symposium, The Combustion Institute, Pittsburgh, PA, pp. 387-394 (1989).

---

* Reprints appended.

PERSONNEL

Professor C. K. Law	Principal Investigator	10%
Dr. M. Birkan	Research Associate	50%
Dr. B.H. Chao	Research Associate	25%
Dr. P.Cho	Research Associate	50%
Mr. F. Egolfopoulos	Ph.D. Student	50%

PRESENTATIONS AND SIGNIFICANT INTERACTIONS

During the reporting period the Principal Investigator gave the following invited and contributed talks.

Invited Talks:

1. "Combustion of Multicomponent Droplets," Ballistic Reserach Laboratory, Aberdeen Proving Ground, Aberdeen, MD, Mar.5 , 1985.

2. "Dynamics of Stretched Premixed Flames," Department of Mechanical Engineering, McGill University, Montreal, Quebec, Canada, Mar. 6, 1985.

3. "Behavior of Non-Dilute Sprays," AFOSR/ARO Workshop on Non-Dilute Sprays, Sandia Laboratories, Livermore, CA, Mar. 20-21, 1985. **Lead Talk**

4. "Recent Advances in Droplet Combustion," Department of Mechanical Engineering, Cornell University, Ithaca, NY, Apr. 30, 1985.

5. "Heat and Mass Transfer in Combustion," Department of Applied Mechanics and Engineering Sciences, University of California, San Diego, CA, Oct. 11, 1985.

6. "Dynamics of Stretched Flames," Department of Mechanical Engineering, University of California, Davis, CA, Jan. 30, 1986.

7. "Recent Advances in Droplet Combustion," Department of Mechanical Engineering, Louisianna State University, Baton Rogue, LA, Feb. 18, 1986.

8. "Dynamics of Stretched Flames," Department of Mechanical Engineering, University of Oklahoma, Norman, OK, Feb. 19, 1986.

9. "Recent Advances in Droplet Combustion," Department of Mechanical Engineering, Texas A&M University, College Station, TX, Feb. 20, 1986.

10. "Recent Advances in Droplet Combustion," Department of Mechanical Engineering, University of Texas, Arlington, TX, Feb. 21, 1986.

11. "Recent Advances in Droplet Combustion," Department of Mechanical Engineering and Aerospace Engineering, Princeton University, Princeton, NJ, April 1, 1986.

12. "Dynamics of Stretched Flames," Department of Mechanical Engineering, University of Colorado, Boulder, CO, April 14, 1986.

13. "Combustion of High Energy Propellants," Martin Marietta Research Lab., Baltimore, MD, July 28, 1986.

14. "Recent Advances in Droplet Combustion," Department of Mechanical Engineering, Washington State University, Pullman, WA, Sept. 10, 1986.

15. "Recent Studies on the Structure of Laminar Premixed Flames," Department of Mechanical Engineering, University of California, Berkeley, CA, Oct. 22, 1986.

16. Recent Advances in Multicomponent and Propellant Droplet Vaporization and Combustion," ASME Winter Annual Meeting, Anaheim, CA, Dec. 8-12, 1986. **Invited Talk**

17. "Recent Advances in Multicomponent Droplet Combustion," Department of Mechanical Engineering, University of California, Davis, CA, April 9, 1987.

18. "Incineration of Chlorinated Hydrocarbons," Workshop on Research in Engineering and System Analysis for the Control of Toxic Substances," University of California, Los Angeles, CA, Oct. 21-22, 1987.

19. "Structure, Propagation, and Stability of Laminar Premixed Flames," Department of Mechanical Engineering, Stanford University, Palo Alto, CA, Nov. 4, 1987.

20. "Single Droplet Considerations in Spray Combustion Processes-Experimental Overview," Workshop on Mass, Momentum and Energy Exchange in Combusting Sprays: Droplet Studies, Sandia National Laboratories, Livermore, CA, March 28-29, 1988. **Lead Talk**

21. "Blending Strategy for the Incineration of Chlorinated Hydrocarbons," Workshop on Incineration Technologies for Municipal, Toxic and Hospital Wastes, National Science Foundation, Washington, DC, April 18-19, 1988.

22. "Dynamics of Stretched Flames," Twenty-Second Symposium (International) on Combustion, Seattle, WA, Aug. 15-19, 1988. **Invited Paper**

23. "Some Recent Advances in Droplet Combustion," Third International Colloquium on Drops and Bubbles, Monterey, CA, Sept. 19-21, 1988. **Keynote Paper**

24. "On Flame Extinction and Flammability Limits of Combustibles," Department of Mechanical and Aerospace Engineering, Rutgers University, New Brunswick, NJ, Nov. 2, 1988.

25. "Vaporization, Combustion, and Collisional Dynamics of Fuel Droplets," Department of Mechanical Engineering, University of Pennsylvania, Philadelphia, PA, Feb. 9, 1989.

26. "Extinction and Flammability of Gaseous Combustibles," Department of Mechanical Engineering, Yale University, New Haven, CT, Feb. 22, 1989.

Contributed Talks

1. "Laminar Flame Speeds of Hydrocarbon/Air Mixtures with Hydrogen Addition," Central and Western States Sections of the Combustion Institute Meeting, San Antonio, TX, Apr. 22-23, 1985.

2. "Droplet Combustion of Organic Azides," AIAA/SAE/ASME/ASEE 21st Joint Propulsion Conference, Monterey, CA, July 8-10, 1985.

3. "Aerodynamic and Kinetic Processes in Flames," AFOSR Contractors' Meeting, California Institute of Technology, Pasadena, CA, July 23-25, 1985.

4. "Combustion of Liquid Propellant Droplets," JANNAF Regenerative Liquid Gun Propellant Spray Combustion Workshop, Aberdeen Proving Ground, MD, Aug. 26-27, 1985.

5. "Stability and Stabilization of Premixed Flames," DOE Third Symposium on Energy Engineering Sciences, Pennsylvania State University, University Park, PA, Oct. 8-10, 1985.

6. "Organic Azides as Jet Fuel Additives," ONR Workshop on Combustion Instability in Compact Ramjets, Johns Hopkins University, Baltimore, MD, Oct. 16-17, 1985.

7. "Propagation and Extinction of Stretched Premixed Flames," Fall Technical Meeting of the Western States Section of the Combustion Institute, University of California, Davis, CA, Oct. 21-22, 1985.

8. "Combustion and Micro-Explosion of Water/Oil Emulsions in High Pressure Environments," Sixth ARO Combustion/Fuels Workshop, University of California, Davis, CA, Mar. 17-18, 1986.

9. "Droplet Combustion of HAN-Based Liquid Propellants," Army Workshop on HAN-Based Liquid Propellants, Aberdeen Proving Ground, MD, July 29, 1986.

10. "Liquid-Phase Diffusional Resistance in Multicomponent Droplet Gasification," 21st Combustion Symposium, Munich, Germany, Aug. 3-8, 1986.

11. "Time-Resolved Gasification and Sooting Characteristics of Droplets of Alcohol/Oil Blends and Water/Oil Emulsions," 21st Combustion Symposium, Munich, Germany, Aug. 3-8, 1986.

12. "Flame Curvature and Preferential Diffusion in the Burning Intensity of Bunsen Flames," 21st Combustion Symposium, Munich, Germany, Aug. 3-8, 1986.

13. "Propagation and Extinction of Stretched Premixed Flames," 21st Combustion Symposium, Munich, Germany, Aug. 3-8, 1986.

14. "Vaporization, Combustion, and Microexplosion of Droplets of Organic Azides," 23rd JANNAF Combustion Meeting, NASA-Langley, Oct. 20-24, 1986.

15. "Propagation and Extinction of Stretched Premixed Flames," Sandia Turbulent Flame Workshop, University of California, Davis, CA, April 21-22, 1987.

16. "Aerodynamic and Kinetic Processes in Flames," AFOSR/ONR Contractor's Workshop, Pennsylvania State University, College Station, PA, June 22-26, 1987.

17. "Some Issues Related to Stretched Flames," US-Japan Workshop on Mathematical Combustion, Juneau, Alaska, Aug. 17-21, 1987.

18. "Kinetic Effects in Flame Analysis," US-Japan Workshop on Mathematical Combustion, Juneau, Alaska, Aug. 17-21, 1987.

19. "Droplet Combustion of HAN-Based Liquid Propellants," Worksnop on Liquid Propellants, Aberdeen Proving Ground, Aberdeen, MD, Aug. 25-27, 1987.

20. "Droplet Extinction Studies," Workshop on Hazardous Waste Incineration, University of California, Davis, CA, Sept. 14-15, 1987.

21. "Ignition and Combustion of liquid Gun Propellants," Seventh Army Engine/Fuels Workshop, Detroit, MI, Oct. 13-14, 1987.

22. "Combustion Studies of Energetic Liquid Materials," ONR Contractor's Meeting, University fo California, Berkeley, CA, Nov. 17-19, 1987.

Appendix A

Twenty-Second Symposium (International) on Combustion/The Combustion Institute, 1988/1539-1545

EXPERIMENTAL AND NUMERICAL DETERMINATION OF LAMINAR FLAME SPEEDS OF METHANE/(Ar, N_2, CO_2)-AIR MIXTURES AS FUNCTION OF STOICHIOMETRY, PRESSURE, AND FLAME TEMPERATURE

D. L. ZHU, F. N. EGOLFOPOULOS AND C. K. LAW
Department of Mechanical Engineering
University of California
Davis, California 95616

By using the counterflow method, the laminar flame speeds of methane/(Ar, N_2, CO_2)-air mixtures have been accurately and extensively determined over the stoichiometric range from very lean to very rich, the pressure range from 0.25 to 2 atm, and flame temperature range from 1,550 to 2,250 K; independent variation in the flame temperature is achieved by substituting nitrogen in the air by an equal amount of argon or carbon dioxide. These data are expected to be useful for the partial validation of proposed kinetic mechanisms. In the present study numerical simulation of the experimental flame speeds has been conducted by using a C_1 mechanism and a full C_2 mechanism. The calculated results agree well with the experimental data, for both the C_1 and C_2 mechanisms, except for very rich mixtures for which there is substantial overprediction by the C_2 mechanism. Sensitivity analyses have also been performed where appropriate for enhanced insight into the controlling elementary reactions.

Introduction

Recent studies of the chemical kinetics of complex reactants of interest to combustion have been greatly aided by the ability to simulate numerically the progress of a large number of possible reactions involving many chemical species.[1,2] Such a simulation can serve two purposes. That is, if the kinetics of the elementary steps are accurately known, then the simulation allows the study of the influence of chemistry on the combustion phenomena of interest with confidence. If, however, part of the kinetic mechanism is either unknown or not well established, then the numerical simulation can be used to either identify and/or validate the needed kinetics information through comparisons with results obtained through independent experimentation. It is clear that such a comparison is useful, and meaningful, only if the experimental situation closely simulates that being calculated, and if the experimental data are of the same degree of accuracy, and the same level of detail, as the calculated results.

The model flame configuration that is perhaps most suited for such a simulation, for the study of chemical kinetics, is the steady propagation of the adiabatic, one-dimensional planar premixed flame in the doubly-infinite domain. Since this situation is totally independent of external influences such as those of aerodynamics and heat and radical exchanges, the structure and the propagation rate, S_L^o, of the flame are therefore unique properties of the combustible mixture, representing its reactivity in the presence of diffusive transport. Thus an agreement between the calculated and measured flame propagation speed, as well as the profiles of temperature and species concentrations, should be a strong indication that the kinetic mechanism used in the calculation is a sufficiently accurate, and thereby adequate, representation of the complete mechanism.

Such a requirement, while desirable, is at present not achievable owing to the lack of accurate and sufficient experimental information on the flame structure. On the other hand, extensive data on the laminar flame propagation speed have been accumulated over the years. Therefore much of the focus on the (partial) validation of kinetic mechanisms has been on the comparison between calculated and measured flame speeds.[1-3] Obviously failure to achieve agreement for even such a global flame property is a clear indication that the mechanism requires revision. The usefulness of such a comparison has recently been further enhanced with the development of the counterflow method for the determination of laminar flame speeds.[4,5] That is, except for the flat-flame burner method, all other techniques adopted for measuring flame speeds uti-

lize flames which suffer aerodynamic straining manifested through either flow nonuniformity, or flame curvature, or flame motion. When coupled to the inherent preferential diffusion effects, the flame behavior such as its temperature and propagation speed can be qualitatively and systematically affected.[6,7] This is probably one of the major reasons that previously reported flame speeds, determined by various investigators with great care but by using different flame configurations, can deviate from each other by substantial amounts. For example, values of 25 cm/s to 45 cm/s have been reported as the laminar flame speed of stoichiometric methane/air mixtures at 1 atm.[8] It is therefore clear that such strain-induced effects will have to be subtracted out from the experimentally-determined flame speed S_L to yield the proper, strain-free, one-dimensional flame speed S_L^o before comparison with the numerical results is valid. Failure to do so can lead to falsification of the kinetic mechanism "validated" through comparison. The counterflow method, to be discussed in the next section, offers such a systematic deduction. We mention in passing that the strainless flat-flame burner method, with extrapolation to vanishing heat loss,[9] still cannot totally simulate the model laminar flame because of the potential radical loss at the burner surface.

The general objective of the present study is to provide experimental data of high fidelity and accuracy for the laminar flame speeds S_L^o of methane/inert/oxygen mixtures by using the counterflow method. These results will then be compared with the numerically calculated values by assuming different kinetic mechanisms. Because of the global and somewhat limited nature of the flame speed as a representation of the detailed kinetics, we shall introduce as much kinetics information as possible into the reported values of the flame speed. Specifically, we shall extensively determine the laminar flame speed not only as a function of the mixture equivalence ratio ϕ and pressure p, which are the traditional independent parameters used, but we shall also map it as an explicit function of the adiabatic flame temperature T_{ad}, which has not been attempted before. Thus

$$S_L^o = S_L^o(\phi, p, T_{ad}).$$

Since T_{ad} of a methane/air mixture is fixed for a given ϕ, in the present investigation T_{ad} is to be *independently* varied by substituting N_2 in the air by equal amounts of either Ar or CO_2 such that the O_2 concentration in the (O_2 + inert) mixture is fixed at 21 volume percent. Thus the inert in our "air" can consist of either N_2, or (Ar + N_2), or (CO_2 + N_2).

The fact that a comprehensive representation of the kinetics information of a certain fuel/air system requires the three independent global parameters of ϕ, p and T_{ad} adopted herein can be appreciated by recognizing that the rate of an elementary reaction also requires at least three fundamental thermodynamic parameters. These parameters are needed to represent the local values of the concentration of at least one of the reacting species, the density and thereby pressure to indicate the frequency of collision, and the temperature to indicate the energetics of collision. Therefore in the previous representation of

$$S_L^o = S_L^o(\phi, p, T_{ad}(\phi)),$$

the concentration and temperature sensitivities of the elementary reactions have not been independently tested.

The above discussion basically provides the motivation and approach of the present investigation. In the next two sections the experimental methodology and results will be presented. These will be followed by a comparison with results obtained from detailed numerical simulation by assuming different kinetic schemes.

Experimental Methodology

The various flow variables are defined in Fig. 1a. The experiment basically involved the establishment of two symmetrical, planar, nearly-adiabatic flames in a nozzle-generated counterflow, and the determination of the axial velocity profile along the centerline of the flow by using laser Doppler velocimetry. By identifying the minimum point of the velocity profile as a reference upstream flame speed S_L corresponding to the imposed strain rate K, which is simply the velocity gradient ahead of it, and by plotting S_L versus K, the laminar flame speed without straining S_L^o, can be determined through linear extrapolation to K = 0 (Fig. 1b) in accordance with the theoretical prescription.[6,7] The linear extrapolation is meaningful and accurate only for small values of the nondimensional strain rate

$$Ka = \frac{DK}{(S_L^o)^2} << 1,$$

where Ka is the Karlovitz number and D a representative mass diffusivity.

The diameters of the nozzles used in the present investigation were 7, 10 and 14 mm. They had high contraction ratios and were water-cooled and nitrogen-shrouded.[5] The entire burner assembly was housed in a large stainless steel chamber with adjustable pressure and continuous ventilation. The cross-section of the test portion of the chamber was 14.5 cm by 14.5 cm. Ignition was achieved by a continuous high energy spark produced by retract-

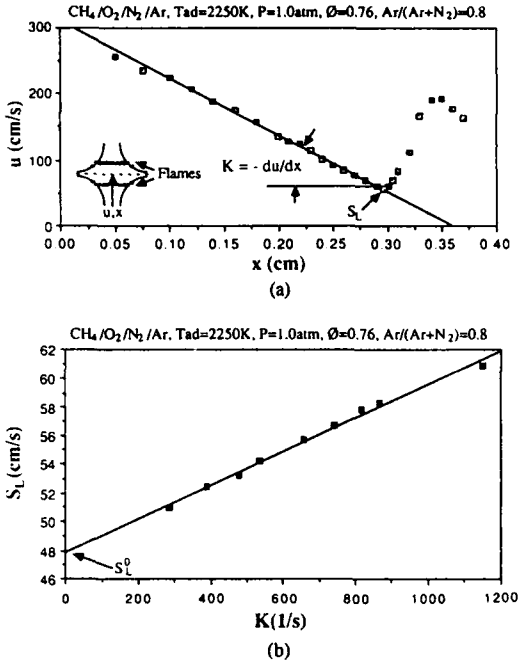

FIG. 1. (a) Typical axial velocity profile across a stagnation flame, showing the definitions of K and S_L. (b) Dependence of the flame speed S_L (K) on the strain rate K.

able electrodes. The LDV operated in the forward scattering mode with 0.3 μm alumina particle seeding.

The flame temperature was independently varied by substituting part of the N_2 in air by equal amount of Ar and CO_2 for higher and lower temperatures respectively. Figure 2 shows the different amounts of substitution used to produce the mixtures for fixed adiabatic flame temperatures.

It is important to mention at this point that this inert substitution affects not only the flame temperature but also the transport properties of the mixture. Specifically, for the same flame temperature and similar equivalence ratios, Ar and CO_2 substitutions tend to increase and decrease the flame speed respectively through changes in the effective (λ/c_p), where λ and c_p are the mixture thermal conductivity and specific heat respectively. Since transport properties of mixtures are known with much greater accuracy than the kinetics, effects due to transport properties can be accurately described such that kinetics is the only component to be studied.

The major source of inaccuracy in the present experiment comes from the difficulty in accurately controlling the individual concentrations of the various gaseous components in the mixture preparation stage. When the preparation involves only three components, as in the case of $CH_4/Ar/O_2$ in Fig. 3, the control is quite tight and the data have higher accuracy. However, when four gaseous components (i.e., CH_4, O_2, N_2, Ar or CO_2) are involved as in the constant flame temperature experiments, the simultaneous control is more delicate. Slight uncertainties in the mixture concentration could lead to corresponding uncertainties in the flame temperature and equivalence ratio. It is estimated that these uncertainties could result in maximum scatters of ±1.5 cm/s in the measured flame speed and ±0.01 in ϕ. These uncertainties are quite small and represent an improvement over previously reported data *in addition* to the elimination of systematic strain rate effects.

Experimental Results

Figure 3 is the traditional plot of flame speed S_L^o versus equivalence ratio ϕ for methane/Ar-air, methane/N_2-air, and methane/CO_2-air mixtures at 1 atm pressure. The symbol I-air here, as in Ar-air, designates an air mixture in which all the N_2 has been substituted by Ar. All of the present results are bounded by the Ar-air and CO_2-air data, from the top and bottom, respectively. We further note that for the same ϕ, flames above and below the N_2-air data have higher and lower temperatures respectively. The data for Ar-air flames obtained by

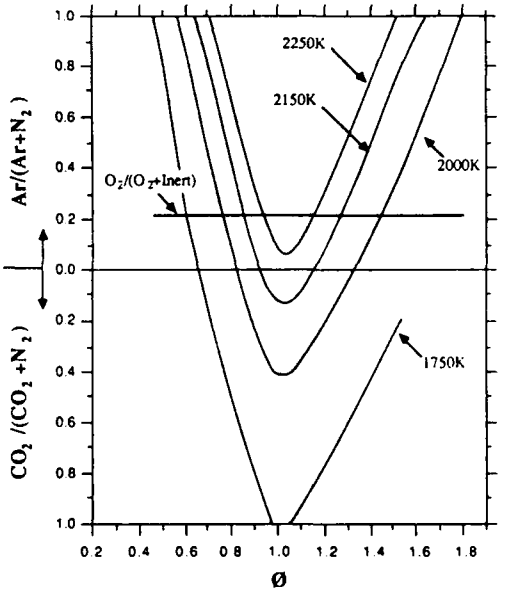

FIG. 2. Relative molar amounts of the various inerts required to achieve different adiabatic flame temperatures, as functions of ϕ.

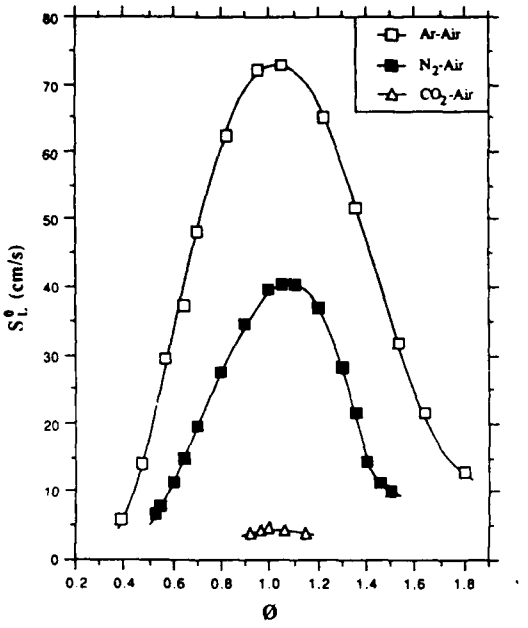

FIG. 3. Experimental laminar flame speeds S_L^o (ϕ) for methane/Ar-air, methane/N_2-air, and methane/CO_2-air mixtures, at 1 atm.

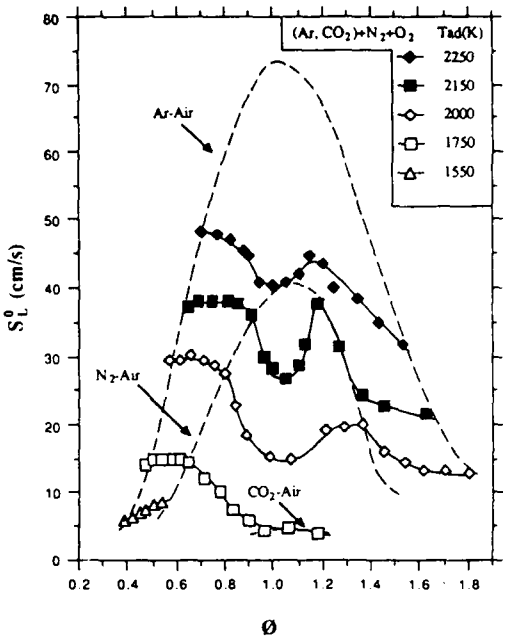

FIG. 4. Experimental laminar flame speeds S_L^o (ϕ) for constant flame temperatures, T_{ad}, at 1 atm.

Clingman et al.,[10] using the area method, show maximum flame speeds nearly 40% higher than those obtained in the present work.

Figure 4 shows the measured S_L^o as a function of ϕ, on constant flame temperatures T_{ad} and at 1 atm. The experimental results of Fig. 3 are shown as dashed curves. The data set of T_{ad} = 2,250 K corresponds to the lowest T_{ad} for which all the S_L^o are higher than the methane/N_2-air curve. For lower values of T_{ad}, CO_2 substitution is needed to obtain flame speeds below those of the methane/N_2-air curve. It is significant to note that S_L^o varies quite non-monotonically with ϕ; this behavior will be explained later.

Figure 5 shows the experimental S_L^o (ϕ) for various pressures p with a constant T_{ad} = 2,250 K. It is seen that, for the same ϕ, S_L^o decreases with increasing pressure. Since the eigenvalue for laminar flame propagation is the mass burning rate (per unit area) $\rho_u S_L^o$ instead of S_L^o, where ρ_u is the density of the unburnt mixture, the data of Fig. 5 are replotted in Fig. 6 as $\rho_u S_L^o$. Now we see that $\rho_u S_L^o$ increases with increasing pressure. Since for a given ϕ one can define an overall reaction order $n(\phi)$ such that $\rho_u S_L^o \sim p^{n/2}$, the increasing trend of $\rho_u S_L^o$ indicates positive values of n. Figure 7 shows n determined as a function of p for a given ϕ. It is seen that while n is positive, it decreases with increasing p for a given ϕ. This illustrates the progressive im-

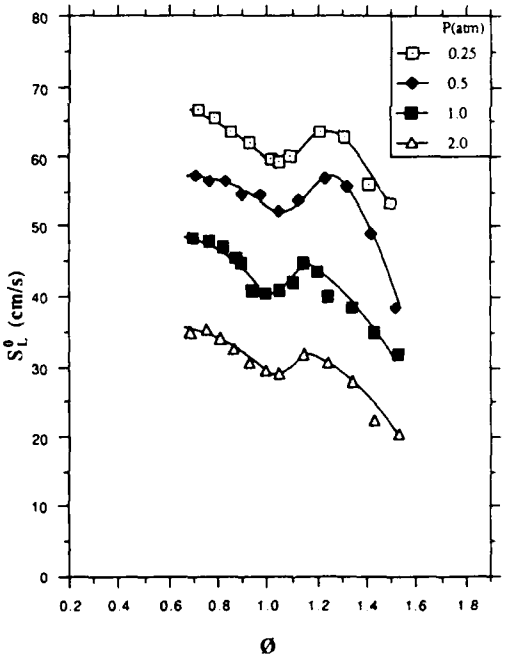

FIG. 5. Experimental laminar flame speeds S_L^o (ϕ, ρ), for T_{ad} = 2,250 K and pressures between 0.25 and 2 atm.

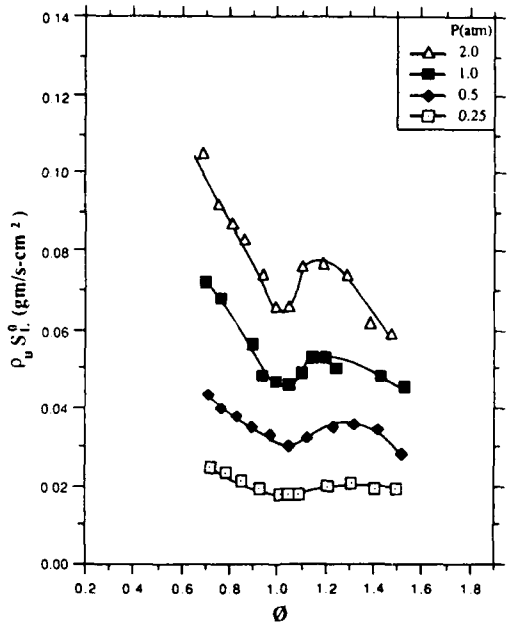

FIG. 6. Experimental mass burning rates $\rho_u S_L^0$ (ϕ, p), for T_{ad} = 2,250 K and pressures between 0.25 and 2 atm.

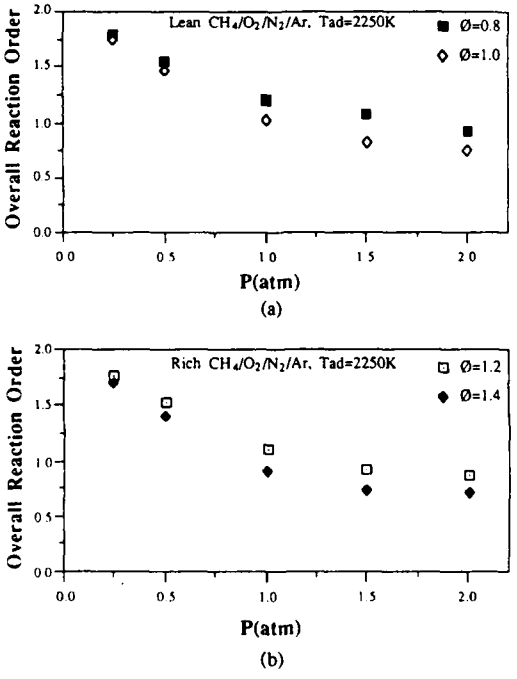

FIG. 7. Experimentally determined overall reaction orders for lean, stoichiometric and rich $CH_4/O_2/N_2/Ar$ flames for T_{ad} = 2,250 K.

portance of three-body termination reactions relative to two-body branching reactions as pressure increases and overall reaction rate decreases. It is especially of interest to note that the importance of the termination reactions is manifested even for the present situations involving relatively low pressures and strongly burning flames.

Numerical Results

Numerical simulation of the one-dimensional flame propagation was conducted by using the flame code developed by Kee and co-workers,[11-14] with the minor modification that diffusion of species k is given by the multicomponent diffusion relation[15]

$$\nabla X_k = \sum_1^N \left(\frac{X_j X_k}{D_{jk}}\right)(V_j - V_k) \qquad (1)$$

without the assumption of trace species diffusion, where X_j, V_j and D_{jk} are respectively the molar fraction and diffusion velocity of species j and its mass diffusivity relative to species k. Overall mass conservation is achieved by applying Eq. (1) to the (N − 1) species while using

$$\sum_1^N Y_i V_i = 0 \qquad (2)$$

for the Nth species, where Y_i is the mass fraction.

In adopting the kinetic mechanisms of methane oxidation needed for simulation, we note that in a previous study on methane/air flames,[16] an extensive evaluation was conducted for the various kinetic mechanisms reported in the literature. Through such an evaluation, two mechanisms emerge as being highly predictive of the experimentally-determined laminar flame speeds. These are the C_1 mechanism of Kee et al.[13] and the full C_2 mechanism of Warnatz,[2] which are predictive up to ϕ = 1.2 to 1.3. These comparisons are reproduced for the methane/N_2-air data in Fig. 8. The C_1 mechanism has the advantages of being predictive up to moderately rich conditions and is also considerably less time consuming for simulation. Furthermore, it has also been suggested[17] that the methane/air laminar flame speeds may not be sensitive to C_2-reactions up to ϕ = 1.3. On the other hand the more complex C_2 mechanism has the advantage of extended applicability over the entire concentration range. It may also be noted that since development of these two mechanisms have probably involved some implicit calibration around the stoichiometric condition, the C_1 part of the full C_2 mechanism of Warnatz[2] slightly underpredicts the experimental

data and therefore does not degenerate to the C_1 mechanism of Kee et al.[13]

In the present simulation these two mechanisms are subjected to further validation by comparing the calculated results with the present data which incorporate variations in concentration, pressure and flame temperature. The constraints imposed on the validation criterion are therefore more stringent than those of the previous validation studies.

Figure 8 shows the calculated flame speeds of methane/Ar-air mixtures by using both the C_1 and C_2 mechanisms. The flame speeds of methane/CO_2-air have not been calculated because they have very low values and the calculations are very difficult to converge. These calculated results are compared with the experimental data, shown in Fig. 8 as dashed curves which are reproduced from the solid curves of Fig. 3. The comparison shows that the C_1 mechanism predicts well the flame speeds of methane/N_2-air and methane/Ar-air mixtures even up to about $\phi = 1.2$ to 1.3. The C_2 mechanism slightly underpredicts the flame speed for Argon mixtures up to $\phi \approx 1.0$, although the difference is too small to be significant. For richer flames, however, it overpredicts the flame speed by somewhat larger amounts.

Figure 9 compares the constant T_{ad} data of Fig. 4, shown as the dashed curves here. Most of the calculations were conducted with the C_1 mechanism because numerical solution with the C_2 mechanism is very time consuming. It is seen that the calculated results satisfactorily reproduce the highly non-monotonic behavior of the experimental data. The C_1 mechanism again shows good agreement while the limited amount of solutions with C_2 mechanism yield higher flame speeds for the richer mixtures. It is perhaps somewhat surprising that the agreement with the C_1 mechanism is better for the methane/N_2-air and methane/Ar-air flames of Fig. 8 than those of the present constant T_{ad} flames which are bounded by them. This is believed to be caused by the increased scatter in the data for the constant-T_{ad} experiments, as mentioned earlier.

Finally, Fig. 10 shows the comparison for the constant pressure data, at $T_{ad} = 2{,}250$ K. The agreement can again be considered to be mostly satisfactory.

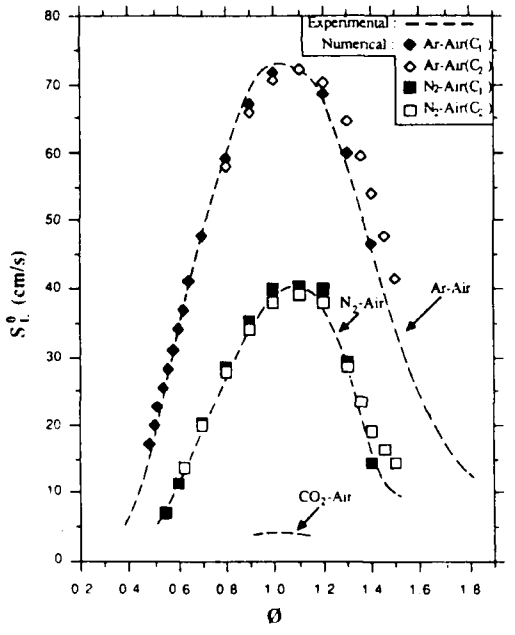

FIG. 8. Comparison between experimentally and numerically determined S_L^0 (ϕ) for methane/Ar-air mixtures at 1 atm, using C_1 and C_2 kinetic schemes.

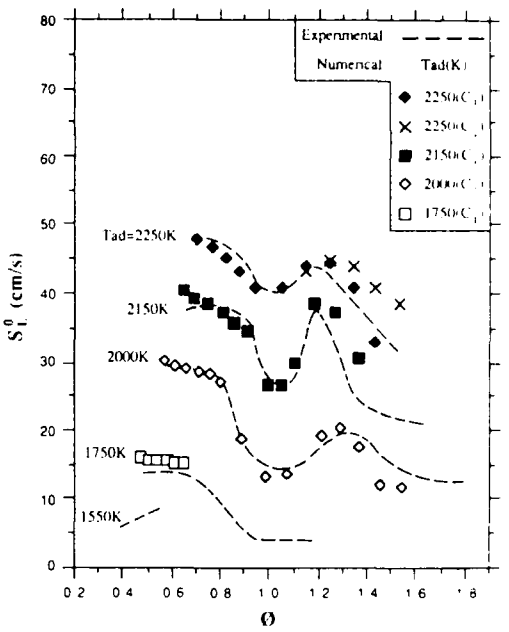

FIG. 9. Comparison between experimentally and numerically determined S_L^0 (ϕ) for various T_{ad} at 1 atm, using C_1 and C_2 kinetic schemes.

Discussions

In order to explain the present experimental and numerical results, which largely agree with each other and are therefore consistent, it is necessary to consider both transport effects due to inert substitution and kinetic effects due to changes in stoichiometry. Let us first discuss the non-monotonic behavior of, say, the 1 atm and $T_{ad} = 2{,}250$ K data of Fig. 6; $\rho_u S_L^0$ is adopted for discussion because it

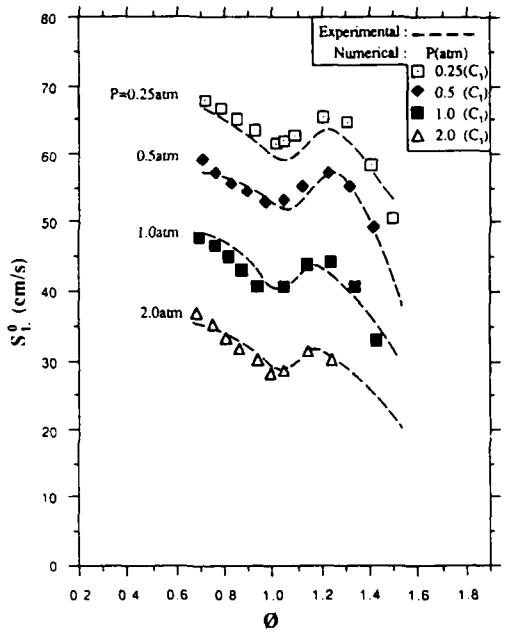

FIG. 10. Comparison between experimentally and numerically determined S_L^o (ϕ, p) for T_{ad} = 2,250 K, using the C_1 kinetic scheme.

is the actual eigenvalue of flame propagation. The results show that $\rho_u S_L^o$ increases in both the lean and rich directions from the stoichiometric regime. Since flame temperature is held constant on a given curve, and since $\rho_u S_L^o$ should decrease based on concentration effect alone, the observed increase is therefore due to the higher values of (λ/c_p) of the mixture with increasing concentration of Ar. The same explanation can be extended to CO_2-diluted flames.

The behavior of $\rho_u S_L^o$ with further departures from stoichiometry becomes quite asymmetrical in that it continues to increase for leaner mixtures but decreases for richer mixtures. The increase on the lean side is of course partly still due to transport effects. We have, however, found that kinetic effects could also be partly responsible in that among the three leading-order reactions

$$H + O_2 = OH + O \qquad (A)$$

$$H + O_2 + M = HO_2 + M \qquad (B)$$

$$CH_3 + H + M = CH_4 + M, \qquad (C)$$

the reaction rates of (A) and (B) are minimally affected with decreasing ϕ, while the recombination rate of reaction (C) is substantially reduced, by about 40%, from ϕ = 1.0 to 0.7. Thus the overall reaction rate is enhanced.

The decreasing trend for rich flames is kinetic in nature. For moderately rich flames ($1 < \phi \lesssim 1.3$) the forward reaction rates of (A) and (B) respectively decrease and increase with increasing ϕ. This eventually causes a significant decrease in $\rho_u S_L^o$ in spite of the positive influence of (λ/c_p). For very rich flames ($\phi \gtrsim 1.3$) the forward reaction rate of (A) increases again, although the forward reaction of

$$C_2H_5 + H = CH_3 + CH_3 \qquad (D)$$

also becomes important and tends to slow down (A) by competing for the H radicals.

Figure 6 also shows that the curves "flatten out" with decreasing pressure. This can be simply explained by considering the relations

$$\rho_u S_L^o \sim p^{n/2} f(\phi), \quad \frac{\partial(\rho_u S_L^o)}{\partial \phi} \sim p^{n/2} f'(\phi). \qquad (3)$$

Thus for a given ϕ and for the range of n encountered in the present study (Fig. 7), the slopes of the curves in Fig. 6 decrease with decreasing p.

It is also of interest to assess whether CO_2 can have any significant direct kinetic effect resulting from its substitution. A comparison between the CH_4/N_2-air flame and a $CH_4/O_2/N_2/CO_2$ flame with T_{ad} = 2,150 K, while keeping p = 1 atm and ϕ = 1 for both flames, shows that the sensitivity on S_L^o of all the crucial reactions is minimally affected and the maximum CO concentrations also remain almost the same. Thus CO_2 substitution does not directly contribute to kinetic effects.

In view of the higher flame speeds predicted by the C_2 mechanism for rich flames, a sensitivity analysis was conducted for the T_{ad} = 2,250 K and p = 1 atm flames at ϕ = 1.15 and 1.435. The results show that reactions of leading order importance are (A) and (C) as would be expected. For the reactions at the next order of importance, it is found that the sensitivity of reaction (D) increases by a factor of 3.2 from ϕ = 1.15 to ϕ = 1.435, while the sensitivities of all the other reactions are not affected much. By slightly modifying the kinetic constants of this reaction, the calculated flame speeds can be substantially lowered and improved agreement with the experimental data is achieved. However we have not attempted to calibrate these kinetic constants against our data. Rather we feel it is more appropriate for a study of the present nature to recommend that the rate constants of this elementary reaction may need to be either re-examined and/or re-determined through basic kinetics studies.

Concluding Remarks

There are two aspects of contributions from the present study. First, we have performed the tedious task of accurately determining the stretch-free, laminar flame speeds of methane/(Ar N_2, CO_2)-air mixtures over extensive parametric ranges of stoichiometry, pressure, and flame temperature. These data are expected to be useful for the partial validation of proposed kinetic mechanisms. Second, we have also performed detailed numerical calculations which partially validated a C_1 mechanism and a full C_2 mechanism for lean to moderately rich mixtures. The need for possible modification of the C_2 mechanism has also been identified. It is clear that such concrete conclusions cannot be made without an accurate experimental data set as a reference.

The present study also emphasizes that agreement in the flame speed is only a necessary but not sufficient criterion for the validation of a kinetic mechanism. For example, we have shown that calculated flame speeds using the C_1 and C_2 mechanisms both agree well with the experimental data even for moderately rich mixtures, while there exist ample kinetically-related experimental phenomena which can only be explained by including the C_2 reactions. Thus there exists an urgent need for accurate experimentally-determined temperature and concentration profiles of laminar flames which can be used for full validation. In conducting such experiments or validations, we again caution the need to either remove or account for the effects due to flame straining. These effects can be especially significant in the potential modification of the local concentrations of such highly mobile species as the important hydrogen radicals.

Acknowledgment

This research was supported by the Division of Basic Energy Sciences, Department of Energy under Grant No. DE-FG03-87ER13274 and the Air Force Office of Scientific Research under Grant No. 85-0147. Additional computer time was provided by the NSF Supercomputer Center at the University of California at San Diego. We thank Dr. David B. Smith of British Gas who suggested the potential usefulness of flame speed data determined as a function of flame temperature.

REFERENCES

1. Westbrook, C. K. and Dryer, F. L.: Eighteenth Symposium (International) on Combustion, p. 749, The Combustion Institute, 1981.
2. Warnatz, J.: Combustion Chemistry (W. C. Gardiner, Jr., Ed.), p. 197, Springer-Verlag, NY, 1984.
3. Dixon-Lewis, G.: Phil. Trans. Roy. Soc. Lond., A 292, 45, 1979.
4. Wu, C. K. and Law, C. K.: Twentieth Symposium (International) on Combustion, p. 1941, The Combustion Institute, 1985.
5. Yu, G., Law, C. K. and Wu, C. K.: Comb. Flame 63, 339 (1986).
6. Matalon, M. and Matkowsky, B. J.: J. Fluid Mech. 124, 239 (1982).
7. Law, C. K.: Dynamics of Stretched Flames, this Symposium.
8. Andrews, G. E. and Bradley, D.: Comb. Flame 18, 133 (1972).
9. Botha, J. P. and Spalding, D. B.: Proc. Roy. Soc. London 225A, 71 (1954).
10. Clingman, W. H., Brokaw, R. S. and Pease, R. N.: Fourth Symposium (International) on Combustion, p. 310, The Combustion Institute, 1953.
11. Kee, R. J., Miller, J. A. and Jefferson, T. H.: CHEMKIN: A General Purpose, Problem-Independent, Transportable, FORTRAN Chemical Kinetics Code Package, Sandia Report SAND80-8003, 1980.
12. Kee R. J., Warnatz, J. and Miller, J. A.: A FORTRAN Computer Package for the Evaluation of Gas-Phase Viscosities, Conductivities, and Diffusion Coefficients, Sandia Report SAND83-8209, 1983.
13. Kee R. J., Grcar, J. F., Smooke, M. D. and Miller, J. A.: A FORTRAN Program for Modeling Steady Laminar One-Dimensional Premixed Flames, Sandia Report SAND85-8240, 1985.
14. Grcar, J. F., Kee, R. J., Smooke, M. D. and Miller, J. A.: Twenty-First Symposium (International) on Combustion, p. 1773, The Combustion Institute, 1988.
15. Williams F. A.: Combustion Theory, Appendix D, Benjamin-Cummins, Palo Alto, 1985.
16. Egolfopoulos, F. N., Cho P. and Law, C. K.: Laminar Flame Speeds of Methane/Air Mixtures under Reduced and Elevated Pressures, submitted to Comb Flame.
17. Miller, J. A.: Personal communications.

COMMENTS

J. Warnatz, Physikalisch-Chemisches Institut, Fed. Rep. of Germany. I do not agree with your conclusion that the high flame velocities calculated on the rich side with the C_2-mechanism are due to deficiencies in the C_2 chemistry. To our present knowledge, the weakest point in these mechanisms is CH_3 oxidation though we do not know the reaction(s) responsible. Removal of this deficiency (hopefully in the near future) should lower both the results with C_1 and C_2 mechanism and low results for the C_1 mechanism.

Author's Reply. We appreciate very much your comment. We have adopted a neutral tone in replying because there just do not exist enough information for a definitive statement. We hope this reply is satisfactory to you. Let us know when you get additional insight/results regarding this issue.

Twenty-Second Symposium (International) on Combustion/The Combustion Institute, 1988/1381-1402

DYNAMICS OF STRETCHED FLAMES

C. K. LAW*
Department of Mechanical Engineering
University of California
Davis, California 95616

Recent advances in the understanding of the structure, propagation, and extinction of laminar flames under the influence of stretch, as manifested by the existence of flame curvature, flow nonuniformity, and flame motion, are reviewed. The emphasis is on premixed flames because of the richness and subtlety of the phenomena involved. The review distinguishes the influences of the tangential and normal velocity gradients on the flame response, both at the hydrodynamic scale and within the flame structure, and emphasizes the importance of the preferential diffusion nature of heat and mass transport, as well as the extent to which the flame can freely adjust its location in response to stretch in order to achieve complete reaction. It is then demonstrated that stretch has only minimal effect on an adiabatic, unrestrained, diffusionally-neutral flame with complete reaction in that the temperature, propagation rate, and thickness of the flame are invariant to stretch, and that stretch alone cannot extinguish such a flame. In the presence of preferential diffusion and/or when the flame movement is restrained, the response of the flame to stretch becomes more sensitive and extinction is also possible. The concept of flame stretch is applied to interpret such practical flame phenomena as flame stabilization and flame-front instability, determination of laminar flame speeds and flammability limits, concentration and temperature modifications in flame chemistry, and modeling of turbulent flames. The properties of stretched diffusion flames are then briefly discussed. The review closes with suggestions for further research.

Introduction

Historically, the concept of flame stretch was first introduced by Karlovitz[1] to describe flame extinction in velocity gradients. It was subsequently adopted by Lewis and von Elbe[2] to explain and quantify the various phenomena associated with flame stabilization. The flame curvature aspects of stretch also formed the basis for the study of flame-front instability by Markstein.[3] In the past fifteen years or so significant advances have been made in our understanding of flame stretch and its influence on the flame structure. These include a fundamental generalization of the definition of stretch, mathematically rigorous analyses of the structure and propagation of stretched flames, experimental and numerical verification and quantification of predicted properties via model flames, and re-interpretation of certain flame phenomena. Some recent reviews[4-11] have summarized the various aspects of these advances.

The objectives of the present review are to synthesize the current understanding of stretched flames from a unified viewpoint, and to identify areas for further research. In the next section the mathematical definition of stretch and its physical interpretation will be presented. We then study the influence of stretch on the flame structure through its coupled effect with heat and mass diffusion. Since the flame response turns out to depend critically on the unequal rates of heat and species diffusion, as signified by $Le_{ij} \neq 1$, the flame behavior without, and with, preferential diffusion are separately discussed. We then review the role of stretch in such practical flame problems as flame stabilization, flame speed determination, flammability limits, flame-front instability, concentration and temperature modifications as related to studies of chemical kinetics, and modeling of turbulent flames.

While much of the present review is on premixed flames because of the richness and subtlety of the response of a premixed flame to stretch, the properties of stretched diffusion flames are also

*Present address: Department of Mechanical and Aerospace Engineering, Princeton University, Princeton, NJ 08544.

briefly discussed and contrasted with those of premixed flames. The paper closes with suggestions for further research.

Definition of Stretch and Preliminary Considerations

Understanding of the structure and propagation of premixed flames, both at the fundamental level as well as for the analysis of practical combustion phenomena, is frequently based on the classical model involving the steady propagation of an adiabatic, one-dimensional, planar flame into a combustible medium of temperature T_u and reactant concentrations $Y_{i,u}$, as shown in Fig. 1a in the flame-stationary frame. This flame is characterized by its final, equilibrium temperature T_b^o, which is simply the adiabatic flame temperature T_{ad} of the mixture, and by its mass burning rate (per unit area) m^o, which is a function of the exothermicity, diffusivity, and reactivity of the mixture; the superscript "o" designates properties pertaining to this specific flame propagation mode. Thus if we symbolize the dependence on exothermicity by the specific heat release q, diffusivity by the Lewis number $Le_{ij} = \lambda/(c_p \rho D_{ij})$, and reactivity by the reaction rate w_k of reaction k, then

$$m'' = m''(q, Le_{ij}, w_k) \tag{1.1}$$

$$T_b^o = T_b^o(q). \tag{1.2}$$

Furthermore, if the characteristic chemical times of the major heat release reactions are much shorter than those of heat and mass diffusion, then the flame structure can be considered to consist of a thin reaction zone preceded by a broader transport-dominated, diffusive-convective zone, which are respectively characterized by thicknesses δ_R and δ_D satisfying $\delta_R << \delta_D$. From $m = \rho u$ we can then define an unburnt, upstream flame speed $S_u'' = m''/\rho_u$ at the upstream boundary of the transport zone, and a burnt, downstream flame speed $S_b'' = m^o/\rho_b^o$ for the entire reaction zone because velocity does not change much owing to the thinness of this zone.

The flame configuration of Fig. 1a is only an idealization. In realistic situations the upstream flow can be nonuniform while the flame can also be curved and nonstationary (Fig. 1b), producing what are collectively known as stretch effects. Furthermore, the flame can also be globally nonadiabatic through exchanges in heat and radicals with the surrounding. Thus if we symbolize influences of stretch by a Karlovitz number Ka, to be defined later, and system nonadiabaticity by a "loss" parameter L, then the flame behavior is expected to be described by

$$m = m(q, Le_{ij}, w_k, Ka, L) \tag{1.3}$$

$$T_b = T_b(q, Le_{ij}, w_k, Ka, L) \tag{1.4}$$

which should deviate from m'' and T_b^o of the idealized situation. It may be noted that although in (1.3) and (1.4) we have purposely separated out the functional dependence into the two groups of parameters (q, Le_{ij}, w_k) and (Ka, L), strong coupling between the individual effects is expected. For example, while T_b^o depends only on q, the presence of stretch and/or loss mechanism can cause T_b to

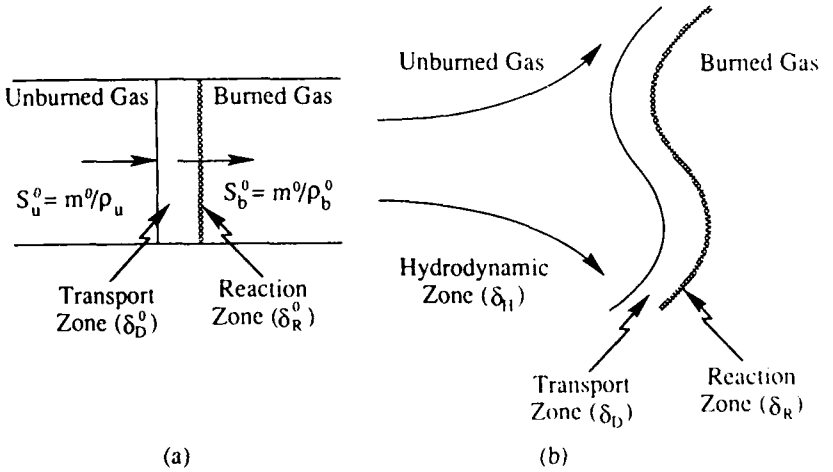

FIG. 1. Schematics of the structure of (a) a one-dimensional planar flame, and (b) a wrinkled flame in a nonuniform flow.

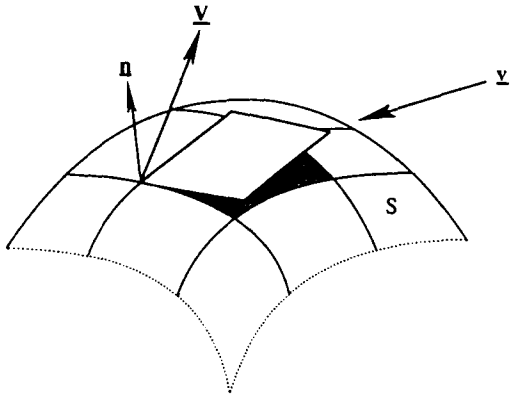

FIG. 2. Schematic of surface element s with velocity $\mathbf{V}$ and unit normal vector $\mathbf{n}$ in a flow field $\mathbf{v}$.

also depend on the diffusive and reactive aspects of the problem. We also note that the presence of flow nonuniformity and flame curvature introduces an additional, hydrodynamic, length scale, δ_H, into the problem.

To define stretch, we first identify an arbitrary surface s, say an isotherm, within the flame structure (Fig. 2). This surface has a velocity $\mathbf{V}$ while the fluid has a velocity $\mathbf{v}$. A general definition[8,10,12-14] of stretch at any point on this surface is the time derivative of the logarithm of the area of an infinitesimal element of the surface,

$$K = \frac{1}{A}\frac{dA}{dt}, \tag{2.1}$$

with the boundary of this surface element moving tangentially to the surface at the local tangential component of the fluid velocity. In terms of the flow variables, it can be shown[13,15,16] that

$$K = \{\nabla_t \cdot \mathbf{v}_t + (\mathbf{V}\cdot\mathbf{n})(\nabla\cdot\mathbf{n})\}_s, \tag{2.2}$$

where ∇_t and $\mathbf{v}_t$ are the tangential components of ∇ and $\mathbf{v}$ evaluated at the surface, and $\mathbf{n}$ is the unit normal vector of the surface, pointed in the direction of the unburnt gas. The stretch rate K has the unit of $\sec^{-1}$.

Equation (2.2) shows the two sources of stretch a flame can be subjected to. The first term represents the influence of flow nonuniformity *along* the flame surface. Since[16]

$$\{\nabla_t \cdot \mathbf{v}_t\}_s = \{-\mathbf{n}\cdot\nabla\times(\mathbf{v}\times\mathbf{n})\}_s, \tag{2.3}$$

this term embodies the effects due to flow nonuniformity through $\mathbf{v}$ and flame curvature through $\nabla\cdot\mathbf{n}$. Furthermore, this term exists only if the flow is oblique to the surface ($\mathbf{v}\times\mathbf{n}\neq 0$). The second term in Eq. (2.2) represents stretch experienced by a nonstationary flame through $\mathbf{V}$, although the flame also has to be curved because $(\nabla\cdot\mathbf{n})$ vanishes otherwise. These three stretch-induced effects can be separately referred to as those due to aerodynamic straining, flame curvature, and flame motion. We further note that since (heat and mass) diffusion is parallel to $\mathbf{n}$, the non-orthogonality requirement of $(\mathbf{v}\times\mathbf{n})$ leads us to anticipate the importance of diffusive transport in the dynamics of stretched flames, even though the discussion so far has been kinematic in nature.

As examples, let us compute the stretch rate K for the three common flame configurations[15] shown in Fig. 3. The flames are assumed to be infinitely thin for simplicity, thus the stretched surface is the flame. Figure 3a shows a planar flame situated in a divergent stagnation flow. Assuming potential flow, the velocity vector is $\mathbf{v} = \{[a/(\sigma+1)]x, -ay, 0\}$,

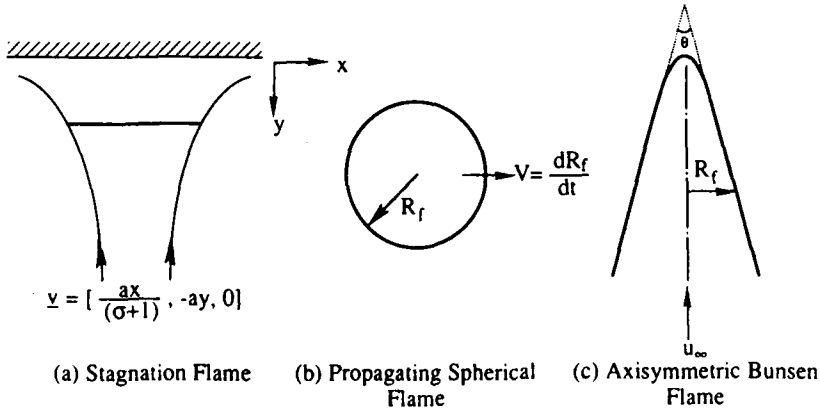

(a) Stagnation Flame (b) Propagating Spherical Flame (c) Axisymmetric Bunsen Flame

FIG. 3. Examples of stretched flames: (a) Stagnation flame, (b) outwardly propagating spherical flame, and (c) axisymmetric Bunsen flame.

where a is the strain rate of the flow, $\sigma = 0,1$ for cartesian and cylindrical coordinates respectively, and the x- and y-velocities in the cylindrical coordinate are those in the radial and axial directions respectively. Since $V = 0$, Eq. (2.2) readily yields

$$K = a. \tag{2.4}$$

Similarly it can be shown that for an outwardly propagating spherical flame (Fig. 3b),

$$K = \frac{2}{R_f}\frac{dR_f}{dt}, \tag{2.5}$$

where R_f is the instantaneous flame radius, while for the conical surface of an axisymmetric Bunsen flame (Fig. 3c),

$$K = -\frac{u_\infty \sin\theta}{2R_f}, \tag{2.6}$$

where u_∞ is the uniform upstream velocity, θ the apex angle, and R_f the flame radius at a given axial cross section. Note that $K > 0$ for the positively-stretched forward stagnation flame and outwardly-propagating spherical flame, while $K < 0$ for the negatively-stretched, or compressed, Bunsen flame. The signs of Figs. 3a, b and c are also reversed for the corresponding flame configurations of the rearward stagnation flame, the inwardly-propagating flame, and the inverted flame if only the effect of flame structure is considered. We shall demonstrate subsequently that the flame response can be qualitatively reversed for positive and negative values of K.

Recently the flame behavior in rotating flow fields has also been studied by using a rotating stagnation flow system[17-20] and via tubular flames.[21-25] Stretch rates experienced by these flames can be individually calculated.

There are also stretchless flames. Examples are the steady and unsteady one-dimensional planar flame, and the stationary cylindrical and spherical flames sustained by line and point sources respectively.

The stretch rate K can be nondimensionalized by the characteristic flow time within the flame,

$$Ka = \left(\frac{\delta_D^o}{S_u^o}\right)K = \left[\frac{D_u}{(S_u^o)^2}\right]K, \tag{2.7}$$

which is the Karlovitz number mentioned earlier. The significance of the functional form of Ka will be discussed in relation to Eq. (4.4). We further note that since stretch is associated with a given surface, for a flame of finite thickness we can define an upstream and a downstream stretch rate, K_u and K_b, for the unburnt and burnt states of the mixture respectively. From the viewpoint of asymptotic analysis with one-step reactions, K_b is a more natural representation of the stretch rate because the reaction zone is thin and is therefore indicative of a well-defined "surface." In realistic situations, however, the multi-step nature of the chemical reaction schemes, and the possibility that complete reaction may not be achievable, render this reaction surface less sharply defined. On the other hand, both numerical and experimental results have shown that K_u, which is not directly affected by diffusion and reaction, can be easily identified. Furthermore, K_u can also be considered as an imposed parameter while K_b is strongly influenced by the flame response. Thus we shall adopt K_u in subsequent discussions.

The influence of stretch on the flame response can be discussed based on the scales as well as the tangential and normal components of the flow field at the flame. Let us first consider stretch at the hydrodynamic scale (Fig. 1b). Here diffusion is not important and the entire flame can be considered to collapse into a flame sheet. Thus the burning intensity of the flame, such as its temperature T_f and burning rate m_u, are not affected by stretch. The presence of stretch, through the *tangential velocity gradient* at the flame and quantified by the Karlovitz number Ka, changes the flame surface area A and consequently the *volumetric* burning rate $m_u A$. Thus positive stretch increases the volumetric burning rate while negative stretch decreases it. We shall refer to this stretch as hydrodynamic stretch. The role of the *normal velocity gradient* is to allow adjustment of the flame location in the normal direction so that the flame situates where the local flame speed balances the local normal velocity, that is $S_u = -v_u$. Thus the combined effects of the tangential and normal velocity gradients are the displacement of the flame surface, distortion of its topography, and modification of the volumetric burning rate.

In the transport zone the *tangential velocity gradient* directly affect the normal mass flux m_f entering the reaction zone. Furthermore, through interaction with heat and mass diffusion, it can also modify the temperature and concentration profiles in this zone and consequently the burning intensity, T_f and m_f, in the reaction zone. We shall refer to this stretch as flame stretch. The *normal velocity gradient* in this zone affects the residence time within the reaction zone and consequently T_f and the completeness of reaction. A measure of this influence is the Damköhler number Da, defined as the ratio of the characteristic flow time to the characteristic reaction time.

Finally, because of the secondary importance of convective transport in the reaction zone, stretch has little influence here except for highly stretched situations.

It is important to emphasize the different roles played by the tangential and normal velocity components in affecting the flame response. Since these two components are coupled through continuity, diffusional interaction, and thermal expansion, there has been some confusion in the literature in distinguishing effects caused by stretch from those caused by residence time, or Damköhler number, considerations.

We also note that hydrodynamic stretch and flame stretch can be strongly coupled in that the hydrodynamic stretch imposes the stretch intensity at the flame needed for flame stretch calculations, while the flame stretch not only yields the burning rate at the flame surface needed for the calculation of the hydrodynamic flow field, but it also predicts such critical phenomena as flame extinction.

The final point to emphasize is the flexibility with which a premixed flame can adjust its location to accommodate changes in the normal velocity gradient. Thus a change in the stretch rate does not necessarily lead to a change of corresponding extent in the residence time. We shall call a flame with total freedom of adjustment an unrestrained flame.

The influence of hydrodynamic stretch is quite straightforward and will not be further discussed. The influence of flame stretch will be studied in the next two sections.

Flame Stretch in Diffusionally-Neutral Mixtures

Adiabatic Unrestrained Flames:

This is perhaps the simplest situation involving stretched flames, with $L = 0$, $Le_{ij} = 1$. The flame is also assumed to be able to freely adjust its position in response to changes in stretch such that complete reaction can be achieved. Simple as it may be, considerable disagreement exists in the interpretation of its basic phenomena. For example Karlovitz[1] and Lewis and von Elbe[2] argued that, with increasing flow divergence, the gradients of temperature and concentration become flatter such that extinction eventually occurs as a result of the continuous reduction in the temperature of the reaction zone. On the other hand, Klimov[26] and then Williams[8] suggested that (positive) stretch tends to thin the flame sheet convectively and to steepen the temperature and concentration gradients within it. Conflicting statements abound in the literature.

To demonstrate the influence of stretch, let us first consider the response of a planar adiabatic flame to aerodynamic stretching (Fig. 4a). A simple phenomenological analysis[27,28] for the control volume bounded by the streamlines and the boundaries of the flame yields relations for the overall mass conservation, overall energy conservation, mass balance at the reaction zone and energy balance at the reaction zone, which are respectively given by

$$m_u A_u = m_b A_b \tag{3.1}$$

$$m_u A_u c_p (T_b - T_u) + \lambda \frac{(T_b - T_u)}{\delta_D} (A_b - A_u) = Y_R k_b \delta_R q A_b \tag{3.2}$$

$$(\rho D)\left(\frac{Y_u}{\delta_D}\right) = Y_R k_b \delta_R \tag{3.3}$$

$$\lambda \frac{(T_b - T_u)}{\delta_D} = Y_R k_b \delta_R q \tag{3.4}$$

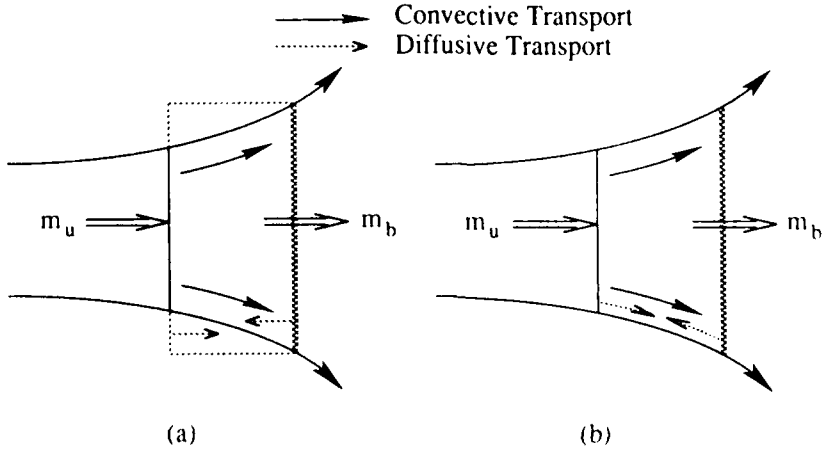

FIG. 4. Phenomenology of an aerodynamically-stretched planar flame: (a) Correct representation allowing for the orthogonality of the diffusive flux, (b) incorrect representation suppressing the effect of stretch.

where c_p, λ and (ρD) are assumed to be constants, $k_b = B \exp(-T_a/T_b)$ is the reaction rate constant evaluated at the reaction zone, and Y_R is a characteristic reactant concentration within the reaction zone.

Approximating $Y_R = \epsilon Y_u$ and $\delta_R = \epsilon \delta_D$, where $\epsilon = T_b/T_a$, Eqs. (3.1) to (3.4) constitute four algebraic relations from which we can solve for the four flame properties, namely the flame temperature T_b, the upstream burning rate m_u, the downstream burning rate m_b, and the flame thickness δ_D:

$$T_b = T_u + (Y_u q/c_p) = T_b^o = T_{ad} \tag{3.5}$$

$$m_u = \epsilon^o(\lambda/c_p)^{1/2}(k_b^o)^{1/2} = m_u^o \tag{3.6}$$

$$m_b = m_u^o(A_u/A_b) = m_b^o(A_u/A_b) \tag{3.7}$$

$$\delta_D = (\lambda/c_p)/m_u^o = \delta_D^o. \tag{3.8}$$

Equations (3.5) to (3.8) show the interesting results that the important parameters T_b, m_u and δ_D of this adiabatic, diffusionally-neutral, unrestrained flame are not affected by stretch and therefore assume the corresponding values of the one-dimensional unstretched flame. The downstream burning rate m_b is modified from the unstretched value m_b^o by the area ratio (A_u/A_b), which can be considered as a measure of the extent of stretch due to effects of both flow divergence and thermal expansion. It is also clear that, because of the invariance of the flame temperature, extinction cannot be achieved for this flame. For a curved flame the above results remain the same except m_u is modified according to Eq. (4.2).

There appear to be different causes leading to the various earlier interpretations of the effect of stretch. For example, the argument in favor of reduced flame temperature discusses only the negative effect of stretch on flame temperature due to the diffusive transport of heat and radicals away from the reaction zone, but it fails to consider the positive effect of reactant diffusion into the reaction zone. The argument based on reduced flame thickness does not account for the fact that the flame, being unrestrained, can move freely in response to changes in stretch. There are also interpretations based on some nondimensional and/or transformed coordinates which however depend on the stretch rate.

Asymptotic analyses[4,8,9] have confirmed that T_b is invariant to stretch while m_b is reduced from the unstretched value m_b^o by a fractional amount Ka. However, the discussions of Refs. 29 and 30 on the reduction of the total extent of reaction across the flame per unit surface area, and on the extinction behavior of such a flame, have overlooked the facts that flow divergence is actually the major cause of this reduction, and that extinction is brought about with only a small amount of incomplete reaction.[31]

To further substantiate the insensitivity of flame thickness to stretch, the temperature profile across an almost adiabatic, diffusionally-neutral, ethane/air flame in a symmetrical counterflow has been experimentally measured.[31] In Fig. 5 these temperature profiles are superimposed by shifting their spatial locations such that the upstream boundaries

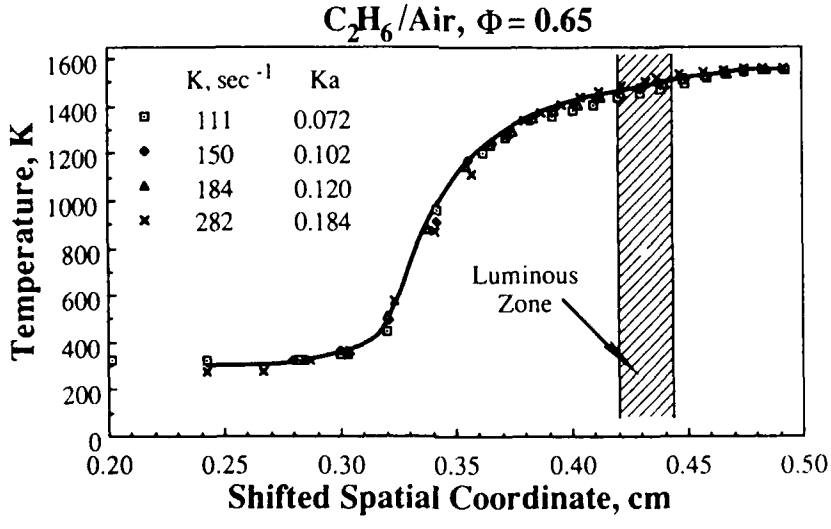

FIG. 5. Experimental temperature profiles of ethane/air flames, with coordinate shifted to demonstrate the minimal influence of stretch on the flame properties, especially the flame thickness, for adiabatic, unrestrained, diffusionally-neutral flames.[31]

of the luminous zones coincide. It is seen that these temperature profiles, and thereby the flame temperatures and thicknesses, are basically unaffected by stretch. The thicknesses of the luminous zones are also not affected. It is significant to note that at the state of extinction, caused by incomplete reaction to be discussed next, the stretch rate for this mixture has been determined to be about 320 s^{-1}. Thus the flame temperature profile remains insensitive to stretch up to stretch rates sufficiently close to that of extinction. This experimental result has also been corroborated by numerical solutions.[31]

Using $D_u = 0.2$ cm^2/s as given in Ref. 32, and $S_u^o = 17.5$ cm/s determined in the manner of Fig. 16 which will be discussed later, the Karlovitz number Ka for the situations of Fig. 5 can also be estimated. It is seen that these values are all sufficiently smaller than unity, specifically, the extinction value is only $Ka_{ex} = 0.2$.

We mention in passing that in writing the overall energy balance of Eq. (3.2), it is essential that the diffusive flux is normal to the reaction zone as shown in Fig. 4a. If the diffusive flux is forced to lie along the streamlines (Fig. 4b), then the diffusion term in Eq. (3.2) is suppressed, resulting in

$$m_u = m_u^o(A_b/A_u),\ m_b = m_b^o, \qquad (3.9)$$

which are completely contrary to Eqs. (3.6) and (3.7), and are incorrect. Thus it is necessary to preserve the orthogonality relation between the flame surface and the diffusive fluxes when performing "quasi-one-dimensional" analysis. In fact, the planar flames in the divergent flow fields of Refs. 33 and 34 are stretchless, according to the definition of K in Eq. (2.2), because diffusive transport has been assumed to occur along the streamlines ($\mathbf{v} \times \mathbf{n} = 0$).

Adiabatic Restrained Flames:

We next consider situations under which the free movement of a flame in response to stretch is restrained, as typified by the strongly-stretched stagnation flame.[29,30] The flame is now situated close to the stagnation surface and thereby loses its flexibility to move freely. If the stagnation surface is adiabatic and effectively impenetrable to net mass transfer, then with further increase in stretch the residence time decreases, the flame becomes thinner, complete reaction cannot be achieved, and extinction eventually occurs. Extinction in this case is caused by stretch-induced incomplete reaction, not by stretch alone. The Damköhler number now exerts a much stronger role in the flame behavior, especially the state of extinction.

If the stagnation surface is penetrable, as in the case of impinging the combustible mixture against a hot product gas stream, then the reaction zone can actually migrate across the stagnation surface and thereby assume a negative flame speed.[26,29] The fuel consumption and heat release rates are of course still positive. Combustion in this situation is supported by diffusion of the reactants against the unfavorable convection. The existence of negative flame speeds has been experimentally verified[35] for superadiabatic flames whose downstream temperature is higher than the adiabatic flame temperature. Adiabatic negative flame speeds have not been observed.

Another example of a restrained flame is the tip segment of a Bunsen flame because the orientation of the shoulder segment is somewhat fixed for a given mixture flow, and because the upstream flame speed at the tip is also fixed at the value of the local flow velocity. Thus the flame speed here is a given parameter instead of a flame response to be solved. Indeed, the exceptionally large value of the "flame speed" at the flame tip[2] has long been an anomaly in combustion science. Some preliminary theoretical and experimental investigations[36,37] have been conducted, although the detailed structure of this restrained, highly-curved flame segment requires further study.

Nonadiabatic Flames:

The effects of heat loss are quite obvious: it slows down the burning rate and can eventually cause extinction. Aerodynamic stretching changes the proximity of a flame to the heat sink while flame curvature also changes the intensity of the heat flux over the flame surface. Thus the influence of stretch and heat loss are intimately coupled. Libby and Williams[39,40] have performed detailed analysis of nonadiabatic counterflow flames. Experimentally, Law et al.[41] have found that downstream heat loss does not strongly affect the flame behavior as long as the flame is not too close to the cold stagnation surface.

Flame Stretch in Diffusionally-Imbalanced Mixtures

Phenomenology:

While pure stretch basically has minimal effect on the propagation of an adiabatic, diffusionally-neutral, unrestrained flame, the flame response can be significantly modified in the presence of preferential diffusion. To demonstrate this influence we first note that there are at least three diffusivities of interest for an inert-abundant mixture, namely those associated with heat (D_T), the deficient reactant (D_i), and the excess reactant (D_j). From these three diffusivities two interpretations for the effects of preferential diffusion have been developed, comparing D_i with D_T, and D_i with D_j, for sufficiently

off- and near-stoichiometric situations respectively. These two interpretations can be respectively termed non-unity Lewis number ($Le = D_T/D_i$) effect and differential diffusion (D_i/D_j) effect.

We again take the stagnation flow as an example (Fig. 6a), and draw a control volume enclosing the transport zone and the divergent streamline as shown. Then with the Lewis number interpretation,[42,43] it is clear that the control volume loses thermal energy to the external streamlines while it gains chemical energy from them due to an increase of the deficient reactant concentration. Thus the flame behavior, especially the flame temperature, depends on the relative rates of heat and mass diffusion. If the diffusivities are equal such that $Le_i = 1$, then total energy conservation is maintained and the flame temperature is the adiabatic flame temperature. This is the case studied in the previous section. However, if $Le > 1$, heat loss exceeds mass gain and we expect $T_b < T_{ad}$. Conversely $T_b > T_{ad}$ if $Le < 1$.

We next take the differential diffusion interpretation. Then if the leaner reactant is also the more diffusive one, the reactant concentration in the reaction zone will become more stoichiometric such that the flame temperature is higher and the burning more intense. The converse holds if the leaner reactant is less diffusive. In the following we shall adopt the Lewis number interpretation because off-stoichiometric burning is more prevalent and because heat diffusion is a crucial mechanism in flame propagation. Experimental results[44] also indicate that the Lewis number interpretation seems to have a wider range of applicability.

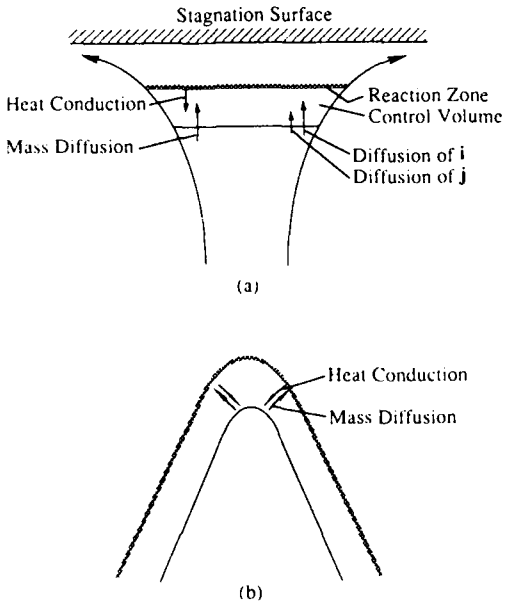

FIG. 6. Schematics of (a) the stagnation flow, and (b) the Bunsen flame, illustrating the coupled influence of flame stretch and preferential diffusion on the flame response.

If we now attempt to extinguish this stagnation flame by increasing the stretch rate, the flame will be pushed closer to the stagnation surface. At the same time it will suffer stronger flame stretch and thereby preferential diffusion effects. Thus it is clear that for $Le > 1$, there exists a critical stretch rate at which T_b will be reduced to such an extent that steady burning is not possible. Extinction occurs when the flame is at a finite distance away from the surface, with the lean reactant almost completely depleted in crossing the flame. On the other hand, for a $Le < 1$ flame, increasing stretch elevates T_b and therefore extinction cannot occur until the downstream boundary of the reaction zone is pushed onto the stagnation surface. With further stretching, reaction cannot be completed because of the reduced residence time. Only then will the flame temperature start to decrease, leading eventually to extinction. Thus the extinction mechanism is similar to that of the $Le = 1$ case studied previously, except the extinction stretch rate with $Le < 1$ is higher in order to compensate for the higher flame temperature initially attained.

The second situation illustrating flame stretch effects involves the burning intensity over the curved surface of an axisymmetric Bunsen cone (Fig. 6b). Here if we assume for simplicity that the flow is uniform, then flame stretch is mainly manifested through curvature effects, especially in the tip region which has the strongest curvature. Thus for a closed tip, its concave nature towards the fresh mixture focuses the heat ahead of the flame, and therefore tends to raise the flame temperature to a value above T_{ad}. On the other hand, this curvature has a defocusing effect on the reactants approaching the flame, and therefore tends to reduce the flame temperature. Thus the temperature of the flame again depends on the relative rates of heat and mass diffusion. The deviation increases progressively from the flame base towards the flame tip because of the corresponding increase in the stretch intensity. Thus for $Le > 1$, the tip will burn more intensely relative to the shoulder region of the flame, while for $Le < 1$ the burning is less intense and can lead to local extinction, commonly known as opening, of the tip. Note that because of the compressive nature of the Bunsen flame, its behavior in response to Lewis number variations is completely opposite to that of the positively-stretched stagnation flame.

Energy Conservation:

The above result that the temperature of the burnt gas of a diffusionally-imbalanced stretched flame can deviate from the adiabatic flame temperature of its

unburnt mixture appears to violate the principle of energy conservation. To explore this point, Figs. 7a and 7b show the profiles of the stoichiometrically-weighted temperature $\tilde{T}$, mass fraction $\tilde{Y}$, and the total energy as represented by the coupling function $\beta = \tilde{T} + \tilde{Y}$, for the case of Le < 1 for which $\tilde{T}_b > \tilde{T}_{ad}$ where $\tilde{T}_{ad} = \tilde{T}_{-\infty} + \tilde{Y}_{-\infty}$. It is clear that in a steady-state situation, as for the stagnation and Bunsen flames, energy is not conserved as the fresh mixture traverses the flame. This is a local phenomenon because only diffusion normal to the flame has been considered. It is reasonable to expect that global energy conservation can again be established by considering diffusion of the excess/deficit heat or mass in the tangential direction along the flame within the transport zone of the entire flame surface.

The consideration is somewhat different for the expanding spherical flame because the entire flame surface is already accounted for. The profiles of Fig. 7 are now instantaneous values. Energy in this case is conserved in that the increase in energy of the burnt gas over $\tilde{T}_{ad}$ is achieved by drawing excess energy in terms of the reactant concentration from the upstream mixture. As the flame expands the amount of excess energy associated with the burnt gas increases because of the increase in volume. However, at the same time the amount of energy deficit in the transport zone also increases because of the corresponding increase in the volume of the transport zone. Thus at any instant the increase in excess energy in the burnt zone is achieved at the expense of the corresponding decrease in energy in the transport zones. Consequently the amount of excess and deficit energies exactly balance.

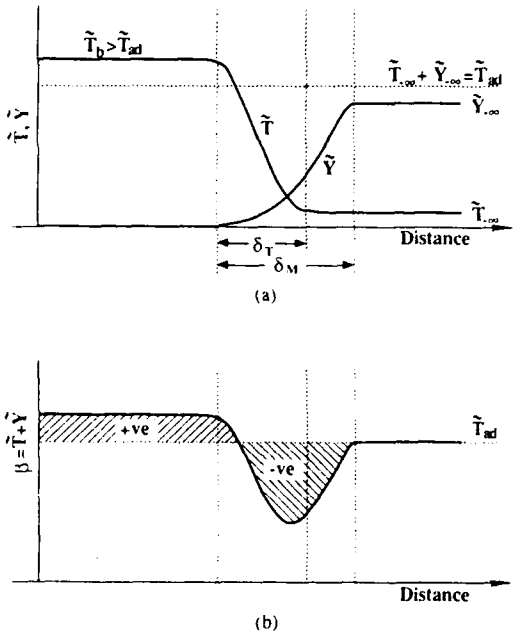

FIG. 7. Schematics of (a) the temperature and concentration profiles, and (b) total energy profile for a Le < 1 positively stretched flame, illustrating the discussions on energy conservation.

Theoretical Results:

Most analytical studies on stretched flames are based on large activation energy asymptotics. These studies can be grouped into three categories, namely (a) multi-scale analyses of a general wrinkled flame in a nonuniform flow,[45-47] (b) detailed analyses of a specific flame configuration such as the stagnation flame,[40-42,43,48-58] the Bunsen flame,[36-42,59-62] the spherical flame,[63-68] or the tubular flame,[20-25] and (c) analyses involving flame/flow situations characterized by some prescribed mathematical forms of stretch.[69-72] The first category, while general in the physical situations, yields only linearized results for weak stretch. The second category, while being specific in the physical configuration, does predict nonlinear phenomena such as extinction. The third category can also be very useful in identifying some specific features of stretched flames. Recently the method of integral analysis has also been applied,[27,28] yielding characteristics of the bulk flame parameters which appear to be both general and capable of exhibiting the nonlinear effects of strong stretch and flame extinction.

The linearized solution of Ref. 27 yields the following explicit expressions of the various flame responses for a wrinkled flame in a nonuniform flow field:

$$\frac{T_b}{T_b^o} = \frac{T_b}{T_{ad}} = 1 + \left(\frac{1}{Le} - 1\right)Ka \qquad (4.1)$$

$$\left(\frac{m_u}{m_u^o}\right) = \frac{S_u}{S_u^o} = 1 - \delta_T^o \nabla \cdot \mathbf{n} + \left(\frac{1}{Le} - 1\right)\frac{Ka}{(2T_{ad}/T_u)} \qquad (4.2)$$

$$\frac{m_b}{m_b^o} = \frac{S_b}{S_b^o} = 1 - \frac{Ka}{Le} + \left(\frac{1}{Le} - 1\right)\frac{Ka}{(2T_{ad}/T_u)} \qquad (4.3)$$

where

$$Ka = \left(\frac{\delta_T^o}{S_u^o}\right)K = \left\{\frac{D_{T,u}^o}{(S_u^o)^2}\right\}K = \left\{\frac{D_{M,u}^o}{[S_u^o(Le = 1)]^2}\right\}K \qquad (4.4)$$

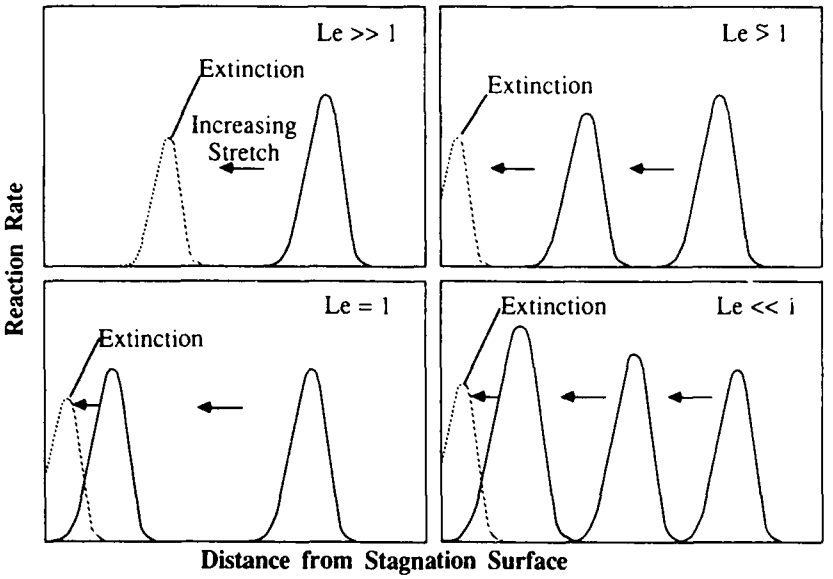

FIG. 8. Schematic showing the response of the reaction rate to increasing stretch in a stagnation flow, for various Lewis numbers.[73]

$$\delta_T^o = \left(\frac{D_{T,u}^o}{S_u^o}\right) = \left\{\frac{(D_{T,u}^o D_{M,u}^o)^{1/2}}{S_u^o(\mathrm{Le}=1)}\right\} = \frac{D_u^o}{S_u^o(\mathrm{Le}=1)} \quad (4.5)$$

and we have used the relation $S_u^o(\mathrm{Le}) = \sqrt{\mathrm{Le}}S_u^o(1)$.

The above results show that the flame temperature can deviate from the adiabatic flame temperature only in the simultaneous presence of stretch (Ka $\neq$ 0) and preferential diffusion (Le $\neq$ 1). The modification in the downstream velocity results from flow divergence and changes in the flame temperature and thereby burning intensity in the presence of preferential diffusion, as given by the second and third terms of Eq. (4.3). The modification in the upstream velocity results from the flame curvature and the preferential diffusion effects. These results essentially degenerate to Eqs. (3.5) to (3.7) for a planar, Le = 1 flame.

Equation (4.4) shows that the effect of stretch as represented by Ka can be increased by increasing the stretch rate or mixture diffusivity, or by decreasing the flame speed. We also note that because the laminar flame speed S_b^o increases with increasing Lewis number, the dependence of S_b on the mixture diffusivity can be actually non-monotonic. It further implies that the preheat zone thickness δ_T^o depends on the geometric average of the thermal and mass diffusivities, from which a weighted diffusivity D_u^o can be defined, as in Eq. (4.5).

A generalized nonlinear theory of wrinkled flames based on differential analysis has not been formulated, although an integral theory has been advanced.[28] The salient features of the flame response, however, can best be illustrated by the numerical solution of the simple adiabatic stagnation flame.[73,74] Figure 8 shows the qualitative behavior of the reaction rate profiles with increasing stretch for various Lewis numbers.[73] For Le >> 1, increasing stretch decreases the maximum reaction rate and extinction occurs when the reaction zone is away from the stagnation surface and reaction is complete. For Le $\gtrsim$ 1, reaction rate still decreases with stretch except now extinction occurs with the reaction zone pressed against the surface and reaction is not complete. For Le = 1, the reaction rate remains unchanged until the reaction zone reaches the surface. Finally, for Le < 1, the reaction rate continuously increases with stretch until the reaction zone reaches the surface, then it decreases. Thus except for the case of Le >> 1, incomplete reaction is essential in causing flame extinction.

Figure 9 shows variation of the maximum flame temperature with stretch for different Le. The behavior basically corroborates that of the reaction rate profiles.

The influence of reaction intermediates on the response of stretched flames has not been adequately studied.[75-79] Numerical solutions of the

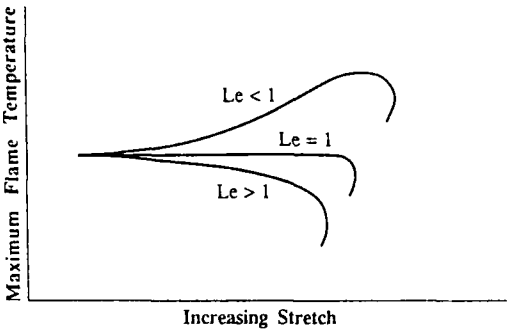

FIG. 9. Schematic of the variation of the maximum flame temperature in response to increasing stretch, for various Lewis numbers.

stagnation flame with complex chemistry[75-77] have shown that the behavior of the bulk flame parameters are in qualitative agreement with interpretations based on a single reactant, without considering the possible preferential diffusion nature of the combustion intermediates. Reference 76, however, has noted the role of incomplete reaction of the H radical in flame extinction, while the asymptotic results[78] obtained with a two-step branching-termination chain reaction model have shown that depending on the parameter range the mass burning rate can be either increased or decreased.

Experimental Results:

The above discussions show that the response of a stretched flame exhibits opposite behavior when the stretch changes from positive to negative, and when the mixture's effective Lewis number is greater or less than a critical value, which is unity for the flame temperature. These completely opposite trends should provide definitive verification of the concept of flame stretch with preferential diffusion.

Two groups of mixtures are especially suitable for the study of preferential diffusion effects. The first group consists of lean methane/air and rich propane/air mixtures. Rough estimates[32] show that their effective Lewis numbers, based on the deficient species, are less than unity. Thus positive (negative) stretch is expected to increase (decrease) the flame intensity of such mixtures. This argument still holds even if we just consider the relative mass diffusivities of the fuel and oxidizer species. That is, based on molecular weight considerations, we expect the diffusivities of the various reactants relative to nitrogen should increase in the order of propane, oxygen, and methane. Thus positive (negative) stretch will increase (decrease) the methane concentration of a lean methane/air mixture but decrease (increase) the propane concentration of a rich propane/air mixture at the flame. Both mixtures are consequently rendered more (less) stoichiometric at the flame, leading to enhanced (reduced) burning intensity.

The second group consists of rich methane/air and lean propane/air mixtures, whose effective Lewis numbers are greater than unity while positive (negative) stretch also renders the mixture less (more) stoichiometric. Thus the responses of these two groups of mixtures to stretch are expected to be qualitatively opposite.

Three series of experiments have been conducted using these mixtures in flame configurations exhibiting positive and negative stretches. For positive stretch, extensive experiments have been performed by using the symmetrical counterflow system.[32,80-83] This system has the advantage over the one created by impinging a single stream onto a solid surface in that, because of symmetry, the stagnation surface in a counterflow is close to being adiabatic.

Although theoretical results show that both the flame temperature and flame speed exhibit flame stretch and non-unity Lewis number effects, experimental determination of the flame temperature is more definitive as compared with that for the flame speed, whose value depends on where it is evaluated. Thus in Fig. 10 we show the measured flame temperature T_f and the distance of the center of the luminous zone y_f from the stagnation surface with varying stretch rate. If we exclude the small regimes near extinction, the results agree with previous discussions in that with increasing stretch the flame temperature increases for a lean methane/air flame and a rich propane/air flame, decreases for a lean propane/air flame, and slightly decreses for a rich methane/air flame. Furthermore, the flame extinguishes when it is away from the stagnation surface for rich methane/air and lean propane/air flames, and at the stagnation surface for lean methane/air and rich propane/air flames.

Next we examine the flame temperature response to negative stretch, provided by the increasing curvature along the surface of an axisymmetric Bunsen cone.[44,84,85] The behavior should be completely opposite to that of the counterflow flame. Figure 11 shows the measured maximum flame temperature T_f along the flame surface. Excluding the segment near the flame base where burning is weak due to heat loss to the burner rim, it is seen that as the intensity of negative stretch increases by moving along the flame towards its tip, the flame temperature increases for the rich methane/air and lean propane/air flames, but decreases for the lean methane/air and rich propane/air flames. The neutral compositions are approximately $\phi = 1.00$ and 0.94 for methane/air and propane/air flames respectively. Figure 11 further shows that ethylene, whose molecular weight is intermediate between those of methane and propane, shows almost neu-

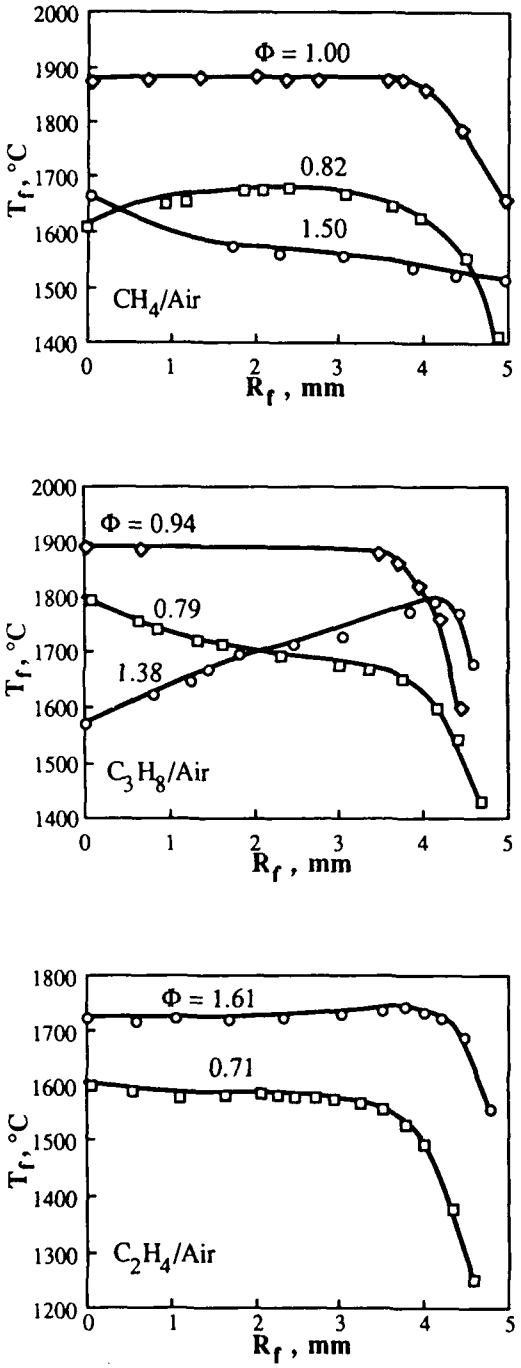

FIG. 11. Experimental results showing the qualitatively different behavior for the flame temperature of negatively-stretched axisymmetric Bunsen flame for mixtures exhibiting (CH_4/Air, C_3H_8/Air) and not exhibiting (C_2H_4/Air) preferential diffusion effects.[84]

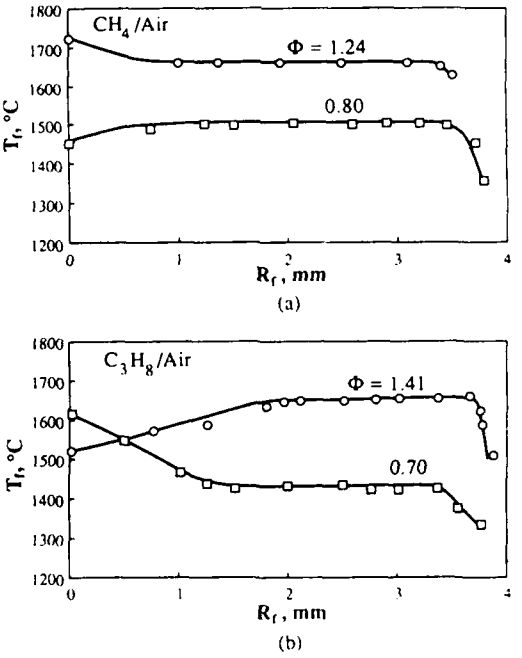

FIG. 12. Experimental results on the flame temperature of two-dimensional Bunsen flames (a) methane/air, and (b) propane/air mixtures, showing the lack of influence of preferential diffusion on stretchless flames.[44]

Eq. (5.2) is essentially the criterion for blowoff (of inverted flames) as originally advanced by Karlovitz[1] and Lewis and von Elbe.[2] This stabilization mechanism is dynamic in nature, and strictly speaking is also not a stretch phenomenon because only the normal velocity gradient is considered. Indirectly, stretch may appear to influence flame stabilization because of the relationship between the normal and transverse velocity gradients, and because S_u can be affected by flame stretch through its coupled effects with heat loss, flow nonuniformity, flame curvature, and preferential diffusion.

The above stabilization mechanism is physically sound. However, in an effort to be quantitatively predictive, Lewis and von Elbe[2] further proposed that blowoff should occur when the velocity varies significantly within the flame, or

$$\left(\frac{\delta_D^o}{S_u^o}\right)\left(\frac{\partial v}{\partial x}\right)_{u,B} = 0(1). \tag{5.3}$$

The validity of Eq. (5.3), or similar expressions with different forms of velocity gradients, has been extensively explored.[2,92–98] However, the meaningfulness of such a criterion and the fidelity of the

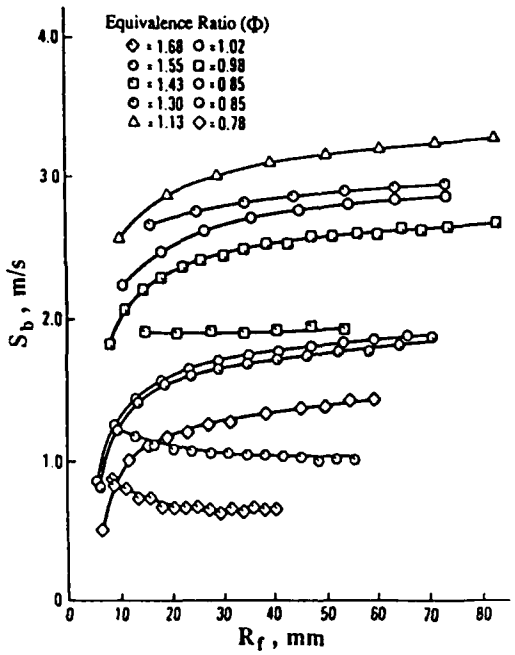

FIG. 13. Experimental results of the flame speeds of the positively-stretched outwardly-propagating flame for propane/air mixtures exhibiting preferential diffusion effects.[86,87]

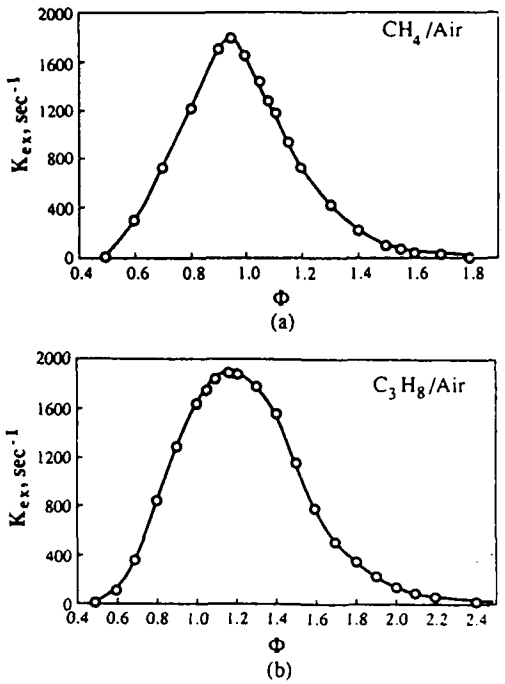

FIG. 14. Extinction stretch rates K_{ex} for the symmetrical counterflow methane/air and propane/air flames.[86]

comparisons have been seriously questioned.[81,99] Kawamura and co-workers[91,100] have also shown that flame curvature, instead of flow gradient as given by Eq. (5.3), yields better correlation with the blowoff data of inverted flames.

In light of our earlier discussion, the possible failure of Eq. (5.3) can be appreciated for several reasons. First, the original postulate[2] of Eq. (5.3) is based on the concept that the flame temperature is reduced with increasing stretch, which eventu-

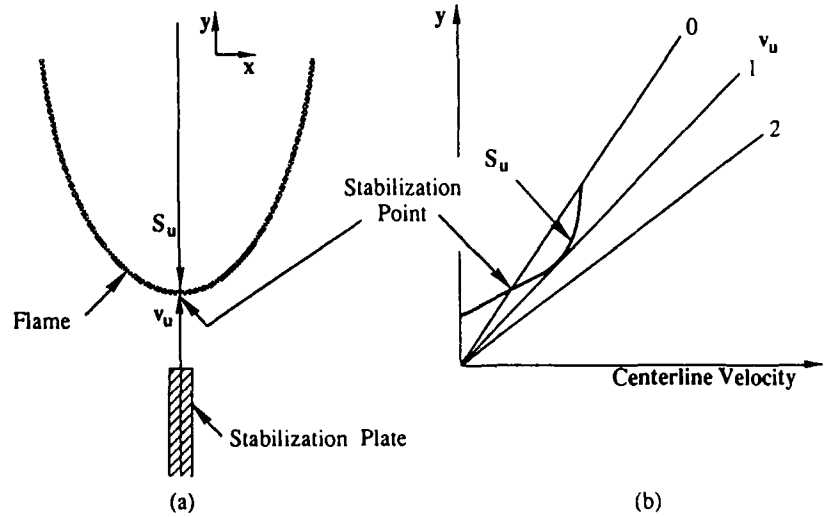

FIG. 15. Schematics showing (a) flame/flow configuration, and (b) blowoff mechanism, of inverted flames.[91]

ally causes extinction. We have, however, shown that the flame temperature can either increase or decrease with stretch depending on the nature of preferential diffusion. Second, Eq. (5.3) also does not account for the influence of heat loss and flame curvature on the flame speed. Third, the inverted flame does not appear to be sufficiently restrained to suffer extensive incomplete reaction. It is therefore quite likely that Eq. (5.3) is not applicable to flame blowoff.

Determination of Laminar Flame Speeds:

In spite of the technological and fundamental importance of the laminar flame speeds S_u^o of combustible mixtures, and the extensive efforts expended to accurately determine their values, substantial systematic spreads still exist in the reported data. While it is not always easy to individually identify the causes for such discrepancies, it is recognized that since most of these determinations involve stretched flames such as the Bunsen and outwardly-propagating spherical flames, the reported data are actually S_u instead of S_u^o. A particularly serious implication of the influence of stretch is the potential inaccuracy in the kinetic information determined or validated through comparison between the numerically-calculated S_u^o and experimentally-determined S_u.[101, 104]

Recently the symmetrical counterflow flame configuration has been used through which stretch effects can be systematically subtracted out.[99, 105, 108] The experiment basically involves determining the axial velocity profile along the centerline of the flow by using LDV (Fig. 16a), and identifying the minimum point of the velocity profile as a *reference* upstream flame speed S_u corresponding to the imposed stretch rate K. Thus by plotting S_u versus K, S_u^o can be unambiguously determined through linear extrapolation to K = 0 (Fig. 16b).

Figure 17 shows close agreement between the experimentally-determined S_u^o and the numerically-calculated values[107, 108] by using the flame code of Kee et al.[109] Such close agreement over extended ranges of equivalence ratio and pressure provides mutual support for the validity of the experimental methodology and the kinetic scheme, as far as flame speed determination is concerned.

An accurate determination of S_u^o also allows an assessment of the overall reaction order n because $S_u^o \sim p^{(n/2)-1}$. Figure 18 shows experimentally- and numerically-determined values of n as a function of pressure for stoichiometric methane/air flames with various amount of nitrogen dilution.[110] It is seen that n decreases with increasing pressure and nitrogen dilution such that it can actually assume negative values. This behavior is caused by the increased relative importance of the three-body termination reactions over the two-body branching reactions with increasing pressure and decreasing flame temperature.

Concept of Flammability Limits:

Although the term "flammability limit" has been widely and loosely applied to diverse situations of unsustainable combustion,[97, 98, 111-124] the general

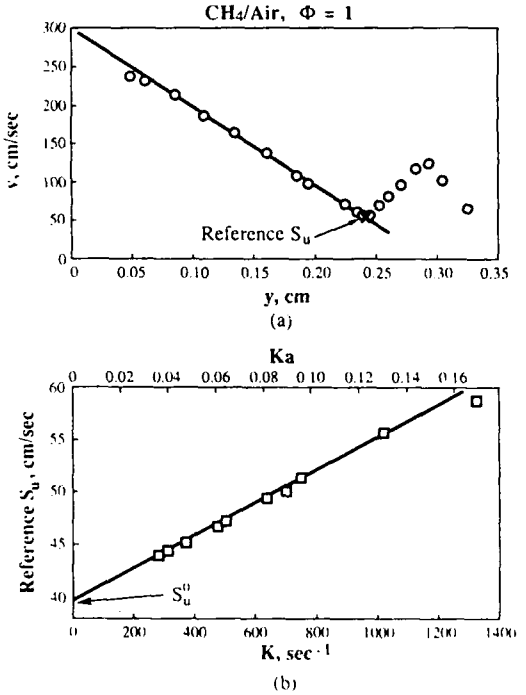

FIG. 16. Principle of counterflow methodology in determining S_u^o: (a) Velocity profile and definition of reference S_u, (b) extrapolation of reference S_u to yield S_u^o.

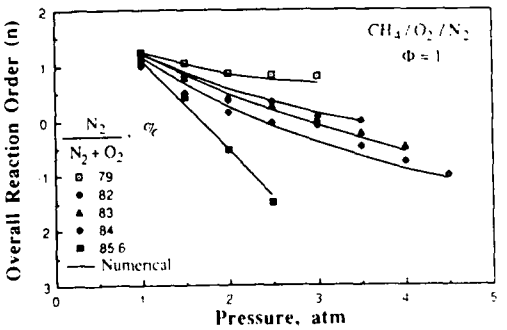

FIG. 17. Comparison between experimentally-determined S_u^o by using the counterflow technique and numerically-calculated values by using the full C_2 kinetics of Warnatz for methane/air flames.

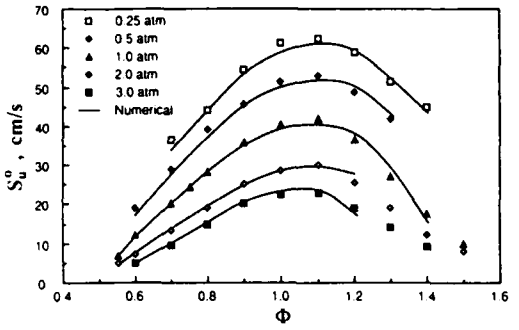

FIG. 18. Experimentally- and numerically-determined values of the overall reaction order n for stoichiometric methane/air flames with various amount of nitrogen dilution, demonstrating the decreasing trend of n with increasing pressure and the existence of negative values of n.

consensus[2,87] is that the flammability limit of a combustible mixture should be a unique physicochemical property of that mixture, being independent of external system parameters. As such, at the flammability limit all external extinction mechanisms such as conductive heat loss and radical loss should have been eliminated such that it is truly the ultimate concentration limit beyond which combustion is absolutely not possible.

As of now it is not clear what is the role of stretch in flammability limits. Certainly if the earth's gravity is counted as an adjunct property of the mixture, then buoyancy induced flame curvature and thereby stretch can extinguish a flame even in the absence of heat loss.[97,98,119] Furthermore it is conceivable that curvature can develop over the surface of a flame in the course of its resistance to extinguishment. Extinction may eventually occur when the curvature attains a certain critical value.

One conceptual difficulty with including stretch as a viable flammability mechanism is the influence of preferential diffusion. That is, depending on the nature of the stretch and the mixture's Lewis number, flame stretch can either extinguish a flame or support the propagation of a sub-limit mixture. An interesting example is the phenomenon[124] of "self-extinguishing flame," in which an outwardly-propagating flame can be initially established in a sub-limit Le < 1 mixture because of the enhanced burning due to preferential diffusion. Extinction eventually occurs as the flame size increases and the stretch effect decreases.

Recently the influence of stretch on the extinction of an adiabatic flame has been experimentally determined[88] by first measuring the extinction stretch rate of the symmetrical counterflow flame as a function of concentration (Fig. 14), and extrapolating the data to zero stretch to yield the corresponding concentration. The values so determined for lean and rich methane/air and propane/air mixtures lie within the previously reported range of flammability limits containing the effect of stretch.[112,125] Since this range is quite narrow, these results suggest that the influence of stretch, even if it does exist, is probably very weak as compared to other internal extinction mechanisms.

There are two possible internal extinction mechanisms which can cause the failure of the stretchless planar flame to propagate, namely radiative heat loss[124] and the emergent importance of chain termination over chain branching with the gradual reduction of the flame temperature as the flammability limit is approached. Theories of flammability have been formulated based on heat loss[126,127] and chain mechanism,[120,128] with the theory of Ref. 128 appearing to be quite quantitatively predictive.

Flame-Front Instability:

When a smooth flamefront is subjected to nonplanar disturbances the resulting wrinkles can either grow or decay. This is a stretched flame phenomenon because the susceptibility to instability depends on the flame response to the development of the flame curvature over its surface.

There are two intrinsic modes of flamefront instability. The first is the Landau, or hydrodynamic instability,[129] which has its origin from thermal expansion of the gas upon crossing the flame. The flame is assumed to be structureless, locally propagating with the constant laminar flame speed S_u^o (Fig. 19a). The gas densities assume constant but different values upstream and downstream of the flame sheet. It can then be easily argued[8] that upon being wrinkled the flow ahead of the convex segment slows down because of widening of the streamtube. However, since the flame speed remains unchanged, a dynamic imbalance results which leads to a further protrusion of this flame segment. Similar argument for the concave segment shows that it will further recede into the burned mixture. Thus the flame is absolutely unstable according to this mechanism, which involves only hydrodynamic stretch without considering the effect of flame stretch within the flame structure.

The importance of diffusional transport on flame stability can be readily appreciated by considering the effect of heat and mass diffusion on the ability of the flame to restore stability (Fig. 19b). Following the same discussion as that for the intensification and weakening of the Bunsen flame tips, it is clear that a Le > 1 flame is stable in that the burning is more (less) intense in the receding (protruding) segment, which tends to advance (recede) to resume its undisturbed position. Similar argument shows that a Le < 1 flame is unstable. Experi-

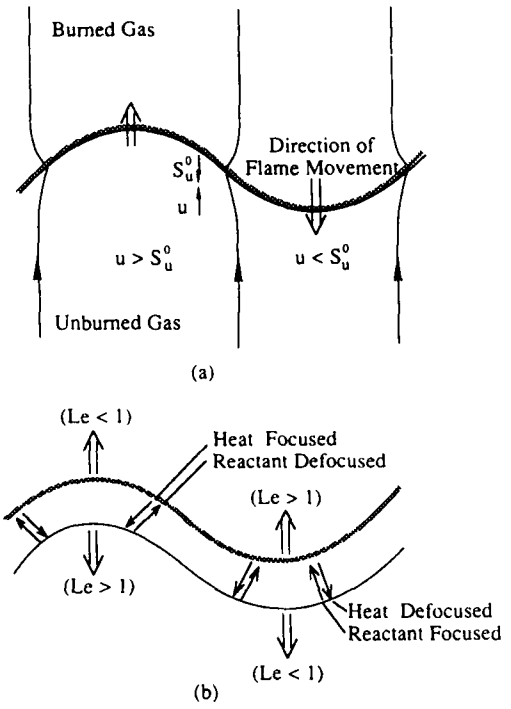

FIG. 19. Schematics demonstrating mechanisms of (a) hydrodynamic instability and (b) diffusional-thermal instability.

mental evidence of the above phenomena can be found in Ref. 3.

Sivashinsky[5,130] has analyzed the diffusional-thermal instability by neglecting thermal expansion. Analyses allowing for both hydrodynamic and diffusional-thermal instabilities have also been advanced by Sivashinsky[131] assuming small heat release, and by Pelce and Clavin[132] and Matalon and Matkowsky[133] through multi-scale analyses. These analyses show that flames are hydrodynamically unstable when subjected to long wavelength disturbances. At short wavelengths the diffusional-thermal mechanism can either stabilize or further destabilize the flame, depending on the Lewis number.

Sivashinsky et al.[134] have also shown that positive aerodynamic stretch has a stabilizing influence on the flame. This effect is further demonstrated in Ref. 66 for expanding spherical flames.

Concentration and Temperature Modifications in Flame Chemistry:

The study of fundamental kinetics is sometimes conducted by employing a particular flame as a "chemical reactor" fed by the freestream mixture, which is assumed to react either at the adiabatic flame temperature or in a temperature environment prescribed by, say, the one-dimensional laminar flame. Recognizing that some of these flames suffer stretch, which can cause modifications in both the mixture composition as well as the flame temperature, failure to account for these modifications can lead to inaccuracies in the deduced chemical information. In fact, the need for an accurate determination of S_u^o, as discussed earlier, stems from such a concern. Another example of the concentration modification is soot formation in flames,[135,136] as evidenced by the formation of soot streak from the tip of the Bunsen flame.[137] Studies of polyhedral flames have also shown substantial composition variations from the ridges to the valleys.[138] Because of the nonlinear nature of chemical kinetics, these effects obviously will not average out in the bulk.

Modelling of Turbulent Flames:

In a turbulent flow the fluctuating nonuniform local velocities impose aerodynamic stretching on the highly-convoluted flame surfaces. Thus the results of stretched laminar flames can be applied to certain situations involving turbulent premixed flames. The minimum requirement for such an application is that the flamelet satisfies the Klimov-Williams criterion,[8,139] which basically states that the laminar flame thickness must be smaller than the Kolmogorov microscale. Peters[11] has further demonstrated that this criterion is equivalent to $Ka < 1$. Since we have shown that the extinction Karlovitz number, Ka_{ex}, is sufficiently smaller than one, it seems the criterion for the existence of laminar flamelets can be further tightened to situations satisfying $Ka < Ka_{ex}$.

The properties of wrinkled laminar flames can be related to turbulent flame propagation by treating the wrinkled laminar flame simply as a surface which locally propagates with the upstream flame velocity S_u. The rates of flame propagation and fuel consumption are then related to the evolution of this surface due to the hydrodynamic stretch of the turbulent flow field, with proper allowance for the variation of S_u with the local stretch rate due to flame stretch.

The propagation of a weakly-strained, weakly-wrinkled flame has already been discussed. Flame propagation in medium- and high-intensity turbulence has recently been analyzed[140,141] by using the renormalization group method. Predicted results agree well with experimental data obtained in high-Reynolds-number turbulent flows, especially in reproducing the "bending" effect observed experimentally.[11]

Another application of stretch in turbulent flames is the flame dynamics in coherent structures.[142] The rolling up of the vortex increases the total surface

area for burning, although excessive stretching can lead to extinction in the vortex core.

Stretched Diffusion Flames

Compared to premixed flames, the response of diffusion flames to stretch is less subtle. First we note that even in a neutrally-diffusive, stretchless situation,[143] incomplete reaction, reactant leakage, and consequently flame extinction are inherent features of a diffusion flame with finite rate kinetics. Furthermore, since a diffusion flame does not have a flame speed and thereby the extent of flexibility of a premixed flame to adjust its location in the presence of convection, convection across the flame always reduces the residence time for reaction. This leads to reduced flame thickness, increased reactant leakage, and consequently increased vulnerability to extinction.

A stretch factor K can still be defined for a given non-uniform flow field and a wrinkled flame sheet, with n pointed opposite to the general direction of the flow velocity v. Stretch-induced concentration and flame temperature modifications also exist for diffusionally-imbalanced mixtures. Preferential diffusion, while still quantitatively important, is only an additional feature of the flame and does not have the profound effect on the flame response as in the case of a premixed flame.

A detailed theory of one-dimensional laminar diffusion flames was formulated by Linan for the counterflow configuration,[144] with the assumption of unity Lewis number. This theory has since been extended to non-unity Lewis number mixtures.[145] Explicit ignition/extinction criteria have been derived as function of the system Damköhler number which depends on the velocity gradient of the flow, allowing a priori assessment of the possible existence of these critical states. A general theory of stretched, wrinkled diffusion flames has not been formulated. Modeling of turbulent diffusion flames on the basis of laminar diffusion flamelets has been reviewed by Peters.[11]

Summary and Suggestions

Summarizing, the basic phenomena of stretched flames are mostly understood, at least qualitatively. Effects of stretch can be distinguished as those caused by hydrodynamic stretch, which does not affect the flame intensity but changes the flame surface area and thereby the volumetric burning rate, and by flame stretch, which modifies the flame intensity and can also cause extinction. Preferential diffusion interacts strongly with stretch and can qualitatively affect the flame response depending on whether the effective mixture Lewis number is greater or smaller than unity, and whether the stretch is positive or negative. The extent with which the flame can freely adjust its location in response to stretch, in order to achieve complete reaction, is also an important factor especially for extinction considerations. It is further clarified that flame stabilization is an issue of dynamic stability, it is neither a stretched-flame phenomenon nor an extinction phenomenon.

More research, however, is still needed for complete understanding and further application of the stretched flame phenomena. Some of the various issues of current interest and importance are

1) A nonlinear analysis of the general stretched premixed flame, allowing for flame extinction is needed. The formulation can be facilitated by the observation that Ka_{e_1} is sufficiently smaller than one. The analysis should provide further insight into the insensitivity of the properties of the adiabatic, unrestrained, diffusionally-neutral flames to stretch, especially for large stretch rates.
2) The anticipation that energy conservation can be satisfied for stagnation and Bunsen flames by considering tangential transport needs to be demonstrated.
3) The role played by the preferential diffusion of reaction intermediates, especially such highly-mobile and chemically-crucial species as the hydrogen radical, on the dynamics of stretched flames requires more detailed study. Asymptotic analysis using reduced kinetic schemes[7,146] appears to be especially suitable for such an investigation.
4) Numerical modelings of stretched flames, especially those in the counterflow configuration have employed different flow fields. While this is acceptable for qualitative studies, a more realistic flow field is needed when performing quantitative comparison with experimental data.[77] The concern is especially serious if the chemical kinetic mechanism used is also not certain and possibly requires "adjustment".
5) Experimental stretched flame results are frequently reported in terms of the global stretch rate. This can be quite different from the local stretch rate determined by using, say, LDV. Caution is needed when comparing these data with the theoretical results obtained by using local stretch rates.
6) Explicit theoretical formulas have already been derived for weakly-stretched flames, at least for one-step reactions. Experimental results, however, have been scarce. A systematic experimental effort should be mounted to obtain data of high fidelity for stretched flames with positive/negative stretches and different preferen-

tial diffusion effects, and to correlate them according to the theoretical formulas.

7) More effort is needed to integrate the theoretical results on stretched flames in the modeling of turbulent flames. Caution is needed to ensure overall energy conservation for diffusionally-imbalanced mixtures. Flame interaction, discussed next, also needs to be accounted for.

8) Most of the studies on stretched flames have employed a solitary flame, which is either premixed or nonpremixed. However, in the interior of a turbulent flame, the individual flamelets interact with each other. Partial premixing also occurs, resulting in partially premixed flames. Some research has been conducted on these issues,[35,147-149] but more is needed.

9) The existence of flammability limits needs to be settled. If they indeed exist, then a general theory of flammability limits is needed. Furthermore, since a sub-limit mixture can be rendered flammable, through either flame stretch and/or flame interaction, the absolute significance of flammability limits also has to be assessed.

10) A general theory of stretched diffusion flames is needed.

Acknowledgments

The author acknowledges with pleasure the technical discussions with and comments from Drs. C. T. Bowman, S. H. Chung, G. H. Markstein, M. Matalon, M. G. Mungal, N. Peters, P. D. Ronney, G. I. Sivashinsky, R. A. Strehlow, H. Tsuji, and F. A. Williams on the various aspects of stretched flames. The continued interest and funding support over the years from NSF, DOE, AFOSR, ARO, and ONR have been essential in the author's pursuit of fundamental combustion research such as the topic reviewed here; the specific efforts on stretched flames have been supported by DOE and AFOSR. The preparation of this manuscript has been ably assisted by Drs. R. L. Axelbaum, B. H. Chao, and S. Nam, and Mr. D. L. Zhu, to whom the author extends his appreciation.

Nomenclature

a	strain rate of stagnation flow
A	area of flame surface
B	frequency factor
c_p	specific heat
Da	Damkohler number
D	diffusivity
k	reaction rate constant
K	stretch rate (sec^{-1})
Ka	Karlovitz number
L	loss parameter
Le	Lewis number
m	mass burning rate per unit area
n	overall reaction order
n	unit normal vector
p	pressure
q	heat of combustion
R_f	radial dimension of flame
t	time
T,$\hat{\text{T}}$	temperature and stoichiometrically-weighted T
T_a	activation temperature
T_{ad}	adiabatic flame temperature
u,u	flow velocity
V	flame velocity
w_k	reaction rate of kth reaction
x,y	spatial coordinate
Y,$\hat{\text{Y}}$	mass fraction and stoichiometrically-weighted Y

Greeks

β	coupling function
δ	thickness of various flame zones
λ	thermal conductivity
Φ	equivalence ratio
ρ	density
σ	geometry factor for stagnation flow
θ	angle of Bunsen cone

Subscripts

B	blowoff
D,H,R	Transport, hydrodynamic, reaction zones
M,T	species and thermal diffusion zones
ex	extinction
f	flame
i,j	index for species
u,b	unburnt and burnt states of mixture
s	surface, especially flames
∞	ambience

Superscripts

o	the adiabatic, unstretched planar flame

REFERENCES

1. Karlovitz, B., Denniston, D. W., Knapschaefer, D. H. and Wells, F. E., Fourth Symposium (International) on Combustion, p. 613, The Combustion Institute, 1953.
2. Lewis, B. and von Elbe, G. Combustion Flames and Explosion of Gases, pp. 220-261, Academic, NY 1961.
3. Markstein, G., Nonsteady Flame Propagation, pp. 5-73, MacMillan, NY, 1964.

4. MATALON, M. AND MATKOWSKY, B. J.: Comb. Sci. Tech. 34, 295 (1983).
5. SIVASHINSKY, G. I.: Ann. Rev. Fluid Mech. 15, 179 (1983).
6. LAW, C. K.: Prog. Energy Comb. Sci. 10, 295 (1984).
7. PETERS, N.: Prog. Energy Comb. Sci. 10, 319 (1984).
8. WILLIAMS, F. A.: Combustion Theory, Chaps. 9 and 10, Benjamin-Cummins, Palo Alto, 1985.
9. CLAVIN, P.: Prog. Energy Comb. Sci. 11, 1–59 (1985).
10. WILLIAMS, F. A.: Combustion and Nonlinear Phenomena (P. CLAVIN, B. LARROUTOUROU AND P. PELCE, Ed.), pp. 93–99, Les Editions de Physique, Les Ulis, France, 1986.
11. PETERS, N.: Twenty-First Symposium (International) on Combustion, p. 1231, The Combustion Institute, 1988.
12. WILLIAMS, F. A.: AGARD Conf. Proc. No. 164, AGARD, Paris, 1975.
13. BUCKMASTER, J. D.: Quart. J. Mech. Appl. Math. 35, 249 (1982).
14. STREHLOW, R. A. AND SAVAGE, L. D.: Comb. Flame 31, 209 (1978).
15. MATALON, M.: Combust. Sci. Tech. 31, 169 (1983).
16. CHUNG, S. H. AND LAW, C. K.: Comb. Flame 55, 123 (1984).
17. CHEN, Z. H., LIU, G. E. AND SOHRAB, S. H.: Comb. Sci. Tech. 51, 39 (1987).
18. LIN, T. H. AND SOHRAB, S. H.: Comb. Sci. Tech. 52, 75 (1987).
19. SIVASHINSKY, G. I., RAKIB, Z., MATALON, M. AND SOHRAB, S. H.: Comb. Sci. Tech. 57, 37 (1988).
20. SIVASHINSKY, G. I. AND SOHRAB, S. H.: "The influence of rotation on premixed flames in stagnation-point flow," to be published.
21. ISHIZUKA, S.: Twentieth Symposium (International) on Combustion, p. 287, The Combustion Institute, 1985.
22. TAKENO, T. AND ISHIZUKA, S.: Comb. Flame 64, 83 (1986).
23. TAKENO, T., NISHIOKA, M. AND ISHIZUKA, S.: Comb. Flame 66, 271 (1986).
24. ISHIZUKA, S.: Lecture Notes in Physics Series, Vol. 299: Math. Modelling in Combustion (J. BUCKMASTER AND T. TAKENO, eds.), p. 93, Springer-Verlag, 1988.
25. KOBAYASHI, H., KITANO, M. AND OTSUKA, Y.: Comb. Sci. Tech. 57, 17 (1988).
26. KLIMOV, A. M.: Zhur. Prikl. Mekh. Tekhn. Fiz. 3, 49 (1963).
27. CHUNG, S. H. AND LAW, C. K.: Comb. Flame 72, 325 (1988).
28. CHUNG, S. H. AND LAW, C. K.: "Analyses of some nonlinear premixed flame phenomena," to appear in Comb. Flame.
29. LIBBY, P. A. AND WILLIAMS, F. A.: Comb. Flame 44, 287 (1982).
30. DARABIHA, N., CANDEL, S. M., AND MARBLE, F. E.: Comb. Flame 64, 203 (1986).
31. LAW, C. K., NAM, S., ZHU, D. L., AND KEE, R. J.: "On the characteristics of adiabatic, diffusionally-neutral, strained flames," to be published.
32. TSUJI, H. AND YAMAOKA, I.: Nineteenth Symposium (International) on Combustion, p. 1533, The Combustion Institute, 1983.
33. DIXON-LEWIS, G. AND ISLAM, S. M.: Nineteenth Symposium (International) on Combustion, p. 283, The Combustion Institute, 1983.
34. KULKARNY, V. A., SCHWARTZ, J. AND FINK, S.: AIAA Paper No. 83-1718, 1983.
35. SOHRAB, S. H., YE, Z. Y. AND LAW, C. K.: Twentieth Symposium (International) on Combustion, p. 1957, The Combustion Institute, 1985.
36. BUCKMASTER, J. AND CROWLEY, A. B.: J. Fluid Mech. 131, 341 (1984).
37. WAGNER, T. C. AND FERGUSON, C. R.: Comb Flame 59, 267 (1985).
38. MUNGAL, M. G. AND ECHEKKI, T.: "Laminar flame speed measurements on a 2-D Bunsen burner," to be published.
39. LIBBY, P. A. AND WILLIAMS, F. A.: Comb. Sci. Tech. 31, 1 (1983).
40. LIBBY, P. A. AND WILLIAMS, F. A.: Comb. Sci Tech. 54, 237 (1987).
41. LAW, C. K., ISHIZUKA, S. AND MIZOMOTO, M.: Eighteenth Symposium (International) on Combustion, p. 1791, The Combustion Institute, 1981.
42. SIVASHINSKY, G. I.: Acta Astronautica 3, 889 (1976).
43. BUCKMASTER, J.: Seventeenth Symposium (International) on Combustion, p. 835, The Combustion Institute, 1979.
44. LAW, C. K., CHO, P., MIZOMOTO, M. AND YOSHIDA, H.: Twenty-First Symposium (International) on Combustion, p. 1803, The Combustion Institute, 1988.
45. CLAVIN, P. AND WILLIAMS, F. A.: J. Fluid Mech. 116, 251 (1982).
46. MATALON, M. AND MATKOWSKY, B. J.: J. Fluid Mech. 124, 239 (1982).
47. CLAVIN, P. AND JOULIN, G.: Journal de Physique—Lettres 44,L-1 (1983).
48. LIBBY, P. A., LINAN, A. AND WILLIAMS, F. A.: Comb. Sci. Tech. 34, 257 (1983).
49. DANESHYAR, H., MENDES-LOPES, J. M. C. AND LUDFORD, G. S. S.: Nineteenth Symposium (International) on Combustion, p. 413, The Combustion Institute, 1983.
50. MENDES-LOPES, J. M. C. AND DANESHYAR, H.: Comb. Flame 60, 29 (1985).

51. ETENG, E., LUDFORD, G. S. S. AND MATALON, M.: Phys. Fluids 29, 2172 (1986).
52. CHUNG, S. H.: Trans. Korean Soc. Mech. Eng. 9, 250 (1985).
53. MIKOLAITIS, D. AND BUCKMASTER, J.: Comb. Sci. Tech. 27, 55 (1981).
54. BUCKMASTER, J. AND MIKOLAITIS, D.: Comb. Flame 47, 191 (1982).
55. MIKOLAITIS, D. AND BUCKMASTER, J.: Comb. Sci. Tech. 27, 55 (1981).
56. MIKOLAITIS, D.: Combust. Sci. Tech. 53, 203 (1987).
57. GIOVANGIGLI, V. AND CANDEL, S.: Comb. Sci. Tech. 48, 1 (1986).
58. KIM, Y. D. AND MATALON, M.: Comb. Flame 73, 303 (1988).
59. SIVASHINSKY, G. I.: J. Chem. Phys. 62, 638 (1975).
60. SIVASHINSKY, G. I.: J. Heat Trans. 11, 530 (1974).
61. BUCKMASTER, J.: Comb. Flame 20, 33 (1979).
62. MITANI, T.: Comb. Sci. Tech. 23, 93 (1980).
63. FRANKEL, M. K. AND SIVASHINSKY, G. I.: Comb. Sci. Tech. 31, 131 (1983).
64. FRANKEL, M. K. AND SIVASHINSKY, G. I.: Comb. Sci. Tech. 40, 257 (1984).
65. FLAHERTY, J. E., FRANKEL, M. K., ROYTBURD, V. AND SIVASHINSKY, G. I.: Comb. Sci. Tech. 43, 245 (1985).
66. MATALON, M. AND ERNEUX, T.: SIAM J. Appl. Math 44, 734 (1984).
67. BECHTOLD, J. K. AND MATALON, M.: Comb. Flame 67, 77 (1987).
68. RONNEY, P. D. AND SIVASHINSKY, G. I.: "A theoretical study of the propagation and extinguishment of nonsteady spherical flame fronts," SIAM J. Appl. Math. (in press).
69. MIKOLAITIS, D. W.: Comb. Flame 56, 327 (1984).
70. MIKOLAITIS, D. W.: Comb. Flame 57, 25 (1984).
71. MIKOLAITIS, D. W.: Comb. Flame 58, 23 (1984).
72. MIKOLAITIS, D. W.: Comb. Flame 63, 95 (1986).
73. SATO, J. AND TSUJI, H.: Comb. Sci. Tech. 33, 193 (1983).
74. GIOVANGIGLI, V. AND SMOOKE, M. D.: J. Computational Physics 68, 327 (1987).
75. GIOVANGIGLI, V. AND SMOOKE, M. D.: Comb. Sci. Tech. 53, 23 (1987).
76. ROGG, B.: Comb. Flame 73, 45 (1988).
77. KEE, R. J., MILLER, J. A., EVANS, G. H., AND DIXON-LEWIS, G.: This Symposium.
78. SESHADRI, K. AND PETERS, N.: Comb. Sci. Tech. 33, 35 (1983).
79. TAM, R. AND LUDFORD, G. S. S.: Comb. Sci. Tech. 43, 227 (1985).
80. TSUJI, H. AND YAMAOKA, I.: First Specialist Meeting, The Combustion Institute, Bordeaux, France, 1981.
81. TSUJI, H.: First ASME-JSME Thermal Engineering Conference, Honolulu, Hawaii, Vol. 4, p. 11, 1983.
82. SATO, J.: Nineteenth Symposium (International) on Combustion, p. 1541, The Combustion Institute, 1983.
83. ISHIZUKA, S. AND LAW, C. K.: Nineteenth Symposium (International) on Combustion, p. 961, The Combustion Institute, 1983.
84. MIZOMOTO, M., ASAKA, Y., IKAI, S. AND LAW, C. K.: Twentieth Symposium (International) on Combustion, p. 1933, The Combustion Institute, 1985.
85. MIZIMOTO, M. AND YOSHIDA, H.: Comb. Flame 70, 1 (1987).
86. PALM-LEIS, A. AND STREHLOW, R. A., Comb. Flame 13, 111 (1969).
87. STREHLOW, R. A.: Combustion Fundamentals, p. 391, McGraw-Hill (1984).
88. LAW, C. K., ZHU, D. L., AND YU, G.: Twenty-First Symposium (International) on Combustion, p. 1419, The Combustion Institute, 1988.
89. YU, G., LAW, C. K. AND WU, C. K.: Comb Flame 63, 339 (1986).
90. TSUJI, H.: Personal communications.
91. KAWAMURA, T., ASATO, K. AND MAZAKI, T.: Comb. Flame 45, 225 (1982).
92. REED, S. B.: Comb. Flame 11, 177 (1967).
93. REED, S. B.: J. Inst. of Gas Engineers 8, 157 (1968).
94. EDMONDSON, H. AND HEAP, M. P.: Twelfth Symposium (International) on Combustion, p. 1007, The Combustion Institute, 1969.
95. EDMONDSON, H. AND HEAP, M. P.: Comb. Flame 15, 179 (1970).
96. REED, S. B.: Comb. Flame 17, 105 (1971).
97. HERTZBERG, M.: "The theory of flammability limits," Bureau of Mines Rept. of Investigation 8865 (1984).
98. HERTZBERG, M.: Twentieth Symposium (International) on Combustion, p. 1967, The Combustion Institute, 1985.
99. MELVIN, A. AND MOSS, J. B.: Comb. Sci. Tech. 7, 189 (1973).
100. KAWAMURA, T., ASATO, K., MAZAKI, T., HAMAGUCHI, T. AND KAYAHARA, H.: Comb. Flame 35, 109 (1979).
101. WESTBROOK, C. K. AND DRYER, F. L.: Eighteenth Symposium (International) on Combustion, p. 749, The Combustion Institute, 1981.
102. WESTBROOK, C. K. AND DRYER, F. L.: Prog. Energy Combust. Sci. 10, 1 (1984).
103. WARNATZ, J.: Eighteenth Symposium (International) on Combustion, p. 369, The Combustion Institute, 1981.
104. WARNATZ, J.: Combustion Chemistry (W. C. GARDINER, JR., Ed.), p. 197, Springer-Verlag, NY, 1984.
105. WU, C. K. AND LAW, C. K.: Twentieth Sym-

posium (International) on Combustion, p. 1941, The Combustion Institute, 1985.
106. Zhu, D. L., Egolfopoulos, F. N. and Law, C. K.: This symposium.
107. Egolfopoulos, F. N., Cho, P. and Law, C. K.: "Laminar flame speeds of methane/air mixtures under reduced and elevated pressures," Combust. Flame (in press).
108. Zhu, D. L., Egolfopoulos, F., and Law, C. K.: This Symposium.
109. Kee, R. J., Grcar, J. F., Smooke, M. D. and Miller, J. A.: "A FORTRAN program for modeling steady laminar one-dimensional premixed flames," Sandi Rept. SAND85-8240, 1985.
110. Egolfopoulos, F. N. and Law, C. K.: "On the existence of negative overall reaction orders in laminar flame propagation," to be published.
111. Egerton, A. C.: Fourth Symposium (International) on Combustion, p. 4, The Combustion Institute, 1953.
112. Zabetakis, M. D., Lambiris, S. and Scott, G. S.: Seventh Symposium (International) on Combustion, p. 484, The Combustion Institute, 1959.
113. Lovachev, L. A., Babkin, V. S., Bunev, V. A., V'yun, A. V., Krivulin, V. A. and Baratov, A. N.: Comb. Flame 20, 259 (1973).
114. Lovachev, L. A.: Comb. Sci. Tech. 20, 209 (1979).
115. Macek, A.: Comb. Sci. Tech. 21, 43 (1979).
116. Sorenson, S. C., Savage, L. D. and Strehlow, R. A.: Comb. Flame 24, 347 (1975).
117. Yamaoka, I. and Tsuji, H.: Seventeenth Symposium (International) on Combustion, p. 843, The Combustion Institute, 1979.
118. Buckmaster, J. and Mikolaitis, D.: Comb. Flame 45, 109 (1982).
119. Jarosinski, J., Strehlow, R. A. and Azarbarzin, A.: Nineteenth Symposium (International) on Combustion, p. 1549, The Combustion Institute, 1983.
120. Peters, N. and Smooke, M. D.: Comb. Flame 60, 171 (1985).
121. Ronney, P. D. and Wachman, H. Y.: Comb. Flame 62, 107 (1985).
122. Ronney, P. D.: Comb. Flame 62, 121 (1985).
123. Ronney, P. D.: Comb. Sci. Tech. 59, 123 (1988).
124. Ronney, P. D.: This Symposium.
125. Ishizaka, S. and Law, C. K.: Nineteenth Symposium (International) on Combustion, p. 327, The Combustion Institute, 1983.
126. Spalding, D. B.: Proc. Royal Soc. London, A-240, 83 (1957).
127. Joulin, G. and Clavin, P.: Acta Astronautica 3, 223 (1976).
128. Law, C. K. and Egolfopoulos, F.: "A kinetic theory of flammability limits," to be published.
129. Landau, L. D. and Lifshitz, E. M.: Fluid Mechanics, Chap. XIV, Pergamon Press (1959).
130. Sivashinsky, G. I.: Comb. Sci. Tech. 15, 137 (1977).
131. Sivashinsky, G. I.: Acta Astronautica 4, 1177 (1977).
132. Pelce, P. and Clavin, P.: J. Fluid Mech. 124, 219 (1982).
133. Matalon, M. and Matkowsky, B. J.: SIAM J. Appl. Math. 44, 327 (1982).
134. Sivashinsky, G. I., Law, C. K., and Joulin, G.: Comb. Sci. Tech. 28, 155 (1982).
135. Haynes, B. S. and Wagner, H. G.: Prog. Energy Comb. Sci. 7, 229 (1981).
136. Axelbaum, R. L., Law, C. K., and Flower, W. L.: This Symposium.
137. Homann, K. H.: Comb. Flame 11, 265 (1967).
138. Markstein, G. H.: Seventh Symposium (International) on Combustion, p. 289, The Combustion Institute, 1958.
139. Williams, F. A.: Comb. Flame 26, 269 (1976).
140. Yakhot, V.: "Propagation Velocity of Premixed Turbulent Flame," Comb. Sci. Tech. (in press).
141. Sivashinsky, G. I.: "Cascade renormalization theory of turbulent flame speed," Comb. Sci. Tech. (in press).
142. Peters, N. and Williams, F. A.: The Role of Coherent Structures in Modelling Turbulence and Mixing, J. Jiminez, Ed., p. 364, Berlin, Springer-Verlag, 1981.
143. Chung, S. H. and Law, C. K.: Comb. Sci. Tech. 29, 129 (1982).
144. Linan, A.: Acta Astronautica 1, 1007 (1974).
145. Chung, S. H. and Law, C. K.: Comb. Flame 52, 59 (1983).
146. Peters, N. and Williams, F. A.: Comb. Flame 68, 185 (1987).
147. Seshadri, K., Puri, I. and Peters, N.: Comb. Flame 61, 239 (1985).
148. Peters, N.: Twentieth Symposium (International) on Combustion, p. 353, The Combustion Institute, 1985.
149. Law, C. K., Li, T. X., Chung, S. H., Kim, J. S., and Zhu, D. L.: "On the structure and extinction dynamics of partially-premixed flames: theory and experiment," Fall Tech. Meeting of the Western States Section of the Combustion Institute, 1988.

Twenty-Second Symposium (International) on Combustion/The Combustion Institute, 1988/379-386

VELOCITY AND SCALAR FIELDS OF TURBULENT PREMIXED FLAMES IN STAGNATION FLOW

P. CHO AND C. K. LAW
Department of Mechanical Engineering
University of California
Davis CA 95616

R. K. CHENG AND I. G. SHEPHERD
Applied Science Division
Lawrence Berkeley Laboratory
Berkeley, CA 94720

Detailed experimental measurements of the scalar and velocity statistics of premixed methane/air flames stabilized by a stagnation plate are reported. Conditioned and unconditioned velocity of two components and the reaction progress variable are measured by using a two-component laser Doppler velocimetry technique and Mie scattering technique, respectively. Experimental conditions cover equivalence ratios of 0.9 and 1.0, incidence turbulence intensities of 0.3 to 0.45 m/s, and global stretch rates of 100 to 150 sec^{-1}. The experimental results are analyzed in the context of the Bray-Moss-Libby flamelet model of these flames. The results indicate that there is no turbulence production within the turbulent flame brush and the second and third order turbulent transport terms are reduced to functions of the difference between the conditioned mean velocity. The result of normalization of these relative veleocities by the respective velocity increase across laminar flame suggests that the mean unconditioned velocity profiles are self-similar.

Introduction

In a recent paper[1] we introduced the use of the turbulent stagnation flow configuration for fundamental studies of premixed turbulent flames. The turbulent flame propagates in the divergent stagnation flow region of a turbulent fuel/air jet impinging on a plate. Depending on flow and mixture conditions the flame brush is stabilized at various distances away from the plate surface where the mean velocity balances the turbulent flame speed. Consequently, flame stabilization is achieved without involving flow recirculation as in the conventional V-flame and conical flame configurations. Moreover, at the centerline, the turbulent flame brush is planar and locally normal to the approach flow so that the turbulent flame speed can be deduced unambiguously from the flow velocity entering the reaction zone. Therefore, this configuration provides a convenient and more accurate means to deduce the turbulent flame speed.[1]

The most significant theoretical implication of this configuration, however, is that it is the closest experimental approximation to the idealized one-dimensional infinite planar flame assumed in many theoretical turbulent combustion models.[2,3] Bray, Champion and Libby[4] (BCL) recognize that a theoretical analysis for the infinite planar flame is limited because the idealized situation cannot be produced in the laboratory. As a result, they have relied on a comparison of their theoretical predictions with experimental measurements made in 2D oblique flames. Although these comparisons have been successful in validating many features of the model, it is however difficult to ascertain whether the discrepancies between predictions and measurements are caused by variations of the flame properties not accounted for in the theory, or by the actual deficiencies in the theory. Hence, encouraged in part by our experimental work, they have recently initiated the modeling of the stagnation flow stabilized flame so that a more direct and compatible comparison can be made between theoretical and experimental studies. Their first analysis[4] is for the case of flames stabilized in two opposed jets and closure is achieved by the use of conventional gradient transport. Subsequent studies[4] will model the turbulent transport using the Bray-Moss-Libby (BML) flamelet concept which assumes infinite rate chemistry and zero flamelet thickness.[2]

The stagnation flame configuration is also significant for other numerical models of turbulent combustion, such as the joint probability density function (jpdf) method developed by Pope[5,6] and a

deterministic model for simulating the interaction of the flamelet with incident turbulence using the vortex dynamics technique.[7] At present, the jpdf model is capable of predicting the turbulent flame speed and other properties similar to those calculated by the BML model. Vortex dynamic simulations of the stagnation flames compute the dynamic movement of the wrinkled flamelet and also predict the conditioned velocity statistics. This configuration is, therefore, important for the further development of fundamental experimental and theoretical turbulent combustion research.

Since very little is known about the behavior of the stagnation flow stabilized flames, it is necessary to improve our understanding of their fundamental properties through detailed experimental measurement of the scalar and velocity statistics. These experimental data will be useful in the development of theoretical models for this configuration. In response to such a need, we report herein results from an investigation of the scalar and velocity statistics which provide further characterization of the flame properties. Measurements were made of the conditioned and unconditioned velocity of two components and the reaction progress variable $\tilde{c}$, a nondimensionalized scalar. Features of the mean and rms velocity profiles significant to modeling are discussed. In addition, implications for the closure requirements of the third order turbulence transport are also considered.

Experimental Methodology

A uniform axisymmetric flow of premixed methane/air is provided by a 50 mm diameter nozzle. This jet of reactants is shielded by a co-flow of air with outer diameter of 100 mm. For this study, the stagnation plate is placed at 75 mm above the exit, and the exit flow velocity is held constant at 5.0 m/s. The incident turbulence is generated by placing at 50 mm upstream of the exit a square grid of 1.0 mm elements with 5.0 mm openings or a perforated plate with 3.2 mm diameter circular holes which gives a 40% blockage ratio. Mixture and flow conditions of the four flames are listed in Table I. The turbulence Reynolds numbers and Damköhler numbers determined at the nozzle exit indicate that these flame fall within the wrinkled laminar flamelet regime (Table I).

Flow velocities are measured by a four-beam two-color laser Doppler velocimetry (LDV) system which measures the velocity of the two components using a 10 μsec co-validation criterion. Details of the LDV system and the computer controlled data acquisition system can be found in Ref. 1. Seeding for unconditioned velocity measurement is provided by refractory aluminum oxide particles of 0.3 μm introduced into the jet by a cyclone seed generator. Conditioned velocity measurement in the reactant side is made possible by using a silicon oil aerosol as the LDV seed. The technique is based on the principle that the silicon oil droplets evaporate and burn through the flamelets. A blast atomizer is used to generate the aerosol. At each measurement position, 8192 pairs of validated velocity data are recorded. To deduce the conditioned velocity statistics in the products, a procedure which involves deconvoluting the velocity pdf's as described in Cheng and Shepherd[8] is used.

The silicone oil seeding technique is also used for measuring the conserved scalar, $\tilde{c}$, by monitoring the Mie scattering intensity using a photomultiplier and lens assembly. Within the flame brush, the Mie scattering signal resembles a random telegraph signal with sharp transition between the signal levels representing the reactant and product states. By specifying a threshold criterion, the local value of the conserved scalar is determined by evaluating the percentage of the time spent in the products. Using the zero thickness flamelet approximation, the conserved scalar so determined is identical to the normalized density $(\rho - \rho_p)/(\rho_r - \rho_p)$, where ρ is the mean density and subscripts r and p denote reactants and products. The Mie scattering signal can also be analyzed to obtain other time dependent scalar parameters such as the scalar spectra, flame crossing frequency[9] and pdf's of the flame passage times.[10] The turbulent flame brush thickness is obtained from the distance between the

TABLE I
Mixture and flow conditions

Case #	Turbulence generator	u' (cm/s)	Length scale (mm)	Stretch rate (sec^{-1})	ϕ	Re_l	Da	δ_l (mm)	δ_l (mm)	S_l (cm/s)
1	grid	30	2	145	1.0	38	20	5.8	0.12	95
2	grid	30	2	115	0.9	38	14	4.4	0.14	60
3	plate	45	3	110	1.0	87	20	10.4	0.12	135
4	plate	45	3	100	0.9	87	14	8.3	0.14	120

two points on the axial scale intersected by the tangent to the $\tilde{c}$ profile at $\tilde{c} = 0.5$.

Results and Discussions

As reported in our previous study, typical flow velocities in the flame region are of the same order of magnitude as the turbulent flame speed. These velocities are lower than those of the other axisymmetric or plane-symmetric flame configurations in which the velocity of the flow entering the flame region is about the same as that of the freestream. Therefore, it becomes necessary to determine whether or not the models developed for high Reynolds numbers are still valid for the stagnation flames. The two criteria for the models are that Re_l, the turbulent Reynolds number based on the integral length scale and velocity fluctuations, and Da, the large eddy Damköhler number, are both much large than unity. Although these conditions are satisfied at the exit, it is important to determine if the turbulence scales change close to the plate.

Shown in Fig. 1 are the profiles of the time scales of the non-reacting stagnation point flow, t_x, obtained from auto-correlations and the associated length scale, l_x, deduced by Taylor's hypothesis for case #1. The length scale is relatively constant except at $x < 10$ mm where a decrease is found. This decrease seems to be an indication of the breakdown of the Taylor's hypothesis in the low velocity region. Similar features are also found in the turbulence generated by the perforated plate. Although it is not possible to deduce the integral length scale for the transverse component, the time scales show that the grid generated turbulence is isotropic whereas the turbulence generated by the perforated plate is slightly anisotropic with smaller transverse integral time scales. The result that both the length scale and the velocity fluctuations are constant[1] demonstrates that the flow criteria for current turbulent combustion models are satisfied even close to the stagnation flame region.

The mean centerline axial profiles of the conditioned and unconditioned velocities for case #1 are shown in Fig. 2. Also shown is the profile of the reaction progress variable. It shows that the reactant boundary of the flame zone, as indicated by the position where $\tilde{c}$ deviates from zero, occurs at the minimum of the unconditioned velocity profile. This provides an experimental validation of our previous method of determining S_T where the minimum velocity was equated to the turbulent flame speed.[1]

The turbulent flame brush thickness, δ_T, deduced from the $\tilde{c}$ profiles is listed in Table 1. Also listed is the corresponding laminar flame thickness, δ_L, based on the definition of Zeldovich.[11] The ratio between the turbulent and laminar flame thicknesses is a significant parameter in the BML model which assumes infinite rate chemistry. Studies in turbulent V-flames and Bunsen flames have shown that at positions close to the stabilization region, the zero thickness flamelet assumption is not valid because the density pdf's show appreciable contributions from the intermediate burning states. These conditions are satisfied only at positions farther away because the flame brush thickness increases almost linearly with downstream distance. In contrast, since the stagnation flames do not have recirculating stabilization regions, the flame brush thickness remains relatively constant along the flame front. Therefore, the process of choosing a location suitable for comparison with theory is not encountered. Moreover, the smallest turbulent/laminar flame thickness ratio of 30 (case #2) indicates that the zero

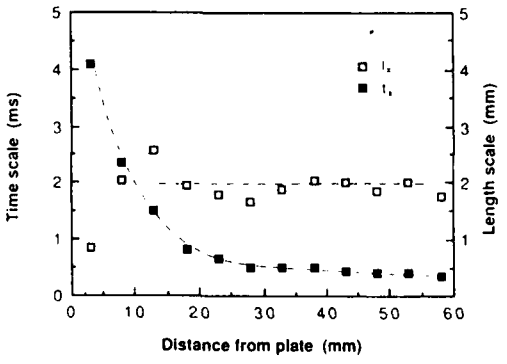

FIG. 1. The time scales of the non-reacting stagnation flow, t_x, obtained from auto-correlation and the associated length scale, lx, obtained by Taylor's hypothesis.

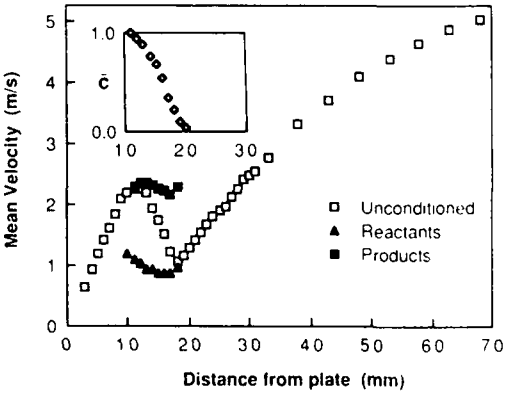

FIG. 2. Mean centerline axial profile of the conditioned and unconditioned velocities for case #1 ($\phi = 1$ and $u' = 40$ cm/s). Inset: profile of the reaction progress variable.

thickness flamelet approximation is valid for turbulent stagnation flames presently considered.

Another important aspect of the scalar field is the heat transfer to the stagnation plate. Since the plate is made of brass, the turbulent flame may be influenced by heat loss from the flame zone. To investigate the possible effect of heat loss, thermocouple measurements were made of the plate temperature and the thermal boundary layer over the plate. The results for case #4 show that, although the plate temperature is only 1500 K, the thermal layer thickness is about 3.0 mm, which is smaller than the standoff distance of the flame brush. This indicates that the wall effect is confined within the product region and is not expected to have any direct influence on flame propagation.

The features of the unconditioned axial velocity profile (Fig. 2) are typical of those measured in the stagnation flames as reported earlier.[1] The unconditioned velocity profile shows three distinct regions. The first region extends from the exit of the nozzle to the upstream boundary of the turbulent flame brush. It is characterized by a steady decrease in the axial velocity due to the divergence of the cold, unreacted flow. The global stretch rate imposed on the flow is given by the mean velocity gradient in this region. The second region is characterized by a rapid increase in velocity, indicating flow acceleration due to combustion heat release. The third region is where the product stream is again decelerated by the presence of negative pressure gradient and the flow is eventually brought to rest at the stagnation plate.

The upstream stretch rate, a, determined from these profiles (Table I) shows that the use of the grid tends to produce a slightly higher upstream stretch rate. This global stretch rate is of the same magnitude as the local stretch rate on the flamelets, which can be estimated by u'/l_t. However, studies on laminar flames[12] have shown that such small stretch rates have minimal effect on the local burning rate.

Within the flame zone, the unconditioned mean velocity increases to form a "hump" at the product boundary as shown in Fig. 2. As discussed previously,[1] this increase is due to intermittent measurement of the conditioned velocities, $\tilde{U}_r$ and $\tilde{U}_p$. The relative velocity between the conditioned mean velocities, $\Delta U = \tilde{U}_p - \tilde{U}_r$, which is referred to as the slip velocity in the BML model, is a major contributor to the unconditioned fluctuations and the second and third order turbulent transport terms. The cause of the so-called counter gradient scalar transport is a direct result of the fact that ΔU is positive in most flames. Shown in Fig. 3 are the four ΔU profiles plotted against $\tilde{c}$ obtained in this study. The data are normalized by the increase in velocity $\Delta u = S_L(\tau - 1)$ across a planar laminar flame where τ is the reactant/product density ratio.

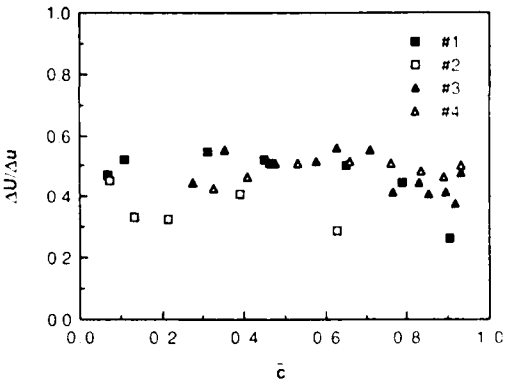

FIG. 3. Dependence of the normalized slip velocity as a function of the reaction progress variable

It can be seen the ΔU's are almost constant and their values are about half of those of Δu. Previous measurements of this ratio in V-flames and conical Bunsen flames have shown that they are independent of $\tilde{c}$ though they are generally lower than unity. As discussed by Cheng et. al.,[13] flow divergence in the products and random flow deflections due to the wrinkled flame could lower this ratio. However, the observation of constant $\Delta U/\Delta u$ ratio for different conditions in the stagnation flames is quite encouraging because it implies that the conditioned and unconditioned velocity profiles may be self-similar. This feature of the stagnation flame profiles is anticipated to facilitate the modeling of these flames. At present, similarity variables for the distance from the plate surface is proposed in BML.[4] The proper means to nondimensionalize the velocity, however, requires further studies.

The conditioned and unconditioned rms fluctuation profiles for the axial and transverse components are shown in Fig. 4. The peak shown in the unconditioned u' profiles (Fig. 4(a)) represents contributions from ΔU. The more significant feature, however, is that the two axial conditioned rms fluctuations are almost equal. This suggests that there is no flame generated turbulence in the axial direction. The lack of a peak in the v' profiles is due to the fact that the transverse component of the relative velocity is zero. The difference in the conditioned fluctuations, $v_p' - v_r'$, is slightly higher at positions close to the product boundary than those shown for the axial component. Recent analysis of turbulence production across turbulent flamelets have shown that the increase in turbulence is associated with vorticity production.[7] Vorticity production is expressed by the baroclinic term which is the cross product between the pressure gradient normal to the flamelet and the local flame curvature due to stretch. In the stagnation flame the adverse mean axial pressure gradient may, by reducing the mag-

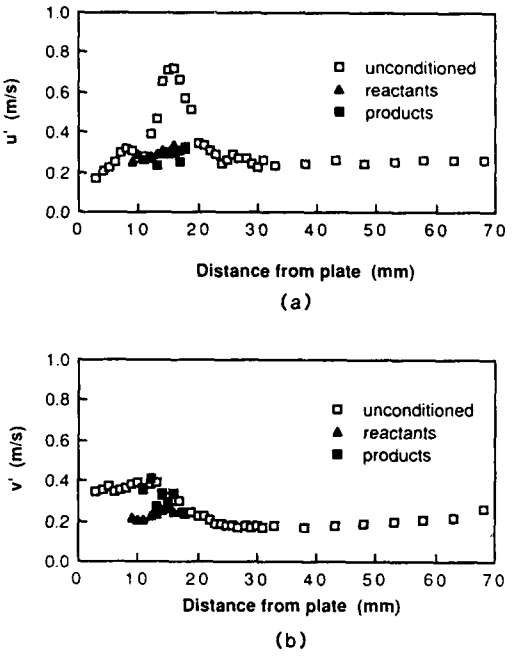

FIG. 4. Conditioned and unconditioned rms velocity fluctuations for (a) axial, (b) transverse components.

nitude of the baroclinic term, suppress production of vorticity. It is, however, important to emphasize the tentative nature of this interpretation, pending further experimental evidence and theoretical analysis.

The lack of significant flame generated turbulence, in particular in the axial fluctuations, also has a significant impact on the modeling of the third order turbulent transport terms. For example, the turbulent diffusion of scalar is modeled[8] as

$$\overline{\rho u''^2 c''}/\bar{\rho} = \bar{c}(1-\bar{c})\{(\tilde{U}_p - \tilde{U}_r)^2[\bar{c}^2 + (1-\bar{c})^2] - \overline{u_r'^2} + \overline{u_p'^2}\}$$

the turbulence flux is

$$\overline{\rho u''^3}/\bar{\rho} = (1-\bar{c})\{3(\tilde{U}_r - \tilde{U})\overline{u_r'^2} + (\tilde{U}_r - \tilde{U})^3 + \overline{u_r'^3}\} + \bar{c}\{3(\tilde{U}_p - \tilde{U})\overline{u_p'^2} + (\tilde{U}_p - \tilde{U})^3 + \overline{u_p'^3}\}$$

where

$$\tilde{U} = \bar{c}\tilde{U}_p + (1-\bar{c})\tilde{U}_r$$

These sub-models consist of contributions from ΔU, the difference in the conditioned turbulence intensities, and the third order terms. However, as the conditioned velocity pdf's are essentially Gaussian, these third order terms may be neglected.[5] In previous theoretical studies, Bray et. al.[3] used an empirical constant to relate the increase in the conditioned velocity fluctuations. To study the relative contributions from the two terms, the ratios $(u_p'^2 - u_r'^2)/(\Delta U)^2$ and $(v_p'^2 - v_r'^2)/(\Delta U)^2$ are plotted in Fig. 5. As can be seen the magnitudes of these ratios are very small, although $(v_p'^2 - v_r'^2)/(\Delta U)^2$ tend to be slightly higher than $(u_p'^2 - u_r'^2)/(\Delta U)^2$ for cases #3 and #4. The lack of significant turbulence production by the flame suggests that all the third order transport can be modeled simply by considering the contributions from the relative velocity ΔU. This again simplifies the modeling scheme.

Concluding Remarks

Reported in this paper is a detailed experimental investigation of the characteristics of the velocity and scalar fields in stagnation flow stabilized premixed

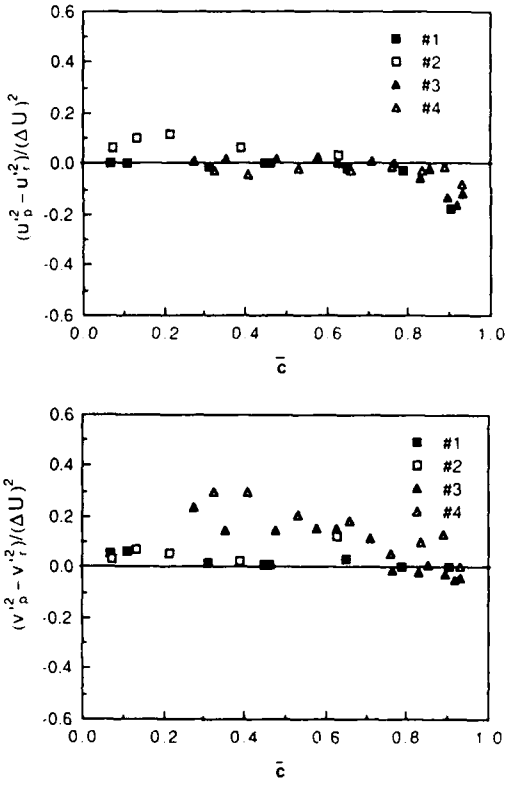

FIG. 5. Relative importance of the first and second moments of conditioned velocities of (a) axial, and (b) transverse components

turbulent flames. This relatively new turbulent flame configuration is considered to be well suited for direct comparisons between experimental and theoretical predictions. The measurements include conditioned and unconditioned velocity statistics of two components, and the profiles of the mean reaction progress variable which is identical to the normalized density in the limit of zero thickness flamelet assumption. The turbulence Reynolds numbers and Damköhler numbers for the four methane/air flames indicate that these flames are within the wrinkled flamelet regime. The experimental results are analyzed to provide insight which will assist in the development of the Bray-Moss-Libby flamelet model for these flames.

For all the flow and mixture conditions considered here, the relative velocity ΔU between the reactants and products, i.e. the difference in the conditioned velocities is constant across the flame brush. Moreover, the relative velocities, when normalized by the velocity increase, $\Delta u = S_L(\tau - 1)$, under laminar condition, have the same value. This suggests that the mean unconditioned velocity profiles across the flame region are self-similar. These characteristics, if confirmed by more extensive studies, would greatly simplify the modeling of the complex turbulent flame flow field.

Within the flame brush, the conditioned turbulence intensities for the axial and transverse velocity components are about equal and constant. That is, the stagnation flames do not create additional turbulence. This is quite different form the results obtained in oblique flames where flame generated turbulence occurs. The most important implication to modeling is that all the second and third order turbulence transport terms are reduced to functions of the relative velocity ΔU. This again implies self-similarity of the turbulence and transport properties.

Acknowledgment

This work was a collaborative effort between the University of California at Davis and the Lawrence Berkeley Laboratories. The work at Davis was supported by the U.S. Air Force Office of Scientific Research under Grant No. 85-0147. The work at LBL is supported by the Director, Office of Energy Research, Office of Basic Energy Sciences, Chemical Science Division of the U.S. Department of Energy under Contract No. DE-AC-03-76SF00098. The authors would like to acknowledge the assistance of Mr. Minh Binh Hua and Mr. David Hackworth in analyzing the conditioned velocity data. It is also a pleasure to thank Prof. Bray, Dr. Champion and Prof. Libby for their helpful discussions.

REFERENCES

1. Cho, P., Law, C. K., Hertzberg, J. H. and Cheng, R. K.: Twenty-First Symposium (International) on Combustion, p. 1493. The Combustion Institute, 1988.
2. Bray, K. N. C., Libby, P. A., and Moss, J. B. Comb. Sci. Tech. 41, p. 143, 1984.
3. Bray, K. N. C., and Libby P. A.: Comb. Sci. Tech. 47, p. 253, 1986.
4. Bray, K. N. C., Champion, M. and Libby, P. A.: Private communication, 1987.
5. Pope, S. B.: Ann. Rev. Fluid. Mech. 19. p 237, 1987.
6. Anand, M. S., and Pope, S. B.: Comb. Flame 67, p. 127, 1987.
7. Pindera, M. Z. and Talbot, L.: Twenty First Symposium (International) on Combustion, p 1357, The Combustion Institute, 1988.
8. Cheng, R. K. and Shepherd, I. G.: Comb. Sci Tech. 52, p. 353, 1987.
9. Cheng, R. K., Shepherd, I. G., and Gokalp, I.: Paper presented at the 6th Symposium on Turbulent Shear Flows, Toulouse, France, 1987.
10. Shepherd, I. G. and Cheng, R. K.: To be published. Comb. Sci. Tech., 1988.
11. Jarosinski, J.: Comb. Flame, 56, 3, p. 337, 1984.
12. Law, C. K., Zhu, D. and Yu, G.: Twenty-First Symposium (International) on Combustion, p 1419, The Combustion Institute, 1988.
13. *Cheng, R. K., Robben, F. A. and Talbot, L.*: Twentieth Symposium (International) on Combustion, p. 453, The Combustion Institute, 1985.

COMMENTS

A. Chomiak, M.I.T., USA. Why did you expect turbulence generation in this stagnation-point flame? Are not the density and pressure gradients almost aligned in this case especially when you consider that the thermal expansion in the radial direction is almost enough to balance the hdrodynamic pressure?

Author's Reply. For other premixed turbulence flames (e.g. v-flames or Bunsen flames), turbulence production is shown by increases in the conditioned rms fluctuations in the product zones. The lack of increase observed here indicates that the centerline of the stagnation flow stabilized flames is an exception. Whether or not this is due to the significant

streamtube divergence as suggested would require the support of data obtained away from the centerline. In particular, measurements made along flowlines (see Cheng, et al., 22nd Combustion Symposium) would be most useful.

•

S. N. B. Murphy, Purdue Univ., USA. A turbulent flow is governed by rather restricted similarity considerations at a stagnation point. What is the basis for the choice of curvature in the experiments? Are there any data to indicate an acceptable curvature for burning rate determination?

Author's Reply. As mentioned in our previous paper (Cho et al. 21st Symposium, p. 1493) the criterion for the plate curvature was to enable the LDA probe to measure flow velocities within 3.0 mm from the plate surface.

At the centerline of the stagnation flow, the only effect of the plate curvature may be the overall stretch rate. This overall stretch rate can be deduced from the velocity profiles. Therefore, the question regarding the "acceptable" range for the curvature is related to the issues concerning the effects of overall stretch on flame propagation. Perhaps the effects of stretch can be studied by varying the plate curvature in contrast to varying the separation distance between the plate and the nozzle exit.

•

T. A. Baritaud, Institut Francais du Pétrole, France. You see that u' remains unchanged when crossing the flame front, when $\bar{U}$ is increased due to the expansion of the gas. Hence, $\rho_u u_u'^2$ is almost instantaneously transformed in a quantity $\rho_b u_b'^2$ much smaller. Where is this turbulent kinetic energy going: increse of the dissipation, effect of the pressure gradient, transfer to the other velocity components . . .?

Author's Reply. As shown in Fig. 4, some of the turbulence kinetic energy is being transferred to the v component. Nevertheless, the total kinetic energy after weighing by the local density is indeed smaller. This is true for most premixed turbulent flames. The present situation may be an extreme case where the effects of streamtube divergence are also significant. As mentioned in the answer to Prof. Ghoniem, conclusions regarding the turbulence production in these flame can only be drawn by comparing measurements made along off-center flowlines.

Twenty-Second Symposium (International) on Combustion/The Combustion Institute, 1988/51-73

PREFERENTIAL DIFFUSION AND CONCENTRATION MODIFICATION IN SOOTING COUNTERFLOW DIFFUSION FLAMES

R. L. AXELBAUM AND C. K. LAW*
Department of Mechanical Engineering
University of California
Davis, California 95616

W. L. FLOWER
Combustion Research Facility
Sandia National Laboratory
Livermore, California 94550

An experimental investigation has been conducted on the influence of the mobility of inert additives on soot formation in propane and ethylene counterflow diffusion flames. Inerts used were helium, neon, argon, or krypton, and the results show that while the mobility of the inert has practically no effect when a small amount of inert is added to the oxidizer side, the influence is significant when added to the fuel side in that krypton, being the least mobile inert, yields the greatest soot loading while helium, being the most mobile, yields the least. By relating the spatially-resolved soot volume fractions to the corresponding profiles of temperature, velocity and species concentrations, it is demonstrated that this influence on soot loading is likely caused by concentration modifications of the fuel and the soot precursors due to the different mobilities of the inert additives.

Introduction

Flame phenomena are strongly influenced by the diffusive processes of the reactants. Since the diffusivities of the various species in a gaseous mixture are in general not equal, it is reasonable to expect that the local reactant concentration will be dependent on the extent with which the diffusivities differ. This concentration modification through preferential diffusion can in turn affect the flame behavior from that anticipated based on the freestream concentrations. Indeed, there exist many flame phenomena which can only be satisfactorily explained on the basis of preferential diffusion. For premixed flames, we cite the earlier works of Refs. 1 and 2 and the recent advances as summarized in Ref. 3. The amount of research on nonpremixed flames, however, has been less; some recent contributions include analyses[4,5] and experiments[6] on flame extinction.

The objective of the present work is to study the effect of preferential diffusion and thereby concentration modification on an important nonpremixed flame phenomenon in which diffusive transport and chemical kinetic processes are inherently coupled, namely soot formation when inerts of different diffusivities are added to either the fuel or the oxidizer stream.

That diffusional stratification may influence the soot formation process can be demonstrated by the following experimental anomaly: In his study of the influence of the various diluents on the soot formation process, McLintock[7] varied the inert diluent on the oxidizer side of an ethylene coflow flame and found that the smoke points decreased in the order of helium, nitrogen and argon. That is, the propensity to soot was least when the oxidizer diluent was helium and greatest when the diluent was argon. With the heat capacities of argon and helium being the same, it was reasoned[7] that the difference was due to the high diffusivity of helium, causing the concentration of helium to be greater within the flame.

An opposite result, however, was reported by Schug et al.,[8] who found that when helium was added to the fuel side of an ethylene coflow diffusion flame, it was not as effective as argon in suppressing soot. In fact, helium was the least effective additive for soot suppression. This behavior was attributed to helium's high thermal diffusivity and its subsequent effect on the temperature distribution and thereby the fuel pyrolysis rate.

While Refs. 7 and 8 have respectively used concentration modification and temperature modifica-

*Present address: Department of Mechanical and Aerospace Engineering, Princeton University, Princeton, NJ 08544

tion to interpret the different trends of their results, it is of interest to note that these observations can also be explained, in a consistent manner, as a consequence of either concentration modification or temperature modification alone. For example, by using the temperature modification interpretation, the difference in the results for helium could be solely a consequence of the broadening of the temperature distribution due to helium.[9] That is, when helium is added to the oxidizer side, the broadened temperature distribution has a greater influence on the rate of particle burnup and a lesser influence on the rate of soot formation, implying that helium would be an effective soot suppressor relative to argon. On the other hand when helium is added to the fuel side, the temperature broadening would promote the soot formation rate but not the burnup rate, implying that helium would be less effective in suppressing soot.

We next adopt the alternate viewpoint that concentration modification could be the physical mechanism responsible for the anomalous results for helium. Recognizing that helium is more mobile than argon, it is clear that when the inerts are added to the fuel, helium will be defocused to a greater extent than argon due to the compressive, concave curvature of the co-flow flame.[3] Consequently, in all but the lowest regions of the flame, the fuel concentration of the helium-diluted mixture will be higher than that of the argon-diluted mixture, implying that the former has a greater propensity to soot. By applying the same reasoning to the oxidizer side, and recognizing that helium is now focused to a greater extent due to the convex flame curvature, the fuel concentration with the helium-diluted oxidizer will be relatively lower, implying that the propensity to soot is reduced.

In order to further understand the relative influences of temperature modification versus concentration modification on the soot formation process, we have adopted an entirely different flame configuration to study the soot response to inert addition. The flame configuration is that of the counterflow diffusion flame. The rationale for such a choice is that in this flame/flow configuration the effect of concentration modification is opposite to that of temperature broadening, thus allowing unambiguous conclusions to be drawn regarding the effect of preferential diffusion. We shall amplify on this point later in the discussion of the experimental results.

In the next section the experimental methodology and arrangement will be specified. This is followed by presentation and discussion of the experimental results.

Experimental Specifications

In this study the counterflow diffusion flame established in the forward stagnation region of a porous cylinder has been used. The flame is amenable to light scattering and extinction measurements and does not suffer from the complication of oxidizer entrainment at the rim as with jet (co-flow) flames. Measurements are taken along the forward stagnation streamline, which is a line of symmetry.

The burner apparatus is similar to that used by Vandsburger et al.[10] and has been described in detail in an earlier work.[11] Briefly, it consists of a porous cylinder mounted horizontally in a vertically oriented wind tunnel that has a uniform velocity profile across its test section. The cylinder is mounted to a vertical translator which allows it to be moved in the streamwise direction. The oxidizer gas is supplied by the wind tunnel while the fuel gas is ejected from the porous cylinder. The cylinder is composed of a sintered stainless steel tube with an outside diameter of 2.5 cm, a length of 8 cm, and is cooled uniformly along its axis.

The fuels used are commercial grade ethylene and instrument grade propane. The inerts used are krypton, argon, neon and helium.

Temperature measurements are obtained with silica-coated Pt/Pt-12%Rh thermocouples. The wire diameters used are 0.076 mm for the diluted-propane flames and 0.127 mm for the diluted-ethylene flames as well as flames where the composition of the oxidizer inert is varied. The smaller thermocouple is preferred because it offers less disturbance to the flame and less measurement error due to radiation loss. However, the temperatures in these latter flames are high enough that the thinner thermocouple would melt, thus necessitating the use of the thicker thermocouple.

Soot measurements are obtained by using standard light scattering and extinction techniques with an apparatus and procedure identical to those of Flower and Bowman[12] and described in greater detail in Ref. 11. Soot volume fraction is obtained from the Lambert-Beer law for light extinction with the assumption that the soot particles behave as spherical Rayleigh scatterers and have a complex refractive index of $\tilde{n} = 1.57 - i0.56$. The soot volume fraction is assumed uniform over the length of the burner, with no correction for end effects. Since this work is concerned with relative changes instead of absolute values, the Rayleigh assumption is acceptable.

Gas sampling of the stable species is performed with an uncooled, quartz microprobe designed with the criterion of Fristrom and Westenberg.[13] To allow for sampling in the sooting region of the flame a probe was designed with an internal plunger[11] that allows soot build-up at the probe orifice to be removed periodically. The orifice diameter is 70 μm and, to ensure that reactions are quenched, sampling is conducted at pressures such that the flow through the orifice is choked. The gas samples are obtained by batch sampling into evacuated vessels and the gas analysis is performed by quantitative

mass spectrometry. Since batch sampling is used, data are not available for water and results are reported on a dry basis.

A standard single-component, laser-Doppler velocimetry (LDV) system is used to measure the velocity component along the forward stagnation streamline. Measurements are made in the forward scattering mode, without frequency shifting. Aluminum-oxide seed particles of 0.05 μm nominal diameter are supplied on the oxidizer side.

The soot loading of the propane diffusion flame in air is too low to measure extinction accurately. To increase the soot loading of propane flames the oxygen volume fraction in the oxidizer is increased from 0.21 to 0.25, with the balance being nitrogen. Ethylene flames do not require enrichment and their oxygen concentrations are maintained at that of air.

For the experimental conditions in this study the flame location is a few millimeters on the oxidizer side of the stagnation point (Fig. 1). The soot formation and growth region lies between the flame and the region of the stagnation point. A consequence of this is that it is the flow field on the oxidizer side that is of primary importance for residence time considerations. Therefore, the upstream velocity of the oxidizer is maintained at 38 cm/s for all studies.

An additional consideration is the gas flow ejected from the burner. Two approaches are used in this study. One is to maintain the volumetric flow rate of the fuel constant. In this case the addition of gas to the fuel increases the ejection velocity from the burner. The other approach is to maintain the fuel ejection parameter constant.[15] The fuel ejection parameter defined for variable gas density is $f_u = -(\rho_u v_u/\rho_\infty)(\kappa\nu_\infty)^{-1/2}$, where ρ_u and v_u are the gas density and velocity at the burner surface, ρ_∞ and ν_∞ the freestream values of density and kinematic viscosity for the oxidizer, and κ the characteristic velocity gradient defined as $\kappa = 2U_\infty/R$, with U_∞ being the freestream velocity of the oxidizer and R the burner radius. The fuel ejection parameter defined in this way allows flow similarity to be maintained even when variable density inerts are added. Only results for constant fuel ejection parameter, $f_u = -3.0$, will be presented herein because maintaining flow similarity allows for an interpretation based on distance from the burner. It is of interest to note that the results were found to be independent of whether fuel flow rate or fuel ejection parameter is held constant.

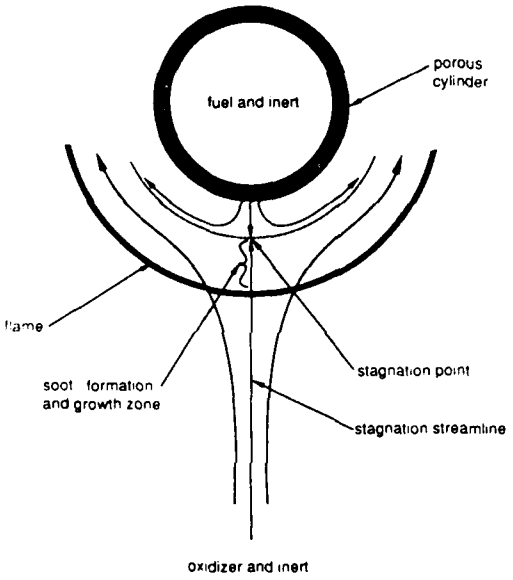

FIG. 1. Cross section of the counterflow diffusion flame established in the forward stagnation region of a porous cylinder.

Results and Discussions

As discussed in the Introduction, both concentration modification and temperature broadening will yield similar trends for inert addition to the coflow flame. Therefore it is difficult to determine with the coflow flame which, if either, mechanism is the dominant cause for the observed trends. This is not the case with the counterflow diffusion flame. By referencing Fig. 1 it can be seen that the fuel reaches the flame by diffusing across the stagnation plane into the oxidizer side. The streamlines on both the fuel and oxidizer sides of the stagnation plane are such that lighter species, which can more easily diffuse across the streamlines, will preferentially accumulate in the region of the stagnation streamline, while heavier species will be preferentially swept away. Consequently, when helium is added to the fuel, concentration modification should lead to a reduction in fuel concentration and, thereby, a corresponding reduction in the soot loading as compared to the situation of adding argon to the fuel.

We further note that soot burn-up does not occur in the forward stagnation region of the counterflow diffusion flame. Therefore, if helium addition were to broaden the temperature distribution, the effect would be to increase the soot loading as based on the reasoning of Ref. 8 discussed in the Introduction. Thus, in the counterflow diffusion flame, the effect of concentration modification is opposite to that of broadening of the temperature distribution and we can compare the relative importance of the two mechanisms for this flame.

In addition to helium and argon we have also used neon and krypton for diluents in this study. All diluents are therefore completely inert and since they are monatomic and have the same heat capacity, they should have a similar influence on the maximum flame temperature.

The soot volume fraction drops off around the

stagnation point because of the inability of the soot particles to propagate past the stagnation point into the fuel side (see Fig. 1). Data in this region have been suppressed as they are not relevant to this work.

The soot volume fraction distributions along the stagnation streamline for the propane/inert mixtures are plotted in Fig. 2. The curves show a strong relationship between the mobility of the inert and the maximum soot loading for the flame. Krypton, being the least mobile inert, yields the greatest soot loading (0.52×10^{-6}) while helium, being the most mobile, yields the lowest soot loading (0.26×10^{-6}).

The results for inert addition to ethylene, shown in Fig. 3, display trends similar to those of the propane flames in both their relationship to the inert mobility and in the extent of the change in soot volume fraction, the soot loading increases with decreasing inert mobility, and the maximum soot volume fraction of the krypton-diluted flame is about twice as high as that of the helium-diluted flame.

The above results indicate that the soot loading varies with the mobility of the inert added. To determine whether the primary cause for the change in the soot loading is indeed modification of the fuel concentration, we have determined the temperature, velocity, and species concentration profiles for these flames.

Figure 4 shows the temperature distributions, uncorrected for radiation losses, for the propane/inert mixtures. The oxygen concentration for the temperature measurements is that of air, or 21 percent by volume, as compared to 25 percent for the soot volume fraction measurements. While the trends in maximum temperature and temperature distribution will not be affected by the lower oxygen concentration, the soot loading is much reduced. Consequently, the accuracy and reproducibility of the measurements are greatly improved due to the fact that soot build-up on the thermocouple is less.

The maximum flame temperatures measured show slight increases with decreases in the mobility (increases in the molecular weight) of the inert, krypton yields the highest temperature (1641° C), he-

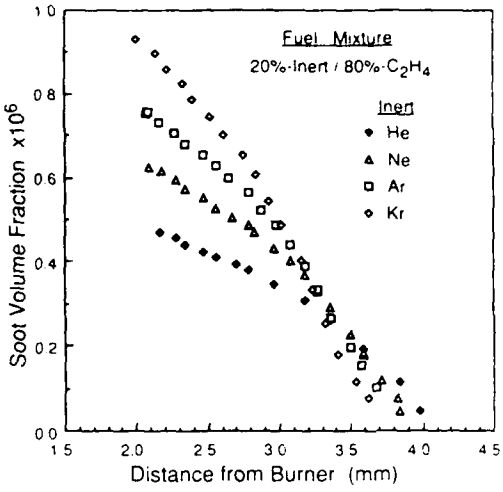

FIG. 3. Soot volume fraction as a function of distance from burner surface for ethylene/air counterflow diffusion flames with inert addition on the fuel side.

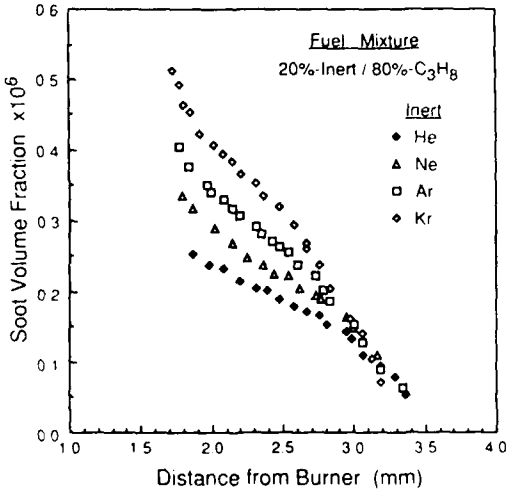

FIG. 2. Soot volume fraction as a function of distance from burner surface for propane/enriched air (25% O_2) counterflow diffusion flames with inert addition on the fuel side.

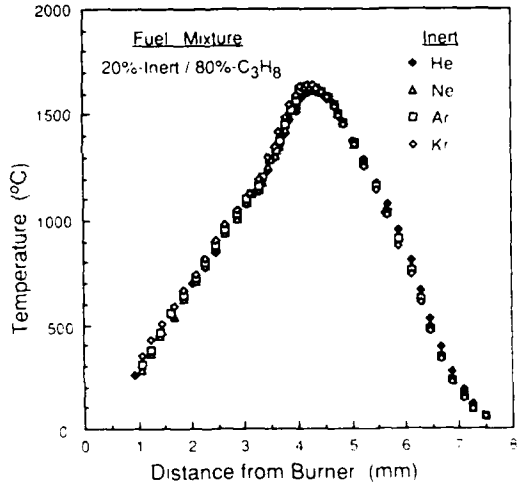

FIG. 4. Temperature distribution for propane/air counterflow diffusion flames with inert addition on the fuel side.

lium the lowest (1607° C), with a difference of 34° C. The temperature profiles are similar with no significant broadening for the lighter inerts.

One may ask, at this point whether the 34° C difference in the maximum measured temperature seen in Fig. 4 could account for the two-fold difference in soot loading. The influence of this temperature difference has been investigated by varying the flame temperature in such a way that the reactive species concentrations are not affected.[11] The results show that even with a 43° C increase in the maximum measured temperature the soot loading increases by only 13%.

For the diluted ethylene flames the maximum flame temperatures were measured and were found to be within 20° C for flames diluted with each of the four inerts. Considering this along with Fig. 4 it is reasonable to expect that temperature effects have only a minor role in explaining how the inerts are influencing the soot volume fractions.

We next note that there is the possibility that the velocity fields vary for the different flames and consequently the residence times are not similar. Since the soot formation and growth region lies nominally between the flame and the stagnation point, it is the velocity field in this region that influences the residence times of the soot particles. Figure 5 is a plot of velocity along the stagnation streamline versus distance from the burner surface for the propane flame when diluted with the inerts. The velocity fields are almost identical, which is reasonable because the temperature fields are almost identical and we have maintained fluid-dynamic similarity by holding $2U_x/R$ and the fuel ejection parameter f_u constant.

A close inspection of Figs. 2–5 reveals that the locations of the flame and stagnation point are shifted away from the burner surface as the mobility of the inert is increased. The shift in stagnation point is most accurately indicated by the locations of maximum soot in Figs. 2 and 3 while the shift in flame location is indicated by both peak temperatures and velocities in Figs. 4 and 5. The shifts are small ($<1/2$ mm) and will not influence soot particle residence times because the flame and stagnation point shift together.

This shift can be understood by considering the fact that in these experiments we have maintained f_u and κ fixed so that, in the nonreactive limit, the flow fields are similar in terms of $\eta = (\kappa/\rho_\infty\mu_\infty)^{1/2} \int_0^y \rho dy$. Therefore, while the stagnation points occur at the same η for all flows, they are shifted in the physical coordinate y. For example, since the density is less in the helium-diluted flame, the physical distance to the stagnation point is greater. Estimates using mean densities show agreement between the anticipated and observed shifts.

With the velocity and temperature fields being largely independent of the additive mobility, the implication is that the local concentrations of the reactive species have been modified. To verify this, a measurement of the species concentrations within the sooting flames is obtained. Probe sampling of the stable species is performed at conditions similar to those of the temperature measurements, in that the oxidizer is 21 percent oxygen as compared to 25 percent used for the soot data. The lower oxidizer concentration reduces the extent of sooting while preserving the important concentration features.

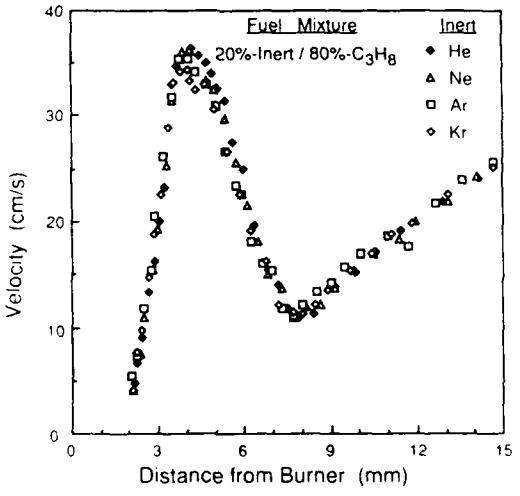

FIG. 5 Velocity as a function of distance from the burner surface for propane/enriched air (25% O_2) counterflow diffusion flames with inert addition on the fuel side.

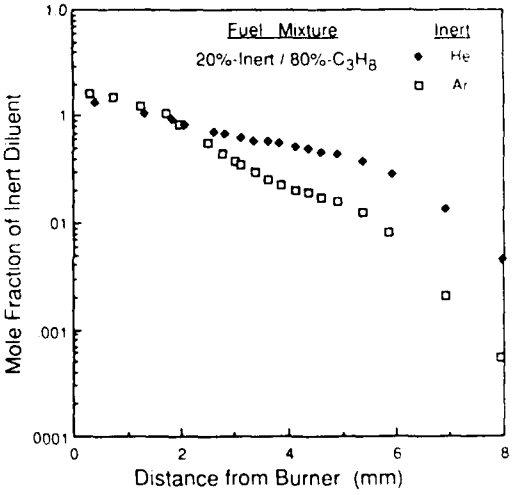

FIG. 6. Mole fraction profiles of inert diluent (helium and argon) in propane/air counterflow diffusion flames with inert addition on the fuel side.

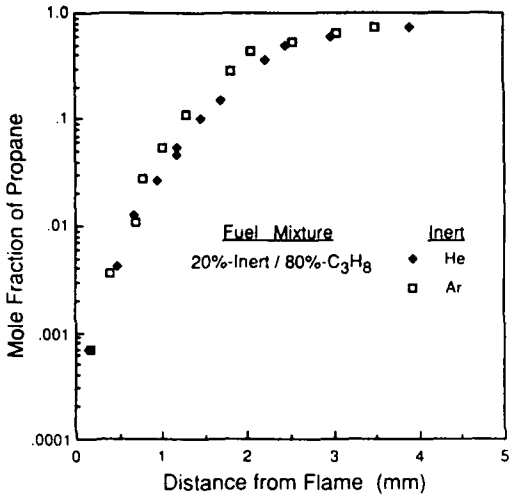

FIG. 7. Mole fraction of parent fuel as a function of distance from the flame for propane/air counterflow diffusion flames with inert addition on the fuel side.

Figure 6 compares the mole fraction profiles of helium and argon for the helium- and argon-diluted flames, respectively. The mole fraction of the inert diluent in the flame region is higher in the helium-diluted flame than in the argon-diluted flame, a consequence of the disparity in the inert mobilities.

Since the local concentrations of the additive differ, the local fuel concentrations could be affected. The relevant coordinate to compare propane concentrations is distance from the flame, rather than distance from the burner because concentration gradients in the flame region are steep and the flame locations are not precisely the same. In Fig. 7 the mole fraction of the parent fuel, propane, is plotted as a function of distance from the flame. Near the flame, the concentration gradients are found to be less for the helium-diluted flame which, in itself, delineates that the mole fraction of the fuel will be locally less, and Fig. 7 illustrates this. However, a caveat is necessary with regard to interpreting Fig. 7. The concentration gradients are so steep near the flame that spatial measurement errors of just 0.1 mm could influence the conclusions drawn. Although care was exercised to maximize the spatial accuracy, there is an alternative means of demonstrating the effects of preferential diffusion that is not as sensitive to spatial accuracy.

Concentration modification of the fuel will necessarily lead to a modification of the concentrations of the fuel-based species in the flame and these species will attain a maximum somewhere within the flame. The maximum is insensitive to location and, where applicable, is a good indicator of the relative availability of soot precursors. Table I lists the maximum mole fractions for all measured species except for ethane and propadiene which did not display obvious maximums. Without exception, the mole fractions are higher in the argon-diluted flame, and, in the case of potentially important soot-particle precursors, notably butadiyne (diacetylene), butadiene and benzene, the mole fractions are 15–25% higher. The results demonstrate that the local mixture composition is indeed modified in the presence of preferential diffusion and this modification can influence soot formation.

TABLE I
Maximum mole fraction of stable species in propane/air counterflow diffusion flames with inert addition on the fuel side.

	Maximum Mole Fraction					
Fuel Mixture	Hydrogen (H_2)	Carbon Monoxide (CO)	Carbon Dioxide (CO_2)	Methane (CH_4)	Acetylene (C_2H_2)	Ethylene (C_2H_4)
20% He/80% C_3H_8	.038	.052	.086	.017	.018	.030
20% Ar/80% C_3H_8	.042	.057	.091	.018	.020	.032
% Difference	10	9	6	6	10	6
	Propene (C_3H_6)	1-3 Butadiyne (C_4H_2)	1-3 Butadiene (C_4H_6)	2-Butene (C_4H_8)	Cyclopentadiene (C_5H_6)	Benzene (C_6H_6)
20% He/80% C_3H_8	.0066	.00042	.00066	.00063	.00021	.00048
20% Ar/80% C_3H_8	.0070	.00049	.00089	.00068	.00024	.00060
% Difference	6	14	26	7	12	20

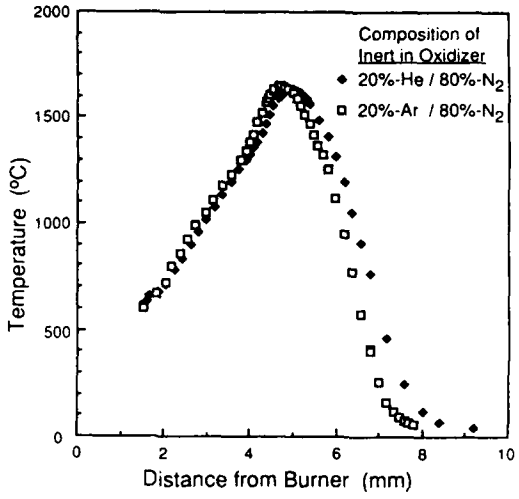

FIG. 8. Temperature distribution for propane/air counterflow diffusion flames with 20% of the nitrogen in the oxidizer replaced with argon or helium.

It may appear somewhat surprising that the stratification of the inert concentrations would affect the composition without affecting the temperature distributions. Although the thermal diffusivities of the inerts used vary widely, these additives are only a small portion of the total gas composition in the region of the flame. Consequently, the thermal transport properties are still dominated by the major species, e.g. nitrogen. The fuel concentration, however, is coupled to the inert concentration so that stratification of the inert can have a significant effect on the concentrations of fuel-related species.

The effects of inert mobility on the oxidizer side of a propane flame are considered in Figs. 8 and 9. Twenty percent of the nitrogen in the oxidizer is replaced with either argon or helium so that the concentration of these test inerts in the oxidizer is 15 percent. Figure 8 reveals that the maximum temperatures of the helium- and argon-diluted flames are still quite similar even though the helium-diluted flame shows some broadening of the temperature distribution. Furthermore, the maximum soot volume fractions seen in Fig. 9 are almost identical. Referring to Fig. 1 it is seen that the transport of fuel from the stagnation point to the flame is totally dependent on diffusion while the transport of the oxidizer to the flame is assisted by convection. Therefore it is reasonable that the mobility of the inert added to the fuel would have a strong influence on fuel concentrations while adding the same inert to the oxidizer side would have little effect on fuel concentrations.

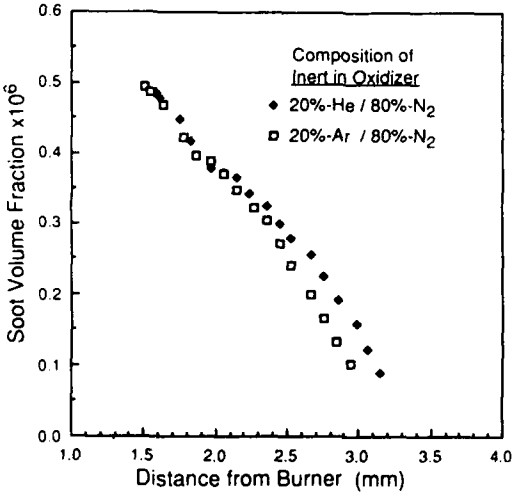

FIG. 9. Soot volume fraction as a function of distance from burner surface for propane/enriched-air (25% O_2) counterflow diffusion flames with 20% of the nitrogen in the oxidizer replaced with argon or helium.

Concluding Remarks

In the present investigation we have provided experimental evidence that gives strong support to the concept that soot formation in diffusion flames can be significantly affected by concentration modification due to preferential diffusion of the reactive/inert species. We have further shown that, while this result is reasonable and possibly not unexpected, a convincing demonstration of this fact requires careful consideration and ultimately elimination of other possible causes, such as those due to the potential modification of the temperature and velocity fields.

Recognizing the existence and importance of diffusional stratification of the concentrations of the reactive mixtures, it would be of interest to extend the present investigation to diffusion flames of other configurations, to premixed flames, and to the formation of other pollutant species which are sensitive to concentration modifications.

Acknowledgments

The work at Davis was supported by the U.S. Air Force Office of Scientific Research under Grant No. 85-0147. The work at Sandia National Laboratories was supported by the U.S. Department of Energy, Office of Basic Energy Sciences, Division of Chemical Sciences. We thank Professor I. Glassman of Princeton University for his valuable insights and comments.

REFERENCES

1. LEWIS, B. AND VON ELBE, G.: Combustion, Flames and Explosions of Gases, 2nd Ed., Academic Press, 1961.
2. MARKSTEIN, G. H.: Non-Steady Flame Propagation (G. H. Markstein, Ed.) Chap. D, Pergamon, 1964.
3. LAW, C. K.: Dynamics of Stretched Flames, this Symposium.
4. LAW, C. K. AND CHUNG, S. H.: Comb. Sci. Tech. 29, 129 (1982).
5. CHUNG, S. H. AND LAW, C. K.: Comb. Flame 52, 59 (1983).
6. ISHIZUKA, S.: Nineteenth Symposium (International) on Combustion, p. 319, The Combustion Institute, 1983.
7. MCLINTOCK, I. S.: Comb. Flame 12, 217 (1968).
8. SCHUG, K. P., Manheimer-Timnat, Y., Yaccarino, P. and Glassman, I.: Comb. Sci. Tech. 22, 235 (1980).
9. GLASSMAN, I.: personal communication, 1986.
10. VANDSBURGER, U., KENNEDY, I. AND GLASSMAN, I.: Comb. Sci. Tech. 39, 263 (1984).
11. AXELBAUM, R. L., FLOWER W. L. AND LAW, C. K.: To appear in Comb. Sci. Tech.
12. FLOWER, W. L. AND BOWMAN, C. T.: Twentieth Symposium (International) on Combustion, p. 1135, The Combustion Institute, 1985.
13. FRISTROM, R. M. AND WESTENBERG, A. A.: Flame Structure Chap. 9, McGraw Hill, 1965.
14. AXELBAUM, R. L., LAW, C. K. AND FLOWER, W. L.: To be published.
15. KENNEDY, I.: Twentieth Symposium (International) on Combustion, p. 1095, The Combustion Institute, 1985.

COMMENTS

R. J. Santoro, Pennsylvania State Univ., USA. In the presentation, you indicated that the temperature was held constant to within about 40K. Could the variation in temperature account for the small changes (approximately 20%) you observed in the species concentration.

Author's Reply. The concentration modification resulting from preferential diffusion influences flame temperature, and any difference in temperature could, in turn, affect the concentrations of the pyrolysis products. For the helium- and argon-diluted flames the measured difference in maximum temperature is 30°C and a similar temperature difference is found throughout the pyrolysis region. (Note that if there was a noticeable broadening of the temperature distribution due to helium addition, the temperature difference of the two flames would have been even less in the pyrolysis region.)

This difference in temperature certainly plays a role in the concentration differences, however we do not believe that temperature alone can account for the measured differences in either soot or species concentrations. While the authors are not aware of any data describing how flame temperature influences species concentrations for this flame, some insight can be gained by considering results where the influence of temperature on soot concentration of a propane flame was studied.[1,2] When flame temperature was increased 43°C without changing either the fuel or oxidizer concentration, the maximum soot concentration increased only 13%, far less than the almost 60% increase observed between the helium- and argon-diluted flames of the present study. The variation in species concentrations resulting from a 30°C increase in temperature would not appear to account for the observed variations in soot concentration.

The species measurements shown in Table 1 and Fig. 7 also imply that factors other than temperature are responsible for the measured differences. Not only are the products and by-products of the fuel greater in the argon-diluted flame, the parent fuel concentration is also locally greater—an unlikely result if temperature is responsible for the concentration differences.

REFERENCES

1. AXELBAUM, R. L.: Fundamental Studies of Soot Formation in Diffusion Flames, Ph.D. Dissertation, University of California, Davis, 1988.
2. AXELBAUM, R. L., LAW, C. K., AND FLOWER, W. L.: The Effects of Diffusional Stratification and Oxygen Addition on Soot Formation in a Counterflow Diffusion Flame, Spring Technical Meeting of the Western and Canadian Sections, the Combustion Institute, Banff, Alberta, Canada, April 28–30, 1986, Paper no. 86-87.

Twenty-Second Symposium (International) on Combustion/The Combustion Institute, 1988/387-394

EXPERIMENTS ON THE SOOTING LIMITS OF AERODYNAMICALLY-STRAINED DIFFUSION FLAMES

D. X. DU, R. L. AXELBAUM AND C. K. LAW
Department of Mechanical Engineering
University of California
Davis, California 95616

An experimental study has been performed with axisymmetric counterflow diffusion flames to investigate the influence of aerodynamic straining on the relevant sooting limits of the lower alkanes. The limits are defined by the critical strain rate at which either soot luminosity, soot particle light-scattering, or fluorescence is negligible compared to the appropriate background signal. The critical strain rates are found to be greatest for the sooting limit based on the fluorescence signal, with those based on luminosity and light-scattering being similar. The fluorescence signal, if attributed to polycyclic aromatic precursors, yields a limit that can be interpreted as the extinction of soot precursors and is suggested to be a possible limit for identifying a completely nonsooting flame condition. The separate effects of flame temperature and fuel concentration on the critical strain rates for soot extinction have also been studied. The results are indicative of how temperature and concentration influence the soot particle inception process and they show that both are potentially important parameters. The critical strain rates display an Arrhenius temperature dependence and this dependence is similar for all alkanes considered.

Introduction

Soot formation is a rate process, and as such is subjected to residence time considerations.[1,2] Since most flames are under the influence of aerodynamic straining, the relevant time scale for such flames is the rate of strain experienced by the flame, expressed in the unit of inverse time.[3] Indeed, Tsuji and Yamaoka[4] have shown that disappearance of the luminous yellow zone in a counterflow diffusion flame can be achieved by increasing the strain rate of the approach flow.

The present study aims to provide a detailed experimental investigation of the influence of aerodynamic straining on particle formation/extinction along the following directions. First, we note that the strain rate of Ref. 4 is a global one, valid in the limit of an inviscid, incompressible, nonreactive, unbounded flow. It is reasonable to expect that the actual, local strain rate as experienced by the flame can be substantially different from the global definition. We shall therefore use the local strain rate, determined by laser Doppler velocimetry, as the parameter to quantify the various soot extinction phenomena to be studied.

Our second objective is to understand and quantify the definition of the sooting limit, i.e., soot inception/extinction limit, in diffusion flames and the various sub-processes associated with it, using the local extinction strain rate as the quantifying parameter. Specifically, it is of interest to explore whether there is a close relation between the visual disappearance of the yellow luminous region and the actual disappearance of the soot particles. This is a relevant concern because for diffusion flames the temperature at the location of the peak soot volume fraction is typically many hundreds of degrees lower than the flame temperature.[5,6] Therefore soot luminosity, with it's T^4 dependence, may not be an accurate indication of soot extinction in these flames. Furthermore, because of this temperature dependence, luminosity may not be appropriate for studying the relative effects of temperature on the sooting limits.

An additional consideration with the definition of soot extinction is that since the formation of soot particles is preceded by the formation of soot precursors, absence of the particles does not necessarily imply the corresponding absence of the precursors and thereby the inability to soot. We shall therefore also provide experimental data and evidence which attempt to distinguish between the sooting limits of the particles and precursors.

Having defined the strain rate and the sooting limits, our third objective is to use these definitions to quantify the influences of temperature and inert addition to the fuel on the sooting limits. Since inert addition changes both the flame temperature as

well as the fuel concentration, it is necessary to isolate these two factors and separately identify their individual effects, as has been done in Ref. 6. In this previous work it was suggested that fuel dilution can have a significant influence on soot volume fraction by changing the total surface area in the particle inception zone. Since the inception limit is concerned with whether particles are produced, not how many are produced, it is not clear a priori whether dilution affects the inception limit as well. Furthermore, while the importance of temperature on soot formation is well documented as it relates to soot yield,[7] there are no known studies on how relevant flame temperature is to the sooting limits. In our study, temperature adjustment will be accomplished by substituting a portion of the nitrogen in the oxidizer with an equal quantity of argon. With this technique the flame temperature can be adjusted without affecting the concentration of the reactants on either the fuel or oxidizer sides of the flame.

The experimental methodology is outlined in the next section, which is followed by presentation and discussion of the experimental results.

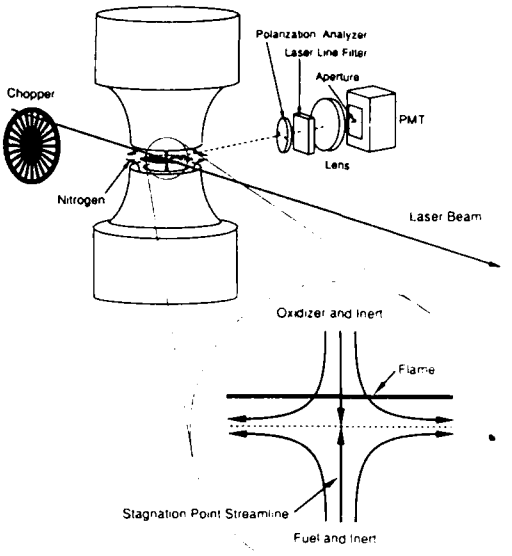

FIG. 1. Schematic of the burner configuration and the optical system used to measure light scattering.

Experimental Methodology

The opposed-jet counterflow diffusion flame is employed in this study. This flame is stable and has a simple, well-defined, axisymmetric flow field.[8] The flame is amenable to light-scattering measurements and does not suffer from the complication of oxidizer entrainment at the rim that occurs in coflow flames. Measurements are taken along the centerline, which is the stagnation point streamline.

The burner configuration is shown in Fig. 1. The flame is stabilized in the region of the stagnation plane established between two converging nozzles. Coflowing nitrogen is employed to eliminate oxidizer entrainment and extinguish the outer flame.

Figure 1 also shows the optical system employed to measure light scattering. The beam of an argon-ion laser operating at 488 nm is modulated by a mechanical chopper and then focused with a 300 mm focal length lens at the midspan of the burner. After passing through a standard set of collection optics, the detection of scattered light is accomplished with a photomultiplier tube whose output is processed by a lock-in amplifier interfaced to a microcomputer.

Close to the sooting limit there are three significant sources of light scattering in these diffusion flames: gaseous Rayleigh scattering, particulate Rayleigh scattering, and broadband fluorescence. Since the species responsible for the fluorescence, assumed[9-11] to be polycyclic aromatic hydrocarbons (PAH), are usually associated with the soot precursor molecules,[10,12,13] then the disappearance of the fluorescence signal may be an indication of the limit at which precursor extinction has been achieved. Therefore, determining a viable method of discriminating between the three sources of scattering is an important aspect of this work; the details are discussed in the Results section.

Temperatures are determined with BeO-Yt_2O_3 coated Pt-20%Rh/Pt-40%Rh thermocouples with a 0.05 mm wire diameter. The lead wires are oriented parallel to the flame to minimize conduction errors. Radiation corrections are performed by assuming a convection/radiation balance on a spherical bead with a value of 0.38 for the emissivity.[14] In the calculation, the Nusselt number is assumed to be constant and equal to 2.0.

A standard single-component, laser-Doppler velocimetry (LDV) system is used to measure the velocity along the forward stagnation streamline. The system is operated in the forward scattering mode, without frequency shifting. Aluminum-oxide seed particles with a 1.0 μm nominal diameter are supplied on the oxidizer side.

For the present axisymmetric counterflow flame we define the strain rate K as the negative of the measured velocity gradient, $-dv/dy$, ahead of the flame. In Fig. 2 a typical curve showing the measured velocity field along the stagnation streamline is shown. The data is taken on the oxidizer side of the stagnation point where the flame and soot formation regions occur. The velocity gradient is found by fitting the data upstream of the flame.

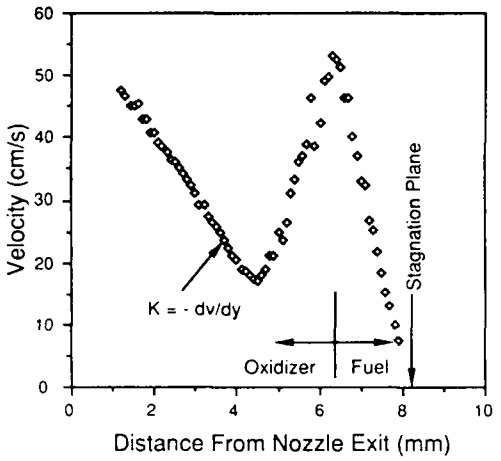

FIG. 2. A typical velocity profile for the axisymmetric counterflow diffusion flame, illustrating the method of determining the local strain rate from the streamwise velocity gradient ahead of the flame.

Results and Discussions

Particle-Inception and Fluorescence Limits:

In obtaining a particle-inception limit, our intention is to find the critical strain rate where particle inception is so small that light scattering from soot particles is negligible compared to background scattering. Near this limit there are three significant sources of light scattering: Rayleigh scattering due to gases and particles, and fluorescence, presumably due to PAH's. The soot particles are spherical in this early stage of their life and therefore, as with Rayleigh scattering from gases, the light remains polarized. Furthermore, since the scattering is elastic, the wavelength is unchanged. On the other hand the inelastic fluorescence signal is depolarized and broadband with both stokes and anti-stokes fluorescence.[15-17] In fact, for a 488 nm excitation wavelength, the spectral peak of the fluorescence signal is located close to the excitation wavelength λ_o, with a large contribution of the signal being at λ = 488 nm. Consequently, near the sooting limit the fluorescence signal can be of the order of the Rayleigh signal even though a laser line filter and polarization analyzer are employed ahead of the detector to diminish the fluorescence signal (Fig. 1).

To obtain a true particle limit it is necessary to discriminate between the Rayleigh signal and the residual fluorescence signal. To do this we exploit the fact that, unlike Rayleigh scattering, fluorescence is depolarizing. Total depolarization of the fluorescence signal has been checked by measuring the vertical (S_{vv}) and horizontal (S_{hv}) scattering components with an edge filter used to remove the elastic scattering signal. It was found that $S_{vv} = S_{hv}$ for $\lambda > 530$ nm. Then it is reasonable to assume that $S_{vv} = S_{hv}$ at λ = 488 nm, and a measurement of S_{hv}(488 nm) will reveal how much of S_{vv}(488 nm) is due to fluorescence.

Figure 3 illustrates the method of obtaining the particle inception limit. First a spatial profile of S_{vv}(488 nm) is obtained (Fig. 3a). This signal contains contributions due to fluorescence and Rayleigh scattering from gases and particles. A profile of S_{hv}(488 nm) is then obtained (Fig. 3a) and this profile is subtracted from the S_{vv}(488 nm) profile to yield a profile that is only due to elastic scattering (Fig. 3b). The peak in Fig. 3b is due to scattering from particles while the balance is due to scattering from molecules. The signal rises after the peak because we are entering the cold fuel zone. The critical strain rate for the suppression of soot is ob-

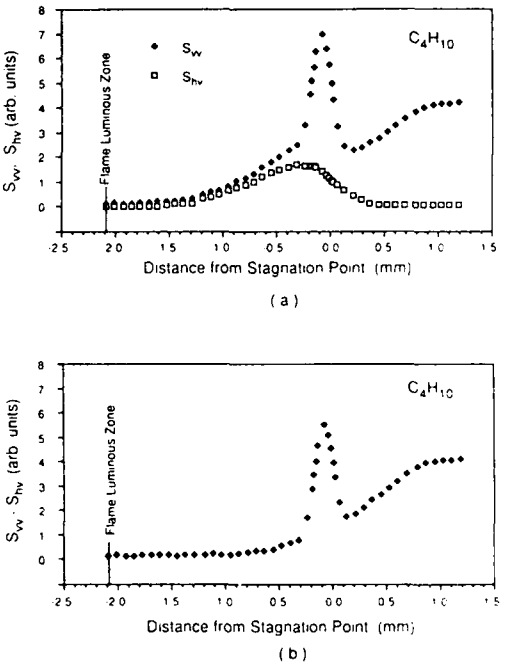

FIG. 3. Profiles of the measured scattering intensity, in arbitrary units, illustrating the method of determining the particle-inception limit. In Fig. 3a the horizontally and vertically polarized components of detected light are plotted as functions of distance from the stagnation point. The detected light has passed through a 1 nm laser line filter centered on the incident wavelength 488 nm and some fluorescence (S_{hv}) is observed to pass through the filter. In Fig. 3b the fluorescence signal has been subtracted from S_{vv} so that the remaining signal is elastic scattering from molecules and soot particles.

tained by increasing the strain rate until the peak is eliminated. This condition is identified as the particle-inception limit K_P which is quite sensitive to changes in strain rate when K is less than K_P, and the limit can easily be determined within around $\pm 3\ s^{-1}$. For K greater than K_P the scattering profile is only weakly affected because the remaining signal is due to scattering by molecules.

It is worthwhile to note that, as with coflow flames,[12] the peak of the fluorescence signal just precedes the particle inception region; this region can be identified by the initial rise of the peak located around 1.5 mm from the luminous zone. This sequential relationship has been used to support the view that the fluorescing molecules are, if nothing else, by-products of the soot inception chemistry.

It is desirable to base the particle and fluorescence limits on the same background signal, i.e., the molecular scattering signal. To accomplish this we continue to measure S_{tt} but the laser line filter is removed so that a large fluorescence signal is obtained. At this strain rate, scattering from particles is negligible because we are already at the inception limit. By again increasing the strain rate, the base-line light scattering signal from molecules is retrieved at another critical strain rate, K_F, which we shall refer to as the fluorescence limit at which production of the fluorescing PAH's is assumed to be suppressed. This limit might be interpreted as a representative precursor limit although it is recognized that there are important precursors at different stages of the soot formation process that do not fluoresce, and that the fluorescing species for $\lambda_0 = 488$ nm may not actually be the precursors themselves.

The sooting limit based on soot luminosity is also measured. Here the limit, indicated by K_L, is defined as the condition where the yellow luminous zone is no longer visibly perceptible when viewed through a 5X stereoscope.

The flame extinction limit, K_E, has also been determined by increasing the strain rate until the flame is extinguished. We then measure the velocity gradient in a flame with a slightly lower strain rate where a stable flame can exist and define this point as the flame extinction limit.

Table I lists the limits of luminosity (K_L), particle inception (K_P), fluorescence (K_F), and flame extinction (K_E) for flames of methane, ethane, propane and butane with air. For a given fuel/air system, the relation $K_L \approx K_P < K_F < K_E$ is evident. Luminosity appears to be an adequate method of determining the particle limit. However, it should be noted that the luminosity measurement is somewhat subjective and potential errors are much greater than for the measurement of K_P. In fact, an acceptable measurement of K_L for methane could not be made. The methane flame has a noticeable amount of emission in the red due to the overtone bands of water[18] and this emission also occurs in the region of the luminous yellow zone. Therefore, it is extremely difficult to determine the limit at which the luminous yellow has disappeared when the background is red. The red emission was evident to a lesser extent in the other flames and did not cause as great an ambiguity.

TABLE I

Critical strain rate limits based on soot luminosity, soot-particle light-scattering, PAH fluorescence and flame extinction. K in units of 1/s.

Fuel	$K_L \pm 6$	$K_P \pm 3$	$K_F \pm 8$	$K_E \pm 20$
Methane	—	32	120	380
Ethane	42	42	130	600
Propane	92	84	190	510
Butane	86	82	190	450

Assuming that the fluorescing species are indicative of soot precursors, the result of $K_P < K_F$ suggests that a substantial amount of precursors may still exist even though the production of soot particles has been suppressed. It is reasonable to anticipate that, in more complex flame configurations, these precursors could survive to other parts of the flame where the residence time and temperature are more conducive to particle generation. Thus attainment of K_P is not necessarily sufficient to guarantee the suppression of soot generation.

The result $K_F < K_E$ is interesting in that it indicates the possibility of completely eliminating soot generation by a sufficiently high strain rate without extinguishing the flame. We hasten to add, however, that this result is obtained only for the present relatively non-sooty fuels of the lower alkanes. It is of interest to explore whether $K_F \rightarrow K_E$ for more sooty fuels such that total soot suppression through straining cannot be achieved without extinguishing the flame. Obviously if the fuel is a highly-fluorescing PAH, then $K_E = K_F$ would be expected to hold.

Effects of Concentration and Temperature:

While soot growth in diffusion flames has been studied in detail,[1,6,12] soot inception has not. Experimental difficulties are largely responsible for this lack of information about inception. However, as noted by Kennedy,[13] the critical strain rate characterizes the inception chemistry; therefore a study of how flame temperature and fuel concentration influence the sooting limits of diffusion flames will yield information about how these parameters influence inception chemistry.

Figure 4 shows the various sooting limits for pro-

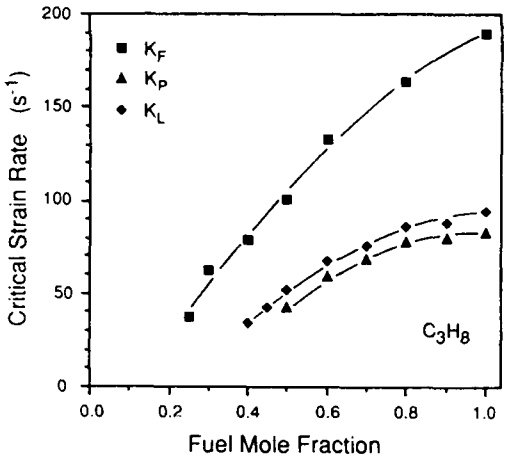

FIG. 4. Sooting limits based on soot luminosity (K_L), soot particle light-scattering (K_P) and PAH fluorescence (K_F) for propane diluted with nitrogen.

pane diluted with nitrogen. These results again demonstrate the differences in the limits based on the various definitions. Furthermore, the results show that the critical strain rates K_L, K_P and K_F all decrease with inert addition and the relative trends of the decrease are similar for all three definitions. In fact, the curve for K_L is similar to that for K_P even though inert addition decreases the temperature (e.g., for X_f = 0.4, ΔT = 113 K) and this decrease will reduce the luminous intensity.

Since the chemistry of soot particle inception is generally a function of both temperature and reactive species concentrations, the results of Fig. 4 do not directly delineate whether the reduction in the critical strain rates with fuel concentration is a consequence of temperature reduction, concentration reduction, or both. To isolate these two effects, we adopt the technique of Ref. 6. That is, after dilution of the fuel by a certain amount of inert, we bring the flame temperature back to the nondiluted value by replacing an appropriate molar amount of nitrogen in the air with an equal amount of argon.

Figures 5 and 6 show the critical strain rates for the diluted flames with and without adjustment of the flame temperature. The difference between the nondiluted value and the diluted value with temperature adjustment is viewed as the effect due to "pure dilution," while the difference between the diluted values with and without temperature adjustment is viewed as the effect due to flame temperature variation. The curve for K_P of Fig. 4 has been duplicated in Fig. 5 to illustrate this technique.

Referring to Fig. 5, it is seen that the effect due to pure dilution is not large for small dilutions but, for fuel mole fractions less than 0.6, the effect can be as large as that due to flame temperature. In Ref. 6 we have demonstrated a similar influence of inert addition on soot volume fraction for flames with low strain rates and high soot loadings. It was suggested[6] that the limited influence of flame temperature when an inert is added to a fuel is a consequence of stoichiometry and the presence of the large amount of nitrogen in air. These facts imply that the flame temperature is only minimally reduced even with a moderate amount of inert addition to the fuel. Reference 6 supports this explanation with calculated adiabatic flame temperatures for different amounts of inert dilution. In the present study we further substantiated these calculated results by experimentally determining the dependence of flame temperature on inert dilution.

The results of Fig. 6b show that the critical strain rates for methane are noticeably more dependent upon inert addition than those for either propane or butane. In Ref. 6 we showed that inert addition influences the flame temperature of methane more than it does that of propane or butane, so inert addition (filled symbols) would be expected to have a greater influence on the critical strain rates of methane. Figure 6b suggests that even when the temperature is not allowed to vary with inert addition, i.e. pure dilution (open symbols), the critical strain rates are more dependent on fuel concentration for methane than for the other fuels. By comparing K_P in Figs. 5 and 6a, it is also seen that

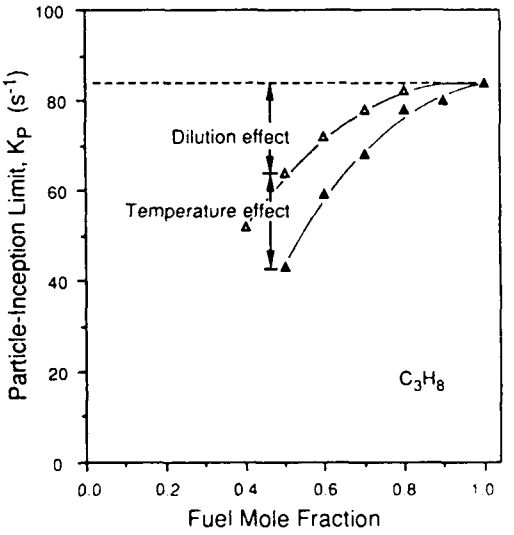

FIG. 5. The effect of nitrogen addition on the particle-inception limit (K_P) for propane. The open symbols represent data for flames where the temperature of the diluted flame has been adjusted to be equal to that of the undiluted flame, so that these data represent pure dilution effects.

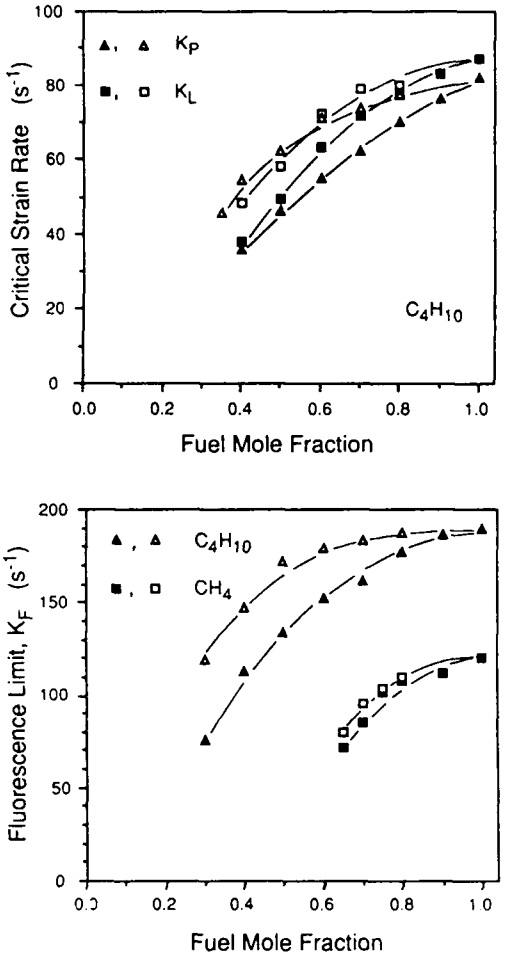

FIG. 6. The effect of nitrogen addition on a) the soot luminosity and particle-inception limit for butane and b) the PAH fluorescence limit for methane and butane. The open symbols represent data for flames where the temperature of the diluted flame has been adjusted to be equal to that of the undiluted flame, so that these data represent pure dilution effects.

the inception limits for propane and butane display similar dependencies on fuel concentration.

Figures 5 and 6 show the influence of pure dilution on the critical strain rates. In Fig. 7 we present the critical strain rates for flames with a fixed concentration of fuel and oxidizer but with different flame temperatures. The fuel mole fractions for ethane, propane and butane are 1.0, 0.5 and 0.4, respectively. The flame temperature is increased by substituting a portion of the nitrogen in air by an equal amount of argon. When the temperature of the flame is increased, it can exceed the operating limits of the thermocouple. Fortunately, experiments as well as adiabatic flame temperature calculations show that the ratio of ΔT to Δ (%Ar) is almost a constant, and this constant is almost independent of fuel concentration. Therefore this ratio is determined at lower fuel concentrations where temperatures are measurable, and is then used to determine ΔT when temperatures are too high to measure.

Figure 7 shows that when concentration effects are eliminated, the flame temperature can have a strong influence on soot extinction by straining. A 200 to 300 K increase in the flame temperature can cause a corresponding increase in the critical strain rates by factor of two to three. Figure 8 shows the Arrhenius plots of the critical strain rates. A linear behavior is observed, implying that the various extinction states can be quantified by a corresponding extinction Damköhler number Da which varies with $K^{-1} \exp(-E_a/R''T_f)$, where E_a is an overall activation energy and T_f the flame temperature. The fact that an Arrhenius correlation exists for T_f is in agreement with the expectation that the flame temperature is useful in characterizing global temperature effects.

The overall activation energies for particle and fluorescence extinction are shown in Fig. 8 for the various fuels. It is of interest to note that the temperature dependence of K_P, depicted by E_a, is similar for all of the alkanes studied. In addition, the

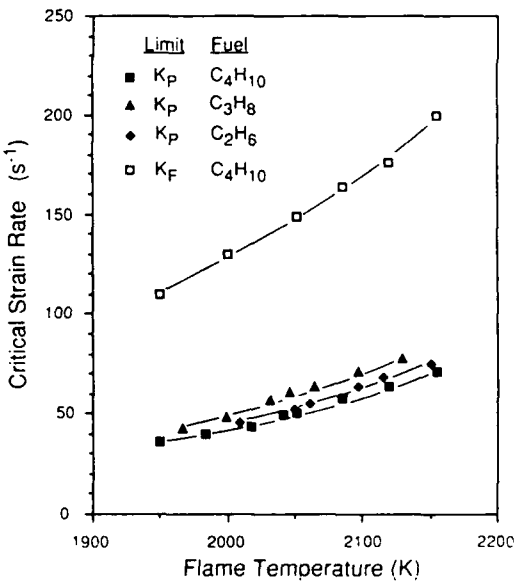

FIG. 7. The effect of temperature on the sooting limits for the various fuels. Temperature adjustment is attained without changing the concentrations of either the fuel or oxidizer. The temperatures have been corrected for radiation loss.

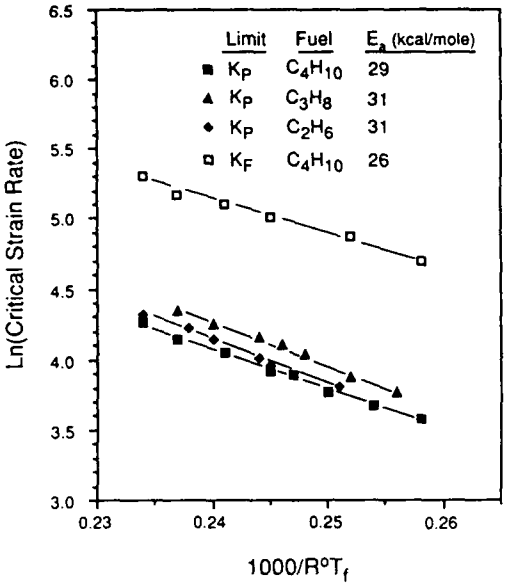

FIG. 8. Arrhenius-type plot for the sooting limits for various fuels, including the global activation energies obtained from least-squares fit to the data.

values of E_a for the particle and fluorescence limits of butane are quite close. This is not surprising if the chemistry of the fluorescing species is related to that of particle formation.

Concluding Remarks

In the present investigation we have distinguished the sooting limits based on luminosity, light scattering by particles, and fluorescence. Each of these extinction phenomena describes a different feature of the soot particle formation process as characterized by the respective critical strain rates. The luminous limit is convenient and a relatively good indicator of the absence of soot particles although the results are strongly dependent on background conditions which can vary greatly with fuel type and flame geometry. The inception limit based on light scattering is an accurate indicator of the absence of soot particles, yet it does not necessarily imply suppression of the soot formation process because gaseous soot precursor species could still be present. It is therefore believed that a sufficiently rigorous indication that the soot formation process is totally suppressed requires the extinction of the soot precursors. The fluorescence limit may be a suitable method of depicting this condition, although further work must be performed to determine if the species that fluoresce when excited at 488 nm are indeed critical to, or at least are by-products of, the chemical processes leading to soot particle inception.

Results further show that soot particle formation is sensitive to both fuel dilution and flame temperature. It is also demonstrated that flame temperature influences both the fluorescence and particle-inception limit in an Arrhenius manner.

Finally, the finding that the parameters important for soot inception are similar to those for soot formation and growth is in agreement with the well-accepted observation that the final soot loading in sooty flames is heavily dependent on the particle inception process.

Acknowledgments

The work was supported by the U.S. Air Force Office of Scientific Research under Grant No. 85-0147. The authors would like to thank Dr. W. L. Flower and Professors I. M. Kennedy and R. J. Santoro for helpful discussions.

REFERENCES

1. VANDSBURGER, U., KENNEDY, I. M. AND GLASSMAN, I.: Twentieth Symposium (International) on Combustion, p. 1105, The Combustion Institute, 1985.
2. HAYNES, B. S. AND WAGNER, H. GG.: Prog. Energy Combust. Sci. 7, 229 (1981).
3. WILLIAMS, F. A.: Combustion Theory, 2nd Edition, p. 415, Benjamin/Cummings, 1985.
4. TSUJI, H. AND YAMAOKA, I.: Eleventh Symposium (International) on Combustion, p. 979, The Combustion Institute, 1967.
5. FLOWER, W. L.: Soot Particle Temperatures in Axisymmetric Laminar Ethylene-Air Diffusion Flames at Pressures up to Seven Atmospheres, SAND87-8704, 1987 (submitted for publication).
6. AXELBAUM, R. L., FLOWER, W. L. AND LAW, C. K.: Dilution and Temperature Effects of Inert Addition on Soot Formation in Counterflow Diffusion Flames, to appear in Comb. Sci. Tech.
7. GLASSMAN, I. AND YACCARINO, P.: Eighteenth Symposium (International) on Combustion, p. 1175, The Combustion Institute, 1981.
8. YU, G., LAW, C. K. AND WU, C. K.: Comb. Flame 63, 339 (1986).
9. MILLER, J. H., MALLARD, W. G. AND SMYTH, K. C.: Comb. Flame, 47, 205 (1982).
10. PRADO, G., GARO, A., KO, A. AND SAROFIM, A. F.: Twentieth Symposium (International) on Combustion, p. 989, The Combustion Institute, 1985.
11. GOMEZ, A., LITTMAN, M. G. AND GLASSMAN, I.: Comb. Flame 70, 225 (1987).
12. SANTORO, R. J. AND SEMERJIAN, H. G.: Twen-

tieth Symposium (International) on Combustion, p. 997, The Combustion Institute, 1985.
13. KENNEDY, I. M.: The Suppression of Soot Particle Formation in Laminar and Turbulent Diffusion Flames, to appear in Comb. Sci. Tech.
14. DU, D. X., AXELBAUM, R. L. AND LAW, C. K.: to be published.
15. BERETTA, F., CINCOTTI, V., D'ALESSIO, A. AND MENNA, P.: Comb. Flame 61, 211 (1985).
16. MULLER DETHLEFS, K.: Optical Studies of Soot Formation and the Addition of Peroxides to Flames, Ph.D. thesis, University of London, 1979.
17. COE, D. S., HAYNES, B. S. AND STEINFELD, J. I.: Comb. Flame 43, 211 (1981).
18. PEARSE, R. W. B. AND GAYDON, A. G.: The Identification of Molecular Spectra, Fourth Ed., Chapman Hall, London, 1976.